TECHNICAL UNIVERSITY OF LIBEREC
Faculty of Textile Engineering

Cellulose Micro Particles from Jute

Dissertation

Study programme: P3106 – Textile Engineering
Study branch: 3106V015 – Textile Technics and Materials Engineering

Author: **Hafiz Shahzad Maqsood, M.Sc.**
Supervisor: Ing. Jana Salačová, Ph.D.

Liberec 2016

TECHNICKÁ UNIVERZITA V LIBERCI
Fakulta textilní

Celulózové mikročástice z juty

Disertační práce

Studijní program: P3106 – Textile Engineering
Studijní obor: 3106V015 – Textile Technics and Materials Engineering

Autor práce: **Hafiz Shahzad Maqsood, M.Sc.**
Vedoucí práce: Ing. Jana Salačová, Ph.D.

Liberec 2016

Prohlášení

Byl jsem seznámen s tím, že na mou disertační práci se plně vztahuje zákon č. 121/2000 Sb., o právu autorském, zejména § 60 – školní dílo.

Beru na vědomí, že Technická univerzita v Liberci (TUL) nezasahuje do mých autorských práv užitím mé disertační práce pro vnitřní potřebu TUL.

Užiji-li disertační práci nebo poskytnu-li licenci k jejímu využití, jsem si vědom povinnosti informovat o této skutečnosti TUL; v tomto případě má TUL právo ode mne požadovat úhradu nákladů, které vynaložila na vytvoření díla, až do jejich skutečné výše.

Disertační práci jsem vypracoval samostatně s použitím uvedené literatury a na základě konzultací s vedoucím mé disertační práce a konzultantem.

Současně čestně prohlašuji, že tištěná verze práce se shoduje s elektronickou verzí, vloženou do IS STAG.

Datum:

Podpis:

Dedicated

to

my Beloved Parents,

Supportive Family and Highly Regarded Teachers

Table of contents

ACKNOWLEDGEMENTS

There have been many people who have helped with the development of this thesis and if I have forgotten to thank anyone, my sincerest apologies.

Firstly, I would like to thank my wonderful family for supporting me through all these years in Liberec, Czech Republic. I would like to give special thanks to my parents, who have always supported me in what I've done and praying for me throughout my life.

I would like to thank my supervisor Ing. Jana Salačová, Ph.D. For her kind behavior, continuous encouragement and great assistance. I would also like to give thanks to my special friend, Dr. Vijaykumar Baheti for his unwavering help.

I would also like to acknowledge Head of the Department, Professor Jiri Militky as well as In-charge textile Chemistry Laboratory, Professor Jakub Wiener for their continual support and guidance. I also appreciate all the support I have had from my colleagues including PhD students and the staff of our Department. Without the help of all of these people this thesis would never have been completed. These people include Miss Mária Průšová, Miss Martina Čimburová, Miss Jana Grabmüllerová, Miss Jana Stránská, Miss Marie Kašparová, Mr. Samson Rawawiire, Mr. Muhammad Zubair and Moaz Ahmad Eldeeb.

Here, at this time I would not forget to thank the kind and nice staff of Dean's Office of Faculty especially Miss Bohumila Keilová, Miss Hana Musilova and Miss Monika Mošničková.

I must acknowledge my parent institution, National Textile University, Faisalabad, Pakistan (NTU) for selecting me for PhD study under its continuous faculty development programme.

I would like to thank Faculty of Textile Engineering, Technical University of Liberec for their financial assistance.

I would also like to offer special thanks to my colleagues there in NTU whoever helped me in my career orientation and development. At last, special thanks to Professor Dr. Niaz Ahmad Akhter, Ex Rector of National Textile University for his dynamic style, kind support, special and sincere efforts for upgrading the overall infrastructure of National Textile University.

ABSTRACT

Jute is an important natural fiber which has a great potential to produce multipurpose products in daily routine life. Unprocessed raw fiber is being utilized as an input source to textile sector for products with high mechanical properties. Jute is one of the longest and most commonly used natural fibers for various technical applications. It is obtained from the inner bark of the plant's stem. Jute is being known as Golden Fiber due to its golden and silky shine. These fibers are composed of the plant materials like cellulose (major component of plant fiber) and lignin (major components of wood). In this specific study, inexpensive jute fibrous waste has been utilized to extract the cellulose particles.

Oxidation of cellulosic materials is required in many fields like textile processing, natural fiber reinforced composites and medical utilization etc. In present study, jute fibers were treated with ozone gas to remove lignin for further utilization of these oxidized fibers.

This study was designed to explore the possibility of ozone treatment as a greener oxidation process of jute fibers. Ozone gas was being used for the treatment of jute fibers for different time periods in a humid atmosphere.

Several characterization techniques, namely physical appearance, fiber mechanical properties, copper number, Fourier Transform Infrared (FTIR) spectroscopy, Wide-angle X-ray diffraction (WAXD), scanning electron microscopy (SEM), moisture regain percentage and lightness values (L) were used to assess the effect of ozone treatment on jute fibres. Results showed that fiber tensile properties weaken gradually as a function of ozone treatment time and surface functional groups alter accordingly. Physically the fiber bundles were split into brittle single fibers and the lightness value increased from brownish shade to lighter colour.

It was clear that physical properties of jute fibers were degraded drastically after certain time of treatment and chemical properties were changed with the change in functional groups present in the fiber morphology. Ozone degrades lignin and slightly solubilizes the hemicellulose fraction, improving resultant fiber morphology for further use. It was concluded in this research that ozonation is a very good and greener substituent of chemical oxidation of cellulose fibers especially jute.

In subsequent step, untreated, chemical (alkali) and ozone pre-treated jute fibers were hydrolyzed by cellulase enzymes for separation of longer jute micro crystals (JMC). The

influence of non-cellulosic contents on the enzyme hydrolysis and morphology of obtained micro crystals was presented.

Later, jute micro crystals were incorporated into poly (lactic acid) matrix to prepare composite films by solvent casting. The reinforcement behavior was evaluated from tensile tests, dynamic mechanical analysis, and differential scanning calorimetry.

In the end, a good level of agreement for maximum reinforcement was confirmed at certain percentage of loading of JMC when compared with predicted values from different mechanical models.

Quadratic regression was applied to the actual values of tensile modulus of composites corresponding to volume fraction of reinforcement and the obtained prediction model was developed using generalized rule of mixture. This model can be used for the prediction of the system properties.

Keywords: Cellulose; Enzymatic Hydrolysis; Jute; Ozone; Oxidation

ABSTRAKT

Juta je důležité přírodní vlákno, které má velký potenciál pro výrobu víceúčelových výrobků v každodenním běžném životě. Nezpracované surové vlákno je využíváno jako vstup v textilním odvětví pro produkty s dobrými mechanickými vlastnostmi. Juta je jedním z nejdelších a nejčastěji používaných přírodních vláken pro různé technické aplikace. Získává se z vnitřních vrstev stonku rostliny. Juta je známa jako "zlaté vlákno" díky své zlatému odstínu a hedvábnému lesku. Vlákna juty se skládají z rostlinných materiálů jako je celulóza (hlavní složka rostlinných vláken) a ligninu (hlavní složky dřevní hmoty). V této konkrétní studii byl použit vláknitý odpad juty k extrakci částic celulózy.

Oxidace celulózových materiálů je důležitá v mnoha oblastech např. při zpracování textilií, kompozitních materiálů z přírodních vláken a využití v lékařství atd. V této studii jutová vlákna byla vystavena účinku ozónu pro odstranění ligninu k dalšímu využití takto oxidovaných vláken.

Tato studie byla navržena tak, aby bylo možné zkoumat možnost úpravy ozónem jako ekologičtější oxidační proces jutových vláken. Ozón byl používán k úpravě jutových vláken po různou dobu expozice a to za přítomnosti vody.

Získané vlastnosti jutových vláken byly analyzovány pro posouzení účinku ozónu pomocí např. změn fyzikálních vlastností, mechanických vlastností vláken, měďného čísla, Fourier Transform Infrared (FTIR) spektroskopie, širokoúhlé rentgenové difrakce (WAXD), rastrovací elektronové mikroskopie (SEM), procenta vlhkosti a hodnoty jasu vzorků (L). Výsledky ukázaly, že pevnost v tahu vláken postupně klesá v závislosti na době zpracování a dochází také ke změnám funkčních skupin v povrchu účinkem ozónu. Ze svazků vláken se oddělily jednotlivé vláken a došlo k zesvětlení nahnědlého odstínu vláken.

Je jasné, že fyzikální vlastnosti jutových vláken se drasticky mění po expozici ozónu. Mění se i chemické vlastnosti jutových vláken, což se projevuje změnami funkčních skupin ve vlákně. Ozón degraduje lignin a mírně napadá frakce hemicelulózy, což má za následek zlepšení výsledné morfologie vláken pro další použití. Z provedeného výzkumu plyne, že ozonizace je velmi dobrá a ekologičtější náhrada chemické oxidace celulózových vláken, zejména juty.

V následujícím kroku jsou neupravená, chemicky (alkalicky) a ozónem opravená vlákna juty hydrolyzována celulázovými enzymy pro separaci celulózových mikrokrystalů z juty (JMC).

Byl prezentován vliv necelulózových složek na enzymovou hydrolýzu a morfologii získaných mikrokrystalů.

Následně byly mikrokrystaly juty začleněny do matrice z kyseliny polymléčné pro přípravu kompozitní fólie litím. Chování výztuže bylo hodnoceno na základě zkoušky pevnosti v tahu, dynamické mechanické analýzy a diferenční skenovací kalorimetrie.

Byla potvrzena dobrá míra shody mezi zvýšením pevnosti kompozitu přídavkem JMC a predikovanými hodnotami z různých mechanických modelů.

Kvadratická regrese byla aplikována na aktuální hodnoty modulu pružnosti kompozitu v závislosti na objemu frakce výztuže a pomocí zobecněného pravidla směsi byl získán predikční model. Tento model lze využít pro predikci vlastností kompozitního systému.

Klíčová slova: Celulóza; Enzymatická hydrolýza; Juta; Ozón; Oxidace

خلاصہ

پَٹ سَن ایک اہم قُدرتی ریشہ ہے جو ہماری روز مرّہ معمول کی زندگی کی مختلف نوعیت کی مصنوعات بنانے کے لیے بہت اچھی صلاحیت رکھتا ہے۔ اِس کا بنیادی ریشہ ٹیکسٹائل کی صنعت میں اچھی طاقت والی مضبوط مصنوعات بنانے کے لیے خام مال کے طور پر استعمال ہوتا ہے۔ پَٹ سَن مختلف تکنیکی مصنوعات کے لیے استعمال ہونے والے سب سے لمبے اور زیادہ استعمال ہونے والے ریشوں میں سے ایک ہے۔ یہ ریشہ پودے کی چھال کے اندرونی خلیوں سے حاصل کیا جاتا ہے اور اپنی سنہری اور ریشمی چمک کی وجہ سے "سنہرے ریشے" کے طور پر معروف ہے۔

پَٹ سَن کے یہ ریشے سیلولوز (پودوں کے ریشوں کا بنیادی جز) اور لِگنن (لکڑی کا بنیادی جز) کا مُرکّب ہوتے ہیں۔ اِس مذکورہ تحقیقی مطالعہ میں سیلولوز مائیکرو اور نینو ذرات حاصل کرنے کے لیے پَٹ سَن کے سستے ضائع شدہ ریشوں کو استعمال کیا گیا۔

سیلولوز کی تکسید بہت سارے شعبوں بشمول ٹیکسٹائل پروسیسنگ، قدرتی ریشوں سے مضبوطی لینے والے کمپوزِٹس اور طِبّی استعمالات وغیرہ میں مطلوب ہے۔ پَٹ سَن کے ریشوں میں موجود لِگنن کو دور کرنے کے لیے اوزون گیس استعمال کی گئی تاکہ وہ ریشے بعد ازاں مائیکرو اور نینو ذرّات حاصل کرنے کے لیے استعمال کیے جا سکیں۔

پَٹ سَن کے ریشوں کی ماحول دوست عملِ تکسید کے امکانات کو تلاش کرنے کے لیے اس تحقیق کر مُرتّب کیا گیا تھا جس میں ریشوں کو ایک مرطوب ماحول میں مختلف اوقات کے ساتھ اوزون گیس کے ساتھ رکھا گیا۔ پَٹ سَن کے ریشوں پر اوزون گیس کا اثر جانچنے کے لیے مختلف تراکیب استعمال کی گئیں جِن میں جسمانی خدوخال کا معائنہ، میکانی

خصوصیات، کاپر نمبر، فوریئر ٹرانسفارم انفراریڈ سپیکٹروسکوپی، وائیڈ اینگل ایکس رے ڈائی فریکشن، سکیننگ الیکٹران مائیکروسکوپی، نمی دوبارہ حاصل کرنے کی خصوصیت اور رَنگت کی تبدیلی شامل ہیں۔ نتائج سے ظاہر ہوا کہ ریشوں کی طاقت کے خواص میں اوزون گیس کے عمل سے بتدریج کمی ہوئی اور ساتھ ہی سطحی فعال گروپوں میں بھی تبدیلی وقوع پذیر ہوئی اور ظاہری طور پر ریشوں کے بَنڈل خَستہ اوور عَلیحدہ عَلیحدہ واحد ریشوں میں تقسیم ہوتے گئے۔ ریشوں کی رنگت بھی گہرے بھورے رنگ سے بدل کر ہلکے بھورے رنگ میں تبدیل ہوتی گئی۔

پَٹ سَن ریشوں کی طَبعی خصوصیات کمزور اور خراب ہونے کے ساتھ ساتھ ان کے اندر موجود فعال گروپوں کے تبدیل ہونے سے کیمیائی خصوصیات بھی تبدیل ہوتی گئیں۔ اوزون گیس نے لِگنن کے خاتمے کے ساتھ ساتھ ہیمی سیلولوز کا کچھ حصہ بھی تحلیل کر دیا جس سے ریشوں کی خصوصیات ذرّات حاصل کرنے کے لیے موزوں ہو گئیں۔ اس تحقیق سے یہ نتیجہ اخذ کیا گیا کہ اوزون گیس کا عمل سیلولوز ریشوں خاص طور پر پَٹ سَن کی عملِ تکسید کے لیے کیمیائی عملِ تکسید کا ایک ماحول دوست نعم البدل ہے۔

بعد اَزاں پَٹ سَن کے خام ریشوں، کیمیائی عملِ تکسید کیے گئے ریشوں اور اوزون کے ذریعے عملِ تکسید کیے گئے ریشوں کی سیلولیز خامروں کی مدد سے آب پاشیدگی کی گئی تاکہ پَٹ سَن کے نسبتاً لمبے اور زیادہ کارآمد مائیکرو ذرّات حاصل کیے جا سکیں۔ اس طرح سیلولیز خامروں کے ذریعے آب پاشیدگی کے عمل میں ریشوں کے اندر موجود

غیر سیلولوزِک مواد کا اثر پیش کیا گیا۔ پھر ان حاصل شدہ مائیکرو ذرّات کو پولی لیکٹک ایسڈ کے میٹرِکس میں ڈال کر کمپوزِٹ فِلم تیار کی گئی جس کی طاقت میں تبدیلی کا اندازہ میکانی تجربات، متحرک میکانی تجزیہ اور ڈیفرینشل سکیننگ کیلوری میٹری سے کیا گیا۔

آخر میں کمپوزِٹ کے اندر ذرّاتی کمک کے نتیجے میں حاصل شدہ ابتدائی معامل کا مختلف میکانی ماڈلوں کے پیش گوئی کردہ اقدار کے ساتھ موازنہ کیا گیا تو ذرّاتی کمک کی ایک خاص فی صدی (حُجم) مقدار تک ان میں تقابلی معاہدہ پایا گیا۔

کمپوزِٹ میں ذرّاتی کمک کے تناسب (فی صدی حُجم) اور حاصل شدہ ٹینسائل معامل کے اوپر چکوری رجعت کا اصول لاگو کرتے ہوئے مُرکّب کے عمومی قاعدے کے استعمال کے تحت ایک ماڈل تیار کیا گیا جو تیار کردہ کمپوزِٹ کے خواص کے متعلّق پیش گوئی کرنے کے لیے استعمال ہو سکتا ہے۔

مطلوبہ اہم الفاظ:

سیلولوز، خامروں کے ذریعے آب پاشیدگی، پَٹ سَن، اوزون، عملِ تکسید

List of tables

List of figures

List of Abbreviations and Symbols

Abbreviation	Description
3D	Three Dimensional
BNC	Bacterial Nano Cellulose
CMC	Carboxymethyle Cellulose
COD	Chemical Oxygen Demand
CTJF	Chemical Treated Jute Fibers
CTJMC	Chemical Treated Jute Micro Crystals
DMA	Dynamic Mechanical Analysis
DSC	Differential Scanning Calorimetry
E	Composite Modulus
E'	Storage Modulus
E_m	Matrix Modulus
E_r	Reinforcement Modulus
FESEM	Field Emission SEM
FTIR	Fourier Transform Infra-Red
g/L	Gram per Litre
GPa	Giga Pascal
Hz	Hertz
JMC	Jute Micro Crystals
kV	Kilo Volt
L/min	Litres per Minute
mg/L	Milligram per Litre
MPa	Mega Pascal
N	Newton
NaOCl	Sodium Hypochlorite
NaOH	Sodium Hydroxide
NCC	Nano Crystalline Cellulose
NFC	Nano fibrillated Cellulose
O_2	Oxygen

O_3	Ozone
^oC	Degrees of Celsius (Temperature)
OP	Ozonation generator Power
OT	Ozonation Time
OTJF	Ozone Treated Jute Fibers
OTJMC	Ozone Treated Jute Micro Crystals
OX	Oxygen flow rate
PHA	Poly Hydroxyalkanoate
PLA	Poly (Lactic acid)
RH	Relative Humidity
rpm	Revolutions per Minute
SEM	Scanning Electron Microscope
T_{cc}	Cold Crystallization Temperature
TEMPO	2,2,6,6-tetramethyle piperidine-1-oxyle
T_g	Glass Transition Temperature
T_m	Melting Temperature
UTJF	Untreated Jute Fibers
UTJMC	Untreated Jute Micro Crystals
WAXD	Wide-angle X-Ray Diffraction
W_r	Weight percentage of Reinforcement
Xc	Percolation Threshold
δ	Standard Deviation
ΔH	Heat of Melting of Sample
ΔH_o	Heat of Melting of 100% Crystalline PLA
η	The shape Parameter of Reinforcement
η_l	Length Correction Factor
η_o	Orientation Factor
ρ_m	Density of Matrix
ρ_r	Density of Reinforcement
ψ	Percolation Volume Fraction

CHAPTER 1

INTRODUCTION

With the rise of living standards of people the demand for textiles has increased significantly in the last few decades. However, the increased demands also brought the challenges to cater the disposal of significant amount of wastes generated during the processing. Generally textile wastes are classified as either pre-consumer or post-consumer textile waste. Pre-consumer textile waste is the leftovers or byproducts from textile, fiber-or cotton industries. On the other hand, post-consumer textile wastes are the wastes of textile products such as fleece, flannel, corduroy, cotton, denim, wool, and linen. These wastes are generally discarded as landfills or incinerated as an alternative fuel source. In recent years, research on recycling and reuse of textile wastes, instead of landfilling or incineration, has gained a lot of importance due to the increased awareness of environmental concerns (Wang 2006), (Horrocks 1996). This is because, textiles in landfill biodegrade to form methane gas which is released into the air and is not suitable for human consumption. Similarly incineration of textile wastes leads to release of toxic fumes which are hazardous in nature. European Union (EU) typically being more progressive on environmental issues have implemented laws (Directive 2000/53/CE) to prevent the landfilling of waste materials.

In the context of environment protection and current disposal of the textile wastes, it becomes essential to recover useful products from the wastes for economic reasons. Traditionally, textile wastes are converted to individual fiber stage through cutting, shredding, carding, and other mechanical processes (Horrocks 1996; Wang 2006). The fibers are then rearranged into products for applications in garment linings, household items, furniture upholstery, automotive carpeting, automobile sound absorption materials, carpet underlays, building materials for insulation and roofing felt, and low-end blankets. In this way, textile waste industries were emerged typically as shredders, shoddy producer, laundry and wiping rag producer. However, due to recent increase in competition and reduced profit margins in these industries, it has become important to search for new recycling techniques of waste textiles in order to utilize them for high end applications. One such interesting way is to separate the nanofibrils or Nano crystals from the textile wastes and subsequently incorporate them as fillers into

high performance composite materials (Klemm et al. 2006; Yuen et al. 2009; Khalil et al. 2012). In this way, the exploration of these inexpensive industrial fiber wastes as bio resource for making industrial products will open new avenues for the utilization and at the same time add value to the creation of economy.

Among various raw materials, cellulose fibers are popularly used in the textile industry due to their high aspect ratio, acceptable density, good tensile strength and modulus (Yuen et al. 2009). These properties make them attractive class of textile materials traditionally used in manufacture of yarn by spinning process. But, due to certain limitations of the spinning process, shorter fibers (i.e. below 10 mm) generated during mechanical processing are not suitable to reuse in yarn manufacture and consequently result into the waste (Yuen et al. 2009). Generally fibers have been used for variety of applications depending on their length (Stevens and Müssig 2010).Here the idea of separation of nanostructures from waste fibers and subsequently incorporating them as fillers in nanocomposite films could provide cost-effective solutions to the struggling textile industries.

The micro/nanostructures of cellulose have gained significant amount of importance due to its higher mechanical properties. The crystalline segments in cellulose have a greater axial elastic modulus than the synthetic fiber Kevlar, and their mechanical properties are within the same range as those of other reinforcement materials such as carbon fibers, steel wires and carbon nanotubes (Klemm et al. 2006; Khalil et al. 2012). The nanostructures of cellulose are considered as bundles of molecules which are elongated and stabilized through hydrogen bonding. The remarkable improvements in mechanical properties of cellulose nanostructures, in range of 130-170 GPa, are considered due to this parallel arrangement of molecular chains which are present without folding (Klemm et al. 2006). Previous work on composites made from cellulose nanostructures showed improved strength and stiffness with a little sacrifice of toughness, reduced gas/water vapor permeability, lower coefficient of thermal expansion, and increased heat deflection temperature (Dufresne et al. 1999; Khalil et al. 2012). These properties thus could promise in replacement of conventional petroleum based composites by new, high performance, and lightweight green nanocomposite materials.

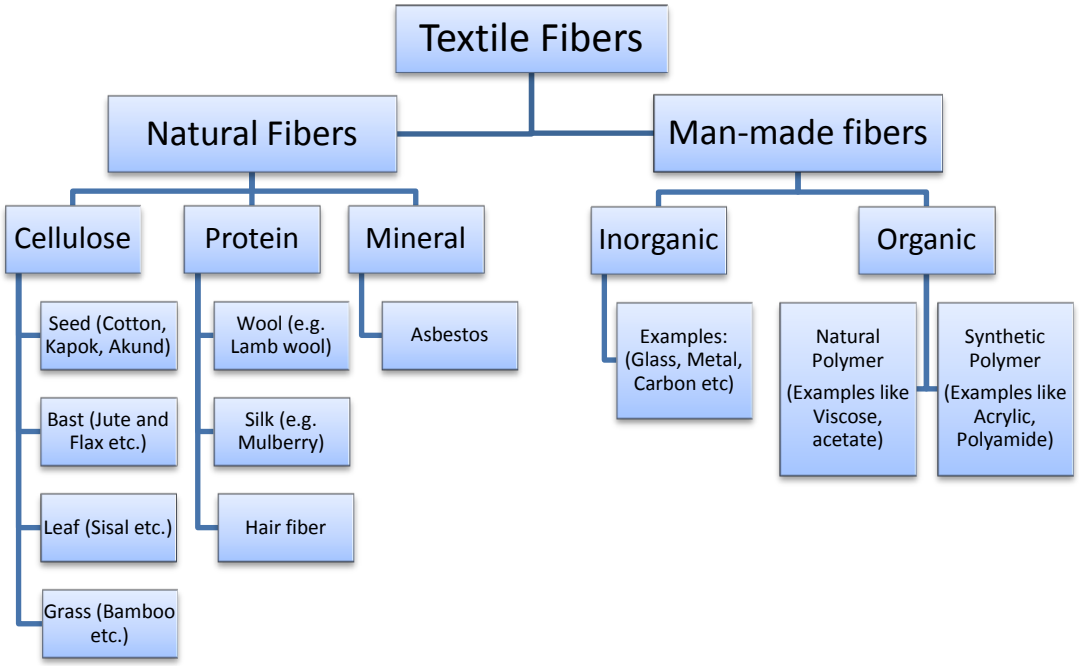

Figure 1. Classification of Different Textile Fibers

Nanocomposites are a relatively new generation of composite materials where at least one of the constituent phases has one dimension of less than 100 nm (Klemm et al. 2006). This new family of composites is reported to exhibit remarkable improvements in material properties when compared to conventional composite materials. The small size of the reinforcement leads to an enormous surface area and thereby to increased interaction with the matrix polymer on molecular level, leading to materials with new properties. Well dispersed nano particles can improve tensile properties and even improve the ductility because their small size does not create large stress concentrations in the matrix. The small size also increases the probability of structural perfection and will in this way be a more efficient reinforcement compared to micro sized reinforcements (Dufresne et al. 1999).

The utilization of different types of cellulosic wastes has been studied in the past in order to obtain cellulose nanostructures at reasonably lower cost. The variety of agricultural wastes like coconut husk fibers (Rosa et al. 2010), cassava bagasse (Pasquini et al. 2010), banana rachis (Zuluaga et al. 2009), mulberry bark (Li et al. 2009), soybean pods (Wang and Sain 2007), wheat straw and soy hulls (Alemdar and Sain 2008)and cornstalks (Reddy and Yang 2005)are investigated for extraction of cellulose nanostructures. However, there is no information available in literature on

utilization of cellulosic wastes of textile industries in spite of large amount of short fibers are generated during the mechanical processing of yarn manufacture.

Although the cellulose nanostructures have a great potential for reinforcement into biopolymers, the major challenge in order to use them is the extraction. The variety of techniques like acid hydrolysis (Liu et al. 2010), enzymatic hydrolysis (Satyamurthy et al. 2011), ultrasonication (Li et al. 2012), high pressure homogenization (Leitner et al. 2007), etc. have been employed. However, most of these techniques used in the extraction are time consuming, expensive in nature and low in yields (Klemm et al. 2006). The commonly used strong acid hydrolysis method has a number of important drawbacks such as potential degradation of the cellulose, corrosivity and environmental incompatibility (Thomas and Pothan 2009). In order to promote the commercialization of cellulose nanofibrils, the development of more flexible and industrially viable processing technique is needed. The core part of thesis describes the enzymatic hydrolysis of jute fibers pretreated with ozone gas in a controlled atmosphere as a practical and greener method to disintegrate the jute fibrous waste to obtain longer micro crystals of cellulose in bulk quantity.

Due to limited availability of petroleum resources and increased concerns over disposal from clean environment point of view, research on renewable materials have gained importance in recent years (Klemm et al. 2006; Khalil et al. 2012). Within the period of 2005 and 2009, global market on the demand of biodegradable polymers was double in size. Among all countries in the World, Europe had the largest growth in the range of 5–10 % on the use of biodegradable polymers in 2009. Moreover, the total consumption of biodegradable polymers has been grown at an average annual rate of nearly 13 % from 2009 to 2014 in North America, Europe and Asia (Platt 2006). Nowadays significant amount of research is being carried out to further increase the market potentials of these materials by reducing their higher price and by improving their properties for different applications. The development of biocomposite materials by incorporation of renewable reinforcing elements is considered as one of the favorable solution to meet these requirements (Klemm et al. 2006).

Over the last two decades, reinforcement potentials of lignocellulose fibers have been investigated in numerous studies of biocomposites made from PLA (Lunt 1998; Petersen et al. 2001; Petersson and Oksman 2006; Sanchez-Garcia et al. 2008; Jonoobi

et al. 2010). However, the reinforcement potentials of lignocellulose fibres are found not enough to meet demands of high performance applications. In addition, there is no clear trend in improvement of mechanical properties after addition of lignocellulosic fibres (Petersen et al. 2001; Petersson and Oksman 2006; Jonoobi et al. 2010). For instance, Oksman (Oksman et al. 2003) produced 30 wt. % flax fibre reinforced PLA biocomposites where only little improvement in tensile strength from 50 MPa to 53 MPa and significant improvement in initial modulus from 3.4 GPa to 8.3 GPa was reported. On the contrary Plackett (Plackett et al. 2003) found the significant improvement in tensile strength from 55 MPa to 100 MPa and similar improvement in initial modulus from 3.5 GPa to 9.4 GPa for 40 wt. % loading of jute fibres into the biopolymer PLA. In another study, Bax and Mussig (Bax and Müssig 2008) also used 30 wt. % flax fibres to reinforce PLA where tensile strength was improved from 44.5 MPa to 54.1 MPa and initial modulus was improved from 3.1 GPa to 6.31 GPa.

This pattern of non-consistent improvements in properties of lignocellulosic fibres composites are explained due to the variations in properties of lignocellulosic fibres derived from different resources (Dufresne et al. 1999; Klemm et al. 2006). Table 1 shows the properties of different types of fibers (Mohanty et al. 2005). As the individual lignocellulosic fibres are made from the packing of several micro/nano cellulose fibrils together, the number of defects present in the structure varies from source to source. One of the basic ideas to further improve fiber and composite properties is to eliminate the macroscopic flaws by disintegrating the fibers, and separating the almost defect-free, highly crystalline nanofibrils. This can be achieved by exploiting the hierarchical structure of the natural fibers (Klemm et al. 2006; Yuen et al. 2009; Khalil et al. 2012).

Table 1. Mechanical properties of textile fibers (Mohanty et al. 2005)

Fiber	Density (g cm^{-3})	Diameter (μm)	Tensile Strength (MPa)	Young's Modulus (GPa)	Elongation at Break (%)
Flax	1.5	40–600	345–1500	27.6	2.7–3.2
Hemp	1.47	25–500	690	70	1.6
Jute	1.3–1.49	25–200	393–800	13–26.5	1.16–1.5
Kenaf			930	53	1.6
Ramie	1.55	—	400–938	61.4–128	1.2–3.8
Nettle			650	38	1.7
Sisal	1.45	50–200	468–700	9.4–22	3–7
Henequen					
PALF		20–80	413–1627	34.5–82.5	1.6
Abaca			430–760		
Oil palm EFB	0.7–1.55	150–500	248	3.2	25
Oil palm mesocarp			80	0.5	17
Cotton	1.5–1.6	12–38	287–800	5.5–12.6	7–8
Coir	1.15–1.46	100–460	131–220	4–6	15–40
E-glass	2.55	<17	3400	73	2.5
Kevlar	1.44		3000	60	2.5–3.7
Carbon	1.78	5–7	3400[a]–4800[b]	240[b]–425[a]	1.4–1.8

1.1. Morphology of lignocellulose fibers

Lignocellulose fibers are basically constituted of cellulose, lignin and hemicellulose. Each fiber is essentially a composite in which rigid cellulose micro fibrils are embedded in a soft matrix mainly composed of lignin (Mohanty et al. 2005). The chemical composition as well as the morphological microstructure of fibers is extremely complex due to the hierarchical organization of the different compounds present at various compositions. Depending on the type, the chemical composition of lignocellulose fiber varies (Table 2).

Table 2. Chemical composition of textile fibers (Mohanty et al. 2005)

Fiber	Cellulose (wt%)	Hemicelluloses (wt%)	Lignin (wt%)	Pectin (wt%)	Moisture Content (wt%)	Waxes (wt%)	Microfibrillar Angle (deg)
Flax	71	18.6–20.6	2.2	2.3	8–12	1.7	5–10
Hemp	70–74	17.9–22.4	3.7–5.7	0.9	6.2–12	0.8	2–6.2
Jute	61–71.5	13.6–20.4	12–13	0.2	12.5–13.7	0.5	8
Kenaf	45–57	21.5	8–13	3–5			
Ramie	68.6–76.2	13.1–16.7	0.6–0.7	1.9	7.5–17	0.3	7.5
Nettle	86				11–17		
Sisal	66–78	10–14	10–14	10	10–22	2	10–22
Henequen	77.6	4–8	13.1				
PALF	70–82		5–12.7		11.8		14
Banana	63–64	10	5		10–12		
Abaca	56–63		12–13	1	5–10		
Oil palm EFB	65		19				42
Oil palm mesocarp	60		11				46
Cotton	85–90	5.7		0–1	7.85–8.5	0.6	—
Coir	32–43	0.15–0.25	40–45	3–4	8		30–49
Cereal straw	38–45	15–31	12–20	8			

Cellulose is main lignocellulosic component of cell wall in plants along with hemicellulose, lignin, pectin and waxes (Rowell 2012). The simple molecular structure of cellulose is given in figure 2. Cellulose is linear polymer of β-d-anhydroglucopyranoside with 1, 4 β-glycosidic linkage. The structure is supported by the free secondary OH groups at C-2, C-3 position and primary OH group at C-6 position (Rowell 2012).

Hemicellulose is a generic term for the various polysaccharides other than cellulose found in native plants (Fig. 2). They are amorphous polysaccharides which are composed from a mixture of carbohydrates comprising 3-6 membered units (Rowell 2012). They consist of polysaccharides of comparatively low molecular weight built up from hexoses, pentoses and uronic acid residues. The chemical composition of hemicelluloses is extraordinarily similar to cellulose (e.g. polymers of various pentoses such as xylose, arabinose, and hexoses like glucose, mannose, galactose, etc.).The main parts are straight chain of d-xylose residues, with two side branches of d-xylose residues. In addition there are other side branches formed from single residues of 4-0-methyl glucoronic acid, to the extent of one for every seven xylose units.

Lignin is a complex dendritic network of phenyl propene which acts as binder in cellulose fiber to give the exact morphology for plant cell wall (Rowell 2012). The main

repeat unit is 3-(4-hydroxy phenyl) prop-2-eneol having a methoxyl group in the ortho position of the phenolic ring (Fig. 2). Lignin is considered to be a thermoplastic polymer exhibiting a glass transition temperature of around 90^{o} C and melting temperature of around 170^{o}C.

Pectin is a generic term for a group of polysaccharides characterized by high uronic acid content, the presence of methyl ester groups, and measurable quantity of acetyl esters. It is heteropolysaccharide of 1-4 linked galacturonic acid with methyl esters of different sugar units (Rowell 2012).

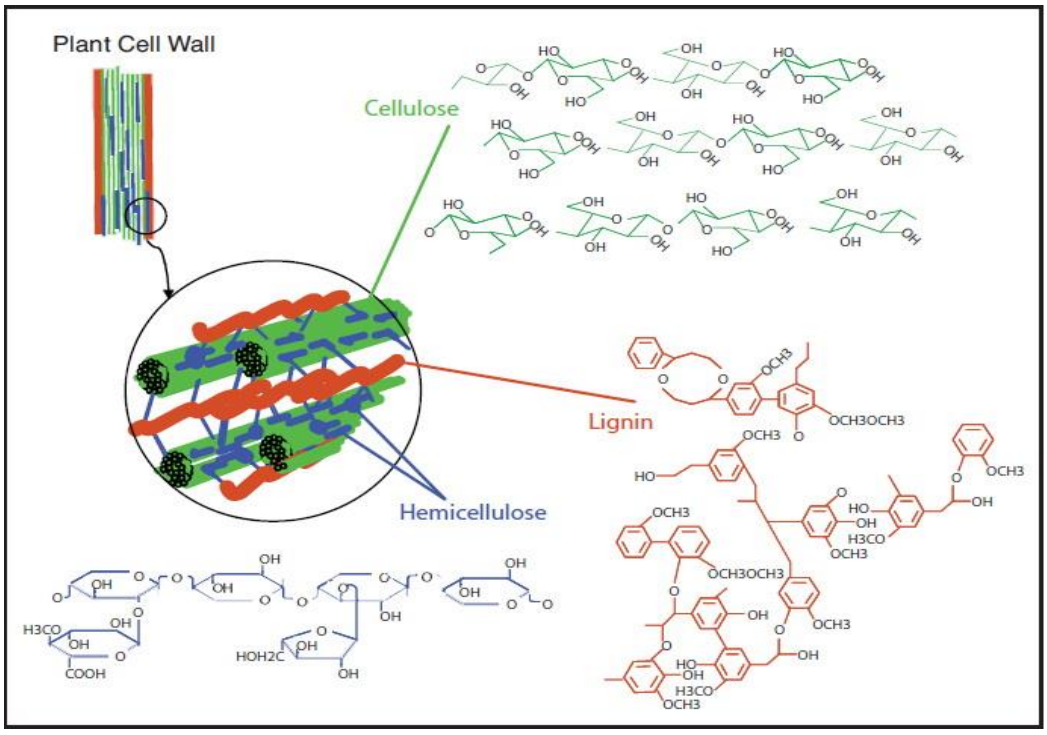

Figure 2. Molecular structure of cellulose, hemicellulose and lignin

A single lignocellulose fiber consists of several cells (except in cotton). These cells are formed out of cellulose-based crystalline micro fibrils, which are connected to a complete layer by amorphous lignin and hemicellulose (Fig. 3). To form a multiple layer composite lignocellulosic fiber, multiples of such cellulose–lignin–hemicellulose layers in one primary and three secondary cell walls stick together. About several hundred to 10 million of glucose units condense to form a straight chain of a polysaccharide unit in the form of cellulose nanofibrils. The free OH groups in one polysaccharide thread have higher possibilities to form hydrogen bonds with another thread. Therefore a number of

nanofibrils bind through intermolecular hydrogen-bonding with each other to form microfibers and then to microscopic cellulose fibers.

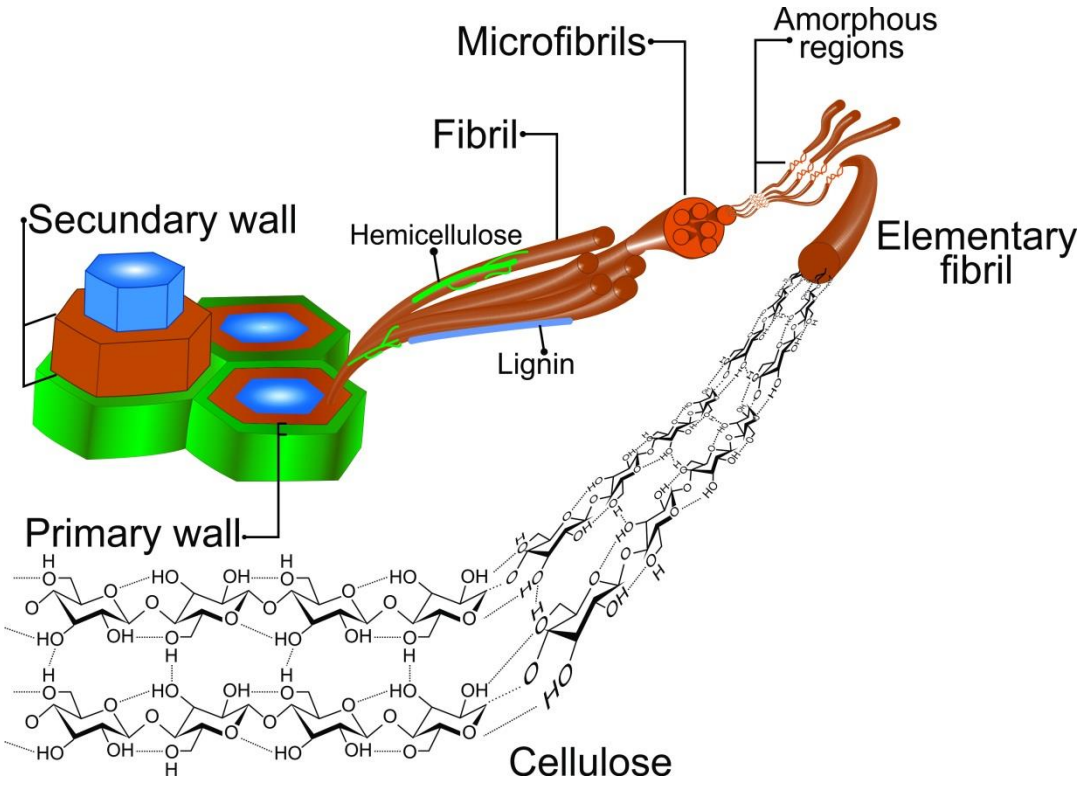

Figure 3. Hierarchical structure of cellulose extracted from plants(Rojas et al. 2015)

The study (Kalia et al. 2011) regarded the micro fibril itself as being made up of a number of crystallites, each of which separated by a para crystalline region and later termed it as elementary fibril. According to this concept, the elementary fibril is formed by the association of many cellulose molecules, which are linked together in repeating lengths along their chains. In this way, a strand of elementary crystallites is held together by parts of the long molecules reaching from one crystallite to the next, through less ordered inter-linking regions (Fig. 4). Their structure consists of a predominantly crystalline cellulosic core which is covered with a sheath of para crystalline polyglucosan material surrounded by hemicelluloses. As they are almost defect free, the modulus of these sub entities is close to the theoretical limit for cellulose.

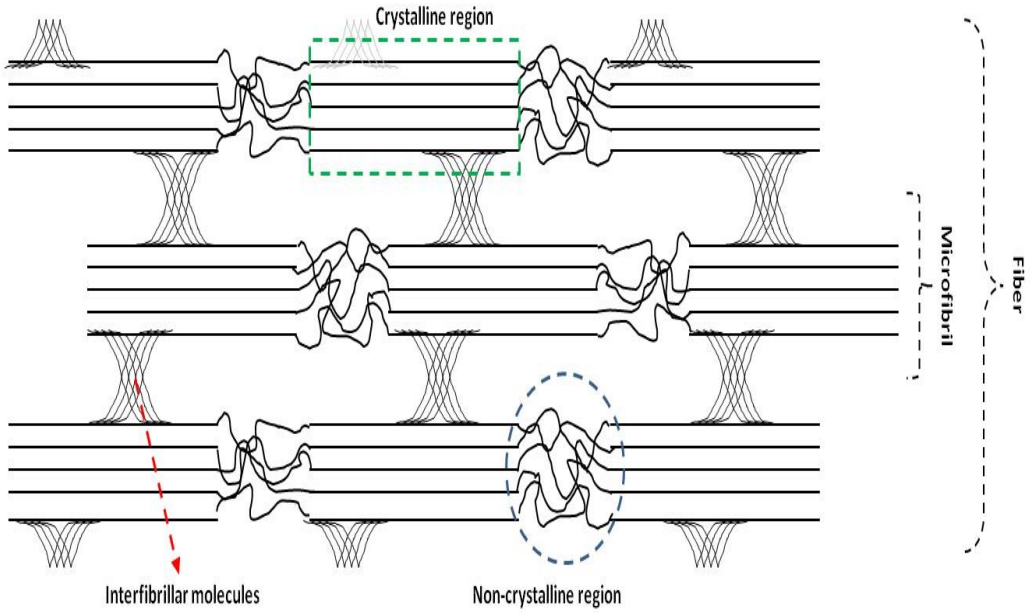

Figure 4. Arrangement of cellulose molecules in fiber (Wallenberger and Weston 2004)

Among various natural plant fibers, jute fibers are extensively used in textile industries for variety of applications. Jute's silky texture, its biodegradability, and its resistance to heat and fire make it suitable for use in industries as diverse as fashion, travel, luggage, furnishings, and carpets and other floor coverings (Kalia et al. 2011). Jute fibers have also been used as reinforcement for partitions, paneling, false ceilings, and other furniture. Extensive studies are carried out in past to fabricate jute/epoxy, jute/polyester, and jute/phenol-formaldehyde composites for applications such as low-cost housing materials, silos for grain storage, and small fishing boats (Kalia et al. 2011).

Jute fibers are obtained from the stem of plants. The suitable climate for growing jute (warm and wet climate) is offered during the monsoon season. The temperatures ranging from 20ºC to 40ºC and relative humidity of 70%-80% are favorable for its successful cultivation. India has its highest cultivation area, largely concentrated in the east and the north-eastern states. The popular varieties of Jute are: Tossa Jute-Corchorusolitorius (Golden yellow color) and White Jute-Corchoruscapsularis (Silvery color). The properties of these varieties are given in table 3.

Table 3. Properties of different varieties of jute fibers

Property	White jute	Tossa jute
Unit cell length (mm)	0.8–6.0	0.8–6.0
Length/breadth ratio	110	110
Hermann's Angle of orientation (X-ray)	7°–10°	7°–9°
Specific gravity	1.4–1.45	2.00–5.00
Moisture regain (%) at 65% RH	12.5	12.5
Transverse swelling (%) in water	20.0–22.0	20.0–22.0
Tenacity – single fibre (g/tex)	27–36	16–35
Elongation at break (%)	1–1.5	1.0–2.0

Jute contains the highest proportion of the stiff natural cellulose in comparison with other lignocellulose fibers. The chemical composition of jute fibers constitutes as cellulose 55–65%, lignin 10–15%, pentosans 15–20%. In addition, jute contains minor constituents such as fats and waxes 0.4—0.8%, inorganic matter of 0.6—1.2%, nitrogenous matter 0.8—1.5% and traces of pigments. In total it amounts about 2%. Cellulose forms the bulk of the ultimate cell walls with the molecular chains lying broadly parallel to the direction of the fiber axis. The hemicellulose and lignin are located in the areas between neighboring cells, where they form the cementing material of middle lamella, providing strong lateral adhesion between the ultimate fibers.

In recent years, renewable materials have gained significant importance due to limited availability of petroleum resources and increased awareness of environmental concerns. The natural fibers are increasingly replacing glass, carbon and other synthetic fibers in composite applications (Rwawiire et al. 2015). Jute is commonly used as reinforcement in composites due to its higher strength and higher aspect ratio. In addition, jute has another important inherent properties such as biodegradability, moderate moisture regain, good thermal and acoustic insulation and low price (Johnson et al. 2016). Nevertheless, for further growth of jute fiber based composites, it is necessary to overcome certain drawbacks. Jute fibers have few disadvantages such as high moisture absorption, swelling, low toughness, limited compatibility with some matrices, low processing temperature, low thermal stability, high biodegradability, and low dimensional stability (Ranganathan et al. 2016). To overcome these drawbacks, considerable efforts have been made by the researchers such as surface modification of jute fibers, isolation of elementary cellulose fibrils/crystals, etc.

Jute fibers consist of lignin (12–14 %), hemicellulose (21–24 %), cellulose (58–63 %), fats and waxes (0.4–0.8 %), inorganic matter (0.6–1.2 %), nitrogenous matter (0.8–1.5 %) and traces of pigments (Militký and Jabbar 2015; Jabbar et al. 2016). However, the presence of non-cellulosic substances found to hinder the reaction between hydroxyl groups of fibers and polymer matrices, which consequently deteriorated the mechanical properties of composites (Baheti et al. 2014). In order to have better bonding between fibers and matrix, the non-cellulosic contents should be removed. The various surface treatments such as sodium hydroxide, peroxide, organic and inorganic acids, silane, anhydrides and acrylic monomers have been attempted by researchers in previous works to improve the compatibility between fibers and matrix (Baheti et al. 2014). However, such chemical treatments are not environment friendly and require more energy, time and water. The motivation of present work was to search for alternative and relatively greener techniques for surface modification of jute fibers.

The oxidation of jute fibers using ozone gas is one of the alternatives over chemical treatments for removal of lignin. Ozone is an oxidizing agent with a strong oxidation potential of 2.07 V (Sargunamani and Selvakumar 2006). It is an unstable allotrope of oxygen containing three atoms. Ozone is highly reactive towards compounds incorporated with conjugated double bonds and functional groups of high electron densities (Perincek et al. 2007). Due to high content of C=C bonds in lignin, ozone treatment of jute fibers is likely to remove lignin by release of soluble compounds of less molecular weight such as organic acids. Therefore, the ozone treatment is environment friendly, causes minimal degradation of cellulose and hemicelluloses, and requires less energy, time and water (Benli and Bahtiyari 2015). The effectiveness of ozone treatments in the textile wet processing has already been demonstrated. The ozone treatment was found suitable for bleaching of cotton (Perincek et al. 2007). In another study, the effect of ozone was found to improve the whiteness degree and dye ability of Angora rabbit fibers (Perincek et al. 2008). The study of ozone treatment on silk reported it to turn into yellowish, harsh and without luster (Sargunamani and Selvakumar 2006).

More recently separation of individual cellulose fibrils or crystals is reported in many research works for achieving extremely higher mechanical properties suitable in high performance composites (Guo et al. 2016). In order to disintegrate fibers to the level of mechanically strong cellulose elementary fibrils without complete dissolution, it

is necessary to work on chemically less aggressive hydrolysis concepts. The ozone pre-treatment of jute fibers before the action of enzyme hydrolysis is considered to be advantageous in this aspect. Due to removal of lignin by ozone pre-treatment, the jute fibers are expected to have less strength and more open structure. In this way, even a less concentration of cellulase enzyme or less hydrolysis time is likely to provide extensively entangled networks, higher strength and higher aspect ratio of the cellulose elementary fibrils. Cellulases are a group of multi component enzyme systems produced by microorganisms that help in the degradation of cellulose. The filamentous fungus Trichodermareesei is one of the most efficient producers of extra cellular cellulase enzyme (Nakayama and Imai 2013). There are further two sub-groups of cellulase that affect crystalline and amorphous regions of cellulose separately. Cellobiohydrolase attacks the crystalline structure of cellulose, whereas endogluconase catalyzes the hydrolysis of amorphous cellulose (Satyamurthy et al. 2011).

In present study, jute fibers were pre-treated with ozone gas for removal of lignin. The change in single fiber strength, fiber surface morphology, whiteness, moisture absorbency, etc. of jute fibers due to ozone pre-treatment is discussed in detail. For comparison purpose, chemical pre-treatment of jute fibers was also carried out. In subsequent step, untreated, chemical and ozone pre-treated jute fibers were hydrolyzed by cellulase enzymes for separation of longer jute micro crystals. The influence of non-cellulosic contents on the enzyme hydrolysis and morphology of obtained micro crystals was investigated. Later, 3 wt. % of jute micro crystals were incorporated into poly (lactic acid) (PLA) matrix to prepare composite films by solvent casting. The reinforcement behavior was evaluated from tensile tests, dynamic mechanical analysis, and differential scanning calorimetry.

Cellulose is considered as one of the most abundant biological polymer existing naturally. Utilization of cellulose in composites is very famous nowadays. Natural cellulosic fibers are hydrophilic in nature and not uniform along the length. In result, these fibers exhibited poor compatibility with polymer matrices. Cellulose can be used in composites due to good specific mechanical properties and low coefficient of thermal expansion. So it becomes necessary to modify the fiber surface for better binding or to disintegrate them for increased surface area to get their maximum mechanical benefit in composites. To derive the elementary units of cellulosic substrates different methods are

being utilized but still much consideration is required for cost effectiveness and environmental protection of the globe already affected to a critical extent.

Many Techniques based on mechanical, chemical and joint chemical-mechanical actions were being utilized for the separation of individual cellulose crystals/fibrils (Krishnamachari et al. 2009; Baheti and Militky 2013). Many important drawbacks like environmental incompatibility and potential degradation of the cellulose are associated with chemical method of fiber disintegration like strong acid hydrolysis (Klemm et al. 2006). Whereas the main hindrance of high energy consumption is associated with mechanical processes for fiber disintegration (Prasad et al. 2005; Krishnamachari et al. 2009; Baheti and Militky 2013). The cost efficient cellulose fiber disintegration or isolation without severe degradation is still not very easy. Scientists are seeking for some environment friendly and relatively less costly methods for fiber treatment/disintegration to micro/nano scale.

Ozone gas is an advanced oxidizing agent having a powerful oxidation potential of 2.07 eV (Sargunamani and Selvakumar 2006). This gas has been used for the oxidation of cellulose to improve the functionality of fluoromonomer. The combination of ozone and fluorocarbon treatments on cotton can increase the contact angle due to higher efficiency of the water repellent polymer on the surface of the ozone-gas treated fibers (Gashti et al. 2013). Ozone gas treatment has the great potential of savings the precious utilities of our daily life like time, energy and water. This treatment also reduces the hazardous impact on environment, especially chemical oxygen demand (COD) values, of the processes (Eren and Anis 2009).

Besides the surface treatments for the oxidation of cellulose, many other surface treatments including physical, chemical, physicochemical and biological methods are being tried for other purposes applicable on natural as well as synthetic fibers (Gashti et al. 2011). For example, atmospheric air-plasma has been tried on polyester fiber to improve the performance of nano-emulsion silicone. This pretreatment modifies the surface of polyester fibers and increases the reactivity of substrate toward nano-emulsion silicone resulting in the decreased moisture absorption due to uniform coating of the silicone emulsion on the surface of fibers (Parvinzadeh and Ebrahimi 2011). Thin film plasma functionalization of polyethylene terephthalate has been suggested to induce Bone-like hydroxyapatite Nano crystals for the its utilization in the field of tissue engineering (Parvinzadeh Gashti et al. 2014).

Corona discharge ionization is another physical surface treatment for polyester to be anionized which will have an increased reactivity of the fibers towards cationic dyes (Parvinzadeh Gashti et al. 2015).

Ozone gas treatment has the great potential of savings the precious utilities of our daily life like time, energy and water. This treatment also reduces the hazardous impact on environment, especially chemical oxygen demand (COD) values of the processes (Eren and Anis 2009).

Ozone treatment is a workable source for some of the treatments in different areas such as pretreatment of waste water before disposal to the environment or treatment of waste water for reusing in the processes (Tzitzi et al. 1994; Lopez et al. 1999). Many scientists have reported their work related to ozone gas utilization for different treatments of textile fibers i.e., cotton (Prabaharan and Rao 2001; Perincek et al. 2007), polyester (Eren and Anis 2009; Eren et al. 2012), wool and angora rabbit hair (Perincek et al. 2008), nylon (Lee et al. 2006), poly lactic acid (Eren et al. 2011), and silk (Sargunamani and Selvakumar 2006). Researchers are trying for the optimization of cotton fabrics bleaching parameters like water content in the cotton woven fabric, pH and the temperature using Ozone gas (Prabaharan and Rao 2001; Perincek et al. 2007). It is also being tried for the multiple reuse of water bath for bleaching of cotton fabrics and in the field of drinking water for color and odor elimination (Lopez et al. 1999; Arooj et al. 2014).

As Ozone gas is used in water treatment and fabric finishing processes, etc., it is interesting to use this gas to treat/oxidize the cellulosic fibers. Keeping in view this idea the present study was designed to explore the possibility of using ozone for the advanced oxidation of jute fiber. The aim of this study was to investigate low cost and energy efficient fiber treatment method with low environmental impact. This oxidized jute may then be utilized for different applications such as medical field or for the production of cellulose Nano fibrils or Micro/Nano crystals.

Ozone gas is an irritating gas with pale blue color. It is heavier than air and it is produced using an Ozone generator in which dry air or oxygen is passed through a very strong electric field which splits the diatomic oxygen molecule (O_2) into two highly excited oxygen atoms (O^-) under corona discharge principle. By combining these unstable oxygen atoms with other oxygen molecules, as illustrated in figure 5, Ozone gas is produced (Manning et al. 2002).

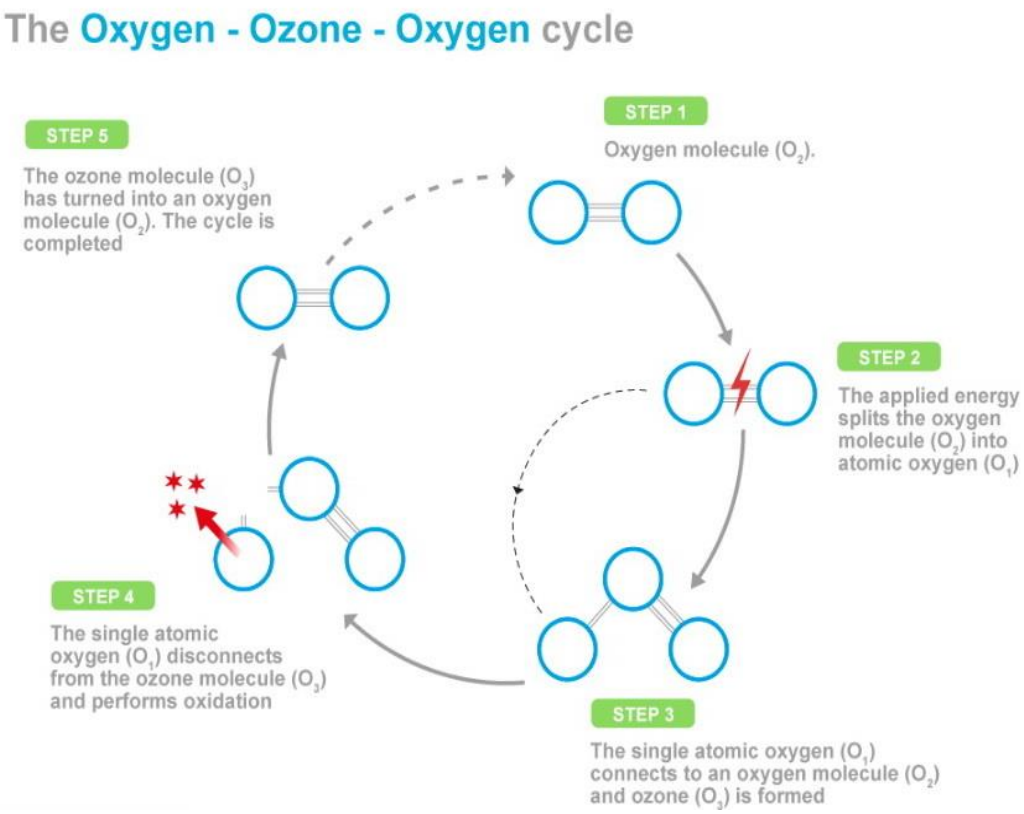

Figure 5. Oxygen-Ozone-Oxygen Cycle

CHAPTER 2

AIMS AND OBJECTIVES

The objectives of the study are

2.1 Extraction and characterization of jute micro/nano particles

The main objective of the work is to obtain jute based cellulose micro/nano particles on large scale quantity from waste jute fibers using environment friendly method of extraction. The enzymatic hydrolysis method was utilized for the extraction of cellulose particles from oxidized jute. The fibers used for the enzymatic hydrolysis were pretreated with Ozone gas for the environment friendly oxidation. These oxidized fibers were then used as a substrate for the enzymatic hydrolysis which is also not a hazardous method for environment.

In this work, enzymatic hydrolysis of untreated, chemically pretreated and the jute fibers pretreated by Ozone gas was carried out to check the effect of pretreatment on the hydrolysis process as well as on the quality of the obtained microcrystals.

Particle size distribution of untreated jute micro crystals (UTJMC), chemical treated jute micro crystals (CTJMC) and ozone treated jute micro crystals (OTJMC) obtained after enzyme hydrolysis was studied on Malvern zetasizer nano series. Deionized water was used as dispersion medium for the particles. It was ultrasonicated before characterization. In addition, morphology of enzyme hydrolyzed UTJMC, CTJMC and OTJMC was observed on scanning electron microscope (SEM).

For Ozone pretreatment, three parameters affecting the oxidation of jute fibers by ozonation i.e. oxygen flow rate, ozonation power and time of treatment were also optimized before enzymatic hydrolysis using Box-Behnken design and response surface modeling was done in order to get the optimum level of deterioration in fiber tenacity and the weight loss.

2.2 Reinforcement of biopolymer by cellulose particles.

The obtained enzymatically hydrolyzed cellulose particles were then incorporated into a biodegradable polymer matrix as reinforcement. Poly lactic acid (PLA) biopolymer was used as a matrix for preparation of composite films which can be used in the applications of biodegradable food packaging, agriculture mulch covers, etc. The incorporation of JMC is expected to improve the mechanical and thermal properties of semi-crystalline polymeric films. The improvements in mechanical properties were investigated from the morphology and crystallization behavior of composite films using differential scanning calorimetry, tensile tests, dynamic mechanical analysis tests etc. In order to have the basic understanding of the stiffening, strengthening and toughening properties of JMC in polymeric matrix, the critical evaluation of experimental results with theoretical models is also performed. The popular theories of composites like rule of mixture, Halpin-Tsai, Cox-Krenchel and percolation are employed for validation of obtained results. In the end, a prediction model was developed using generalized rule of mixture to predict the system property corresponding to volume fraction of reinforcement along with interaction effect of volume fractions of reinforcement (JMC) and matrix i.e. PLA.

CHAPTER 3

OVERVIEW OF THE CURRENT STATE OF THE PROBLEM

3.1 Extraction of cellulose Micro/Nanostructures

Isolation, characterization, and search for applications of novel forms of cellulose (i.e. crystallites, nano crystals, whiskers and nano fibrils) are generating much activity these days (Klemm et al. 2006; Khalil et al. 2012). Such isolated cellulosic materials with one dimension in the nanometer range are referred to generically as nanocelluloses. Novel methods for their production range from top-down methods involving enzymatic, chemical, physical methodologies (Fig. 6) to the bottom-up production from glucose by bacteria. Depending on the source and extraction method, the size and shape of the nanocellulose structures are different. In a unique manner, these nanocelluloses combine important cellulose properties such as hydrophilicity, broad chemical-modification capacity, and the formation of versatile semi crystalline fiber morphologies due to the large surface area of these materials. On the basis of their dimensions, functions, and preparation methods, nanocelluloses are classified in three main subcategories as nanocrystalline cellulose (NCC), nanofibrillated cellulose (NFC) and bacterial nanocellulose (BNC) (Klemm et al. 2006).

The NFC is composed of more or less individualized cellulose nanofibrils, presenting lateral dimensions in the order of 10 to 100 nm, and length generally in the micrometer scale, and consisting of alternating crystalline and amorphous domains. The micro fibrils have a high aspect ratio and exhibit gel-like characteristics in water, with pseudo plastic and thixotropic properties. The NFC fibers are obtained by a simple mechanical shearing disintegration process. The process for isolating NFC consists of the disintegration of cellulose fibers along their long axis (Klemm et al. 2006).

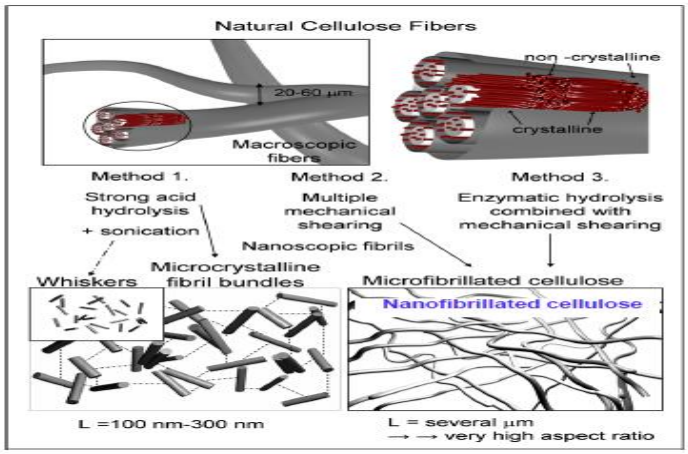

Figure 6. Types of cellulose nanostructures(Abraham et al. 2011)

The NCC also known as whiskers, consist of rod like cellulose crystals with widths and lengths of 5–70 nm and between 100 nm and several micrometers, respectively. They are generated by the removal of amorphous sections of a purified cellulose source by acid hydrolysis, often followed by ultrasonic treatment. Although similar in size to NFC, they have very limited flexibility, as they do not contain amorphous regions but instead exhibit elongated crystalline rod like shapes (Klemm et al. 2006).

The BNC also called bacterial cellulose, microbial cellulose, or bio cellulose is formed by aerobic bacteria, such as acetic acid bacteria of the genus Gluconacetobacter, as a pure component of their biofilms. These bacteria are wide-spread in nature where the fermentation of sugars and plant carbohydrates takes place. In contrast to NFC and NCC materials isolated from cellulose sources, BNC is formed as a polymer and nanomaterial by biotechnological assembly processes from low-molecular weight carbon sources, such as d-glucose. The bacteria are cultivated in common aqueous nutrient media, and the BNC is excreted as exopolysaccharide at the interface to the air. The resulting form-stable BNC hydrogel is composed of a nanofibrils network of 20–100 nm diameters enclosing up to 99 % water. This BNC proved to be very pure cellulose with a high weight-average molecular weight (Mw), high crystallinity, and good mechanical stability (Klemm et al. 2006).

3.1.1 Mechanically induced destructuring strategy

Multiple mechanical shearing actions applied to cellulosic fibers release more or fewer individual micro fibrils or nanofibrils. Different mechanical treatment procedures have been reported to prepare NFC. They mainly consist of steam explosion, high-pressure homogenization and grinding (Leitner et al. 2007; Satyamurthy et al. 2011; Li et al. 2012).

3.1.1.1 Steam explosion.

It is a thermomechanical process to breakdown the structural components of cellulose. The process is accompanied with heat carried by steam. Steam at high pressure penetrates the lignocellulosic biomass through diffusion. The sudden release of pressure generates shear force which hydrolyze the glycosidic bond and hydrogen bonds between the glucose chains, leading to the formation of nanofibrils (Deepa et al. 2011).

3.1.1.2 Homogenization.

The fibers are passed through a valve at high pressure and exposed to a pressure drop to atmospheric condition when the valve is released resulting in high shear force on the fiber surface (Fig. 7). However, this production route is normally associated with high energy consumption for fiber delamination (Leitner et al. 2007). Extensive clogging of the homogenizer was also found to be a chronic problem. Therefore, different pretreatments have been proposed to facilitate this process, for example, mechanical cutting, acid hydrolysis, enzymatic pretreatment, and the introduction of charged groups through carboxymethylation or 2,2,6,6-tetramethylpiperidine-1-oxyl (TEMPO)-mediated oxidation (Lee et al. 2009).

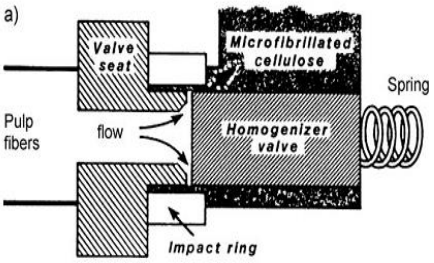

Figure 7. Homogenization (Leitner et al. 2007)

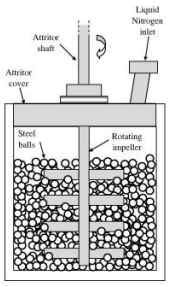

Figure 8. Cryocrushing(Chakraborty et al. 2005)

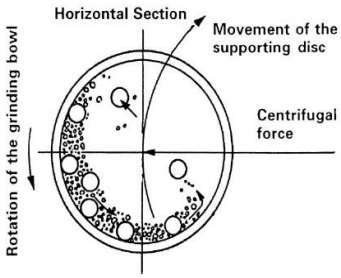

Figure 9. Ball milling (Liimatainen et al. 2011)

3.1.1.3 Cryocrushing.

The fibers are first frozen in liquid nitrogen. The embrittled glassy fibers are then subjected to high speed crushing (Fig. 8). The high shear and impact forces acting on the fibers turn them to powder comprising micro fibrils. The cryocrushed fibers may then be dispersed uniformly into water suspension using a disintegrator (Chakraborty et al. 2005).

3.1.1.4 Ball milling.

Ball milling process is a mechanical process which relies on the energy released at the point of collision between balls as well as on the high grinding energy created by friction of balls on the wall as shown in (Fig. 9). When the mill rotates, balls are picked up by the mill wall and rotate around the wall due to centrifugal force leading to grinding of material due to frictional effect. On the other hand there is also reverse rotation of disc with respect to mill which applies centrifugal force in opposite direction leading to transition of balls on opposite walls of mill giving impact effect (Liimatainen et al. 2011).

The milling machine stresses the maximum number of individual particles in a powder mass to undergo plastic deformation or initiate fracture with a minimum of energy. The motion of the milling medium and the charge varies with respect to the movement and trajectories of individual balls, the mass of balls, degree of energy applied during impact, shear attrition and compression forces on powder particles shown in figure 10 (Suryanarayana 2004). For brittle materials, particle fracture is well described by Griffith theory. According to the theory, stress σ_F, at which crack

propagation leading to catastrophic failure (fracture) occurs in the particle, is approximated by Eq. (1) (Khait et al. 2001)

$$\sigma_F \approx \sqrt{\frac{\gamma E}{c}} \qquad (1)$$

where c is the length of the crack, E is the modulus of elasticity and γ is the surface energy of the milled substance. When stress at the crack tip equals the strength of cohesion between atoms, the crack becomes unstable and propagates, leading to fracture.

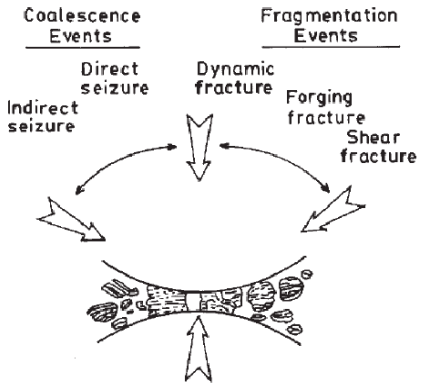

Figure 10. Different forces in ball milling process (Suryanarayana 2004)

3.1.2 Chemically induced destructuring strategy

Cellulose Nano crystals are generated by the liberation of crystalline regions of the semi crystalline cellulosic fibers by hydrolysis with mineral acids. This chemical process starts with the removal of polysaccharides bound at the fibril surface and is followed by the cleavage and destruction of the more readily accessible amorphous regions to liberate rod like crystalline cellulose sections (Brito et al. 2012). The hydronium ions penetrate the cellulosic material in the amorphous domains, promoting the hydrolytic cleavage of the glycosidic bonds and releasing individual crystallites (Liu et al. 2010).When the appropriate level of glucose-chain depolymerization has been reached, the acidic mixture is diluted, and the residual acids and impurities are fully removed by repeated centrifugation and extensive dialysis. The hydrolysis is followed by a mechanical process, typically sonication, which disperses the Nano crystals as a uniform stable suspension. The structure, properties, and phase-separation behavior of cellulose-nanocrystal suspensions are strongly dependent on the type of mineral acid used and its concentration, the hydrolysis temperature and time, and the intensity of the

ultrasonic irradiation (Brito et al. 2012).Different strong acids have been shown to successfully degrade cellulose fibers, but hydrochloric and sulfuric acids have been extensively used. However, phosphoric, hydrobromic and nitric acids have also been reported for the preparation of crystalline cellulosic nanoparticles (Brito et al. 2012). The other processes allowing the release of crystalline domains from cellulosic fibers have also been reported, including enzymatic hydrolysis treatment (Filson et al. 2009), TEMPO oxidation (Habibi et al. 2006), hydrolysis with gaseous acid (Lu and Hsieh 2010), and treatment with ionic liquids (Man et al. 2011).

3.2 Hornification of cellulose micro/nanofibrils

The issue of the redispersion of micro/nanocellulose after drying is difficult, as irreversible aggregation of the fibrils occurs in a process known as "hornification", which results in a material with ivory-like properties that can neither be used in rheological applications nor dispersed for composite applications (Diniz et al. 2004). The main strategy to prevent hornification has been the introduction of a steric barrier or electrostatic groups to block cooperative hydrogen bonding of the cellulose chains (Köhnke et al. 2010). Among the most useful additives are polyhydroxy-functionalized admixtures, particularly carbohydrates or carbohydrate related compounds, such as glycosides, carbohydrate gums, cellulose derivatives (e.g., CMC), starches, oligosaccharides, seaweed extracts, and glycol compounds (Köhnke et al. 2010).

3.3 Applications in biodegradable composites

The replacement of long cellulosic fibers by cellulosic material of smaller axial ratios is an interesting option for composite preparation. With their better dispersibility and their lower susceptibility to bulk moisture absorption, a theoretical elastic modulus of 138 GPa (comparable to that of steel), and a large surface area of several hundreds of square meters per gram (Klemm et al. 2006; Khalil et al. 2012), cellulose micro/nanofibrils are more efficient filler candidates. The small dimensions of cellulose micro/nanofibrils enable direct contact between cellulose and matrix polymers, allowing for a large contact surface and thus excellent adhesion. Favier et al. (Favier et al. 1995)were the first to demonstrate the reinforcing properties of cellulose Nano crystals. They prepared PBA latex composite which showed a significant improvement in the matrix modulus in the rubbery state. Following this advance, the incorporation of cellulose nanostructures from different sources into composite materials with enhanced

properties has been investigated thoroughly and summarized in several review articles (Habibi et al. 2010). The cellulose nanostructures have been incorporated into a wide range of polymer matrices, including polysiloxanes (Grunert and Winter 2000), polysulfonate (Oksman et al. 2006b), poly(caprolactone) (Morin and Dufresne 2002), styrene butyl acrylate latex (Paillet and Dufresne 2001), poly(oxyethylene) (Samir et al. 2004), poly(styrene-co-butylacrylate) (Favier et al. 1995), cellulose acetate butyrate (Petersson et al. 2009), carboxymethyl cellulose (Choi and Simonsen 2006), poly(vinyl alcohol) (Chauve et al. 2005), poly(vinyl acetate) (de Menezes et al. 2009), epoxides (Tang and Weder 2010), polyethylene (Chazeau et al. 1999), polypropylene (Marcovich et al. 2006), poly(vinyl chloride) (Cao et al. 2009), polyurethane (ORTS et al. 2004), and water borne polyurethane (Wang et al. 2006). Their incorporation into biopolymers, such as starch-based polymers (Grunert and Winter 2002), soy protein (Siqueira et al. 2010), chitosan (Azeredo et al. 2010)or poly(lactic acid) (Oksman et al. 2006a), poly (hydroxyoctanoate) (Noishiki et al. 2002), and polyhydroxybutyrates (Angles and Dufresne 2000) have also been reported.

Apart from applications of cellulose nanofibrils in composites, their use in health care areas are also promising due to their high strength and stiffness combined with low weight, biocompatibility and renewability (Ohkawa et al. 2009). Cellulose nanofibrils can also be used as a rheology modifier in foods, paints, cosmetics and pharmaceuticals (Chen et al. 2013). In cosmetics, nanocellulose is suitable as an additive in skin-cleansing cloths and as part of disposal diapers, sanitary napkins, and incontinence pads (Fathi-Azarbayjani et al. 2010).

3.4 Investigation of mechanical properties of composites

The important properties which contribute to the mechanical properties of composites are interaction between matrix and reinforcement, matrix crystallinity, trans crystallization phenomenon and moisture uptake (Jonoobi et al. 2011). The increase in matrix crystallinity due to addition of cellulose nanostructures is studied by Dufresne (Dufresne 2013). They reported an increase in the crystallinity of their plasticized starch matrix as the whisker content was increased. Trans crystallization is the phenomenon whereby a highly oriented layer of a semi crystalline polymer forms at the matrix/filler interface (Dufresne 2013). Such layers only develop under specific conditions and affect the quality of interactions between the matrix components. Dufresne et al. (Dufresne 2013)invoked trans crystallization of PHA latex by cellulose whisker surfaces to explain

the enhanced performance of the composite. The quality of cellulose-matrix adhesion was found to diminish especially in case of hydrophobic matrices due to moisture on the surfaces of hydrophilic cellulose reinforcements (Dhakal et al. 2007).

In addition, the effectiveness of reinforcement is often addressed by percolation theory, which can predict long-range connectivity in the matrix during film formation (Celzard et al. 2009). It was reported from previous studies that percolated network of nanofibrils could slow down the propagation of cracks during the fracture and consequently improve the mechanical properties of composites (Qua et al. 2009). This extended network is presumably generated through hydrogen-bond formation between the cellulose Nano crystals, whose packing structure depends on the distribution and orientation of the rods as well as their aspect ratios. In principle, the higher the aspect ratio, the lower the percolation threshold, which defines the critical value at which continuous connectivity between fillers, first arises.

3.5 Validation of mechanical models

In order to explore the reinforcement potentials of nanofibrils in matrix, the comparison of obtained experimental results with available mechanical models is of great interest (Li et al. 2009). The experimental results of initial modulus obtained from tensile testing are ultimately compared with predicted modulus obtained from theoretical models of rule of mixture, Halpin Tsai and Cox Krenchel which are based on filler-matrix interactions. However it was necessary to consider also the filler-filler interactions due to tendency of cellulose nanofibrilsto generate a percolated network of nanofibrils via hydrogen bonding between adjacent nanofibrils.

3.5.1 The rule of mixtures model

It is used to predict the modulus of composite as combination of filler modulus and matrix modulus by taking volume weighted average of the individual phase properties as given in Eq. (2)

$$E = X_r E_r + (1 - X_r) E_m \qquad (2)$$

where E is composite modulus; $E_r$is reinforcement modulus; E_m is matrix modulus and X_r is volume fraction of reinforcement. The volume fractions of nanoreinforcements can be calculated using following Eq. (3)

$$X_r = \frac{w_r / \rho_r}{w_r / \rho_r + (1 - w_r) / \rho_m} \quad (3)$$

Where W_r is weight % of reinforcements, ρ_r is density of the reinforcement and ρ_m is density of the matrix polymer.

3.5.2 The Halpin-Tsai model

It is used to predict the modulus of composite material as a function of aspect ratio of filler assuming they are linearly oriented in the matrix. The Halpin-Tsai theory is usually used for aligned fiber composites (Agarwal et al. 2006), but it has also been used before to predict the modulus of nanocomposites (Helbert et al. 1996; Wu et al. 2004; Petersson and Oksman 2006). The Halpin–Tsai Eq. (4) was chosen since it demanded the least amount of assumptions about dispersion of fillers in matrix.

$$E = E_m (1 + \xi \eta X_r) / 1 - \eta X_r \quad (4)$$

The shape parameter of reinforcement η was calculated from the Eq. (5)

$$\eta = (E_r / E_m - 1) / (E_r / E_m + \xi) \quad (5)$$

where $\xi = 2 \times Length / Diameter$

3.5.3 The Cox-Krenchel model

Since Halpin-Tsai theory does not consider orientation of fillers into the matrix, Cox-Krenchel theory (Krenchel 1963) is used to predict the modulus based on random orientation of fillers in matrix. The similar Eq. (6) was used before for carbon nanotube composites (Gómez-del Río et al. 2010).

$$E = E_m (1 - X_r) + \eta_l \eta_o E_r X_r \quad (6)$$

where η_l is the length correction factor, η_o is orientation factor and the assumed value is 3/8 (Krenchel 1963) when the fillers are oriented randomly in plane. The η_l was calculated from the Eq. (7)

$$\eta_l = 1 - (\tan h(\beta l / 2) / (\beta l / 2)) \quad (7)$$
$$\beta = 1 / r \left(E_m / 2E_r \ln(R / r)\right)^{1/2}$$

where l is the filler length and r is the radius.

$$R/r = \sqrt{K_r / X_r} \tag{8}$$

where K_r depends on the geometrical packing of fillers, and it is chosen to be π/4, considering the square packing.

3.5.4 The percolation theory model

The previous studies have indicated that not only the filler-matrix interaction but also the filler-filler interactions are important when considering the reinforcing capability of cellulose nanofibrils (Favier et al. 1995; Saïd Azizi Samir et al. 2004). As jute nanofibrils are also hydrophilic in nature, they have strong tendency to generate a percolated network via hydrogen bonding between adjacent nanofibrils. In order to consider the filler-filler interactions, the percolation theory was used to predict the modulus of composite material using Eq. (9) (Sorrentino et al. 2011)

$$E = \left((1-2\psi + X_r\psi)E_m E_r + (1-X_r)\psi E_r^2\right)/\left((1-X_r)E_r + (X_r-\psi)E_m\right) \tag{9}$$

where ψ is a percolation volume fraction and given by Eq. (10)

$$\psi = X_r\left((X_r - X_c)/(1-X_c)\right)^{0.4} \tag{10}$$

where X_c is a percolation threshold given in Eq. (11) (Das et al. 2011) when fillers are strongly interconnected by a 3D network

$$X_c = 0.7/(L/d) \tag{11}$$

3.6 Generalized Rule of Mixtures

The Simple Rule of Mixtures is often utilized in the prediction of various material properties such as modulus, electrical, thermal conductivity etc. However, in most cases, the prediction models as shown above underperform and don't accurately predict the system properties due to the fact that there exists various interactions in the system (Pan et al. 2000).

(Nielsen 1978) showed that the system property can be calculated by a generalized rule of mixtures as shown below:

$$E_s = E_1X_1 + E_2X_2 + IX_1X_2 \tag{12}$$

$$E_s = E_1X_1 + E_2(1 - X_1) + IX_1(1 - X_1) \tag{13}$$

where E_s is the system property and E_n is the properties of the two constituent components.X_n is the volume fraction and $X_1 + X_2 = 1$ whereas I is the coefficient

representing the intensity of the interactions in a two component system. The significance of *I* can be explained as follows:

1. $I > 0$ which implies that the interaction between the two components enhances the overall system property.
2. $I < 0$ implies that the interaction reduces the system property.
3. $I = 0$ shows that the interactions do not exist and the equation reduces to the simple Rule of Mixtures.

Eq. (13) can be simplified in the form of

$$Y = A + BX + CX^2 \tag{14}$$

where $A = E_2$;

$B = (E_1 - E_2 + I)$ and

$C = (-I)$

CHAPTER 4

METHOD USED AND STUDIED MATERIAL

4.1 Materials

Short waste jute fibers were obtained from Jute mills of South Asia. The fibers were measured to have a density of 1.58 g/cm3, modulus of 20 GPa, tensile strength of 440 MPa and elongation at break of 3 %. PLA was purchased from Nature Works LLC, USA through local supplier Resinex, Czech Republic. The PLA had a density of 1.25 g/cm^3 and the average molecular weight (Mw) of 200,000. The chloroform, which was used as solvent, purchased from Thermofisher Czech Republic. The TEXAZYM AP cellulase enzyme was provided by the company INOTEX in Czech Republic. The optimal pH in range of 4.5-5.5 and temperature in range of 50-60 °C was selected for enzyme activity.

In this work, Ozone Generator with identification name plate as "TRIOTECH GO 5LAB-K, made in Czech Republic" was used and the power setting was kept constant at 50% for all treated samples. An Oxygen Concentrator "Krober MEDIZINTECHNIK, Germany" with a controllable output Oxygen flow rate was used as an oxygen supplier/feeder to the Ozone Generator.

4.2 Ozone Treatment of Jute fiber

The substrate fibers of Jute waste were placed in a humid ozonized atmosphere for different times. The outlet gases of the system were analyzed and measured the mass flow of ozone as 4.5 mg/L. The output concentrated oxygen flow rate from Oxygen Concentrator was adjusted at 5.0 L/minute and this oxygen was being fed to the Ozone Generator. As humid atmosphere is more effective for the reaction of Ozone with lignocellulosic material, so this treatment was done in humid atmosphere (Saha et al. 2010).

As the Oxygen provided by Oxygen Concentrator and Ozone produced by Ozone Generator in series are dry in nature. So a humidification system was developed in the way of Ozone to the jute samples. Due to this system the dry nature of Ozone was changed to humid one as shown in figure 11. The jute samples were removed from the

container after each one hour. The ozone treated fibers were immediately pounded in nonionic surfactant solution for one hour to remove the residual ozone. A concentration of 1 g/L of nonionic surfactant in distilled water was used for this solution. After that distilled water was used for rinsing the treated fibers and then dried in an oven at 105 °C for 3 hours. So according to plan there were six samples as shown in table 4.

Table 4. Ozone treatment plan of jute fiber

Jute Fiber	Sample number	Ozone treatment Time (hours)
Untreated	01	0
Treated With O_3 Gas	02	1
	03	2
	04	3
	05	4
	06	5

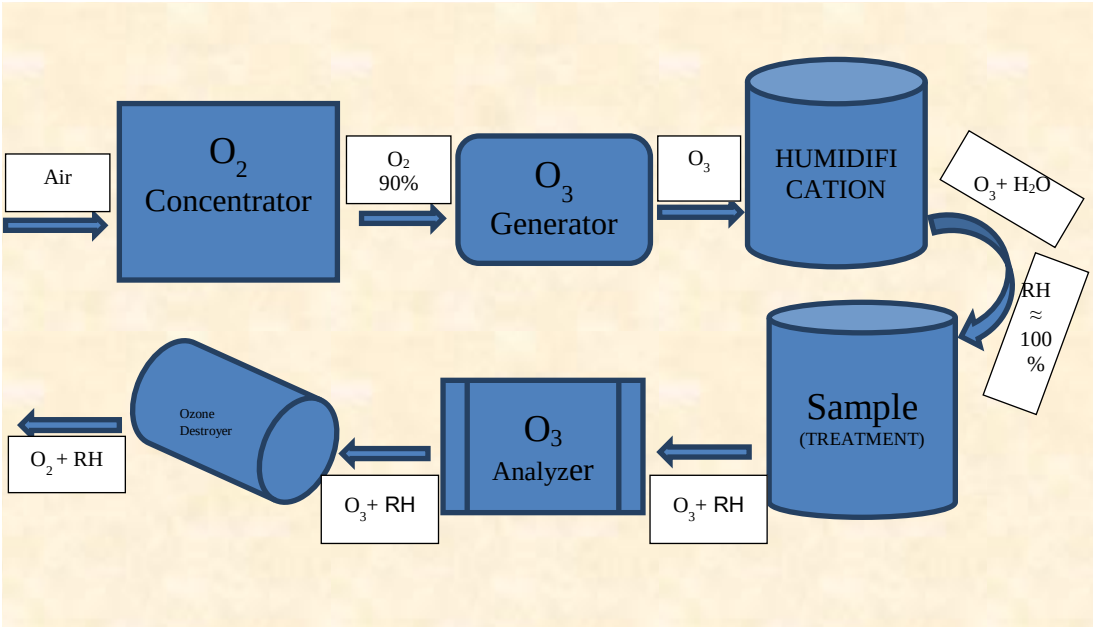

Figure 11.Schematic diagram of the Ozone Treatment Setup.

4.3 Optimization of Ozone Treatment by Response surface methodology:

4.3.1 Objective:

During Ozone treatment of jute fibres for oxidation, different factors were affecting the oxidation phenomenon. These factors include oxygen flow rate from oxygen concentrator, ozonation power of the ozone generator and time for ozone treatment. All of those factors affect the resultant oxidized fibres. Tenacity of the treated jute fibre and the resultant weight loss of the substrate were selected for measuring the effect of ozone treatment. To get the optimum settings for those parameters, response surface methodology was utilized to get some optimum value of treatment.

The objective of present study is to optimize these three parameters of ozone treatment for oxidation i.e. oxygen flow rate (OX), ozonation power of the generator (OP) and ozone treatment time (OT) with use of Box-Behnken design and response surface methodology.

In recent years, response surface methodology has been widely used as an optimization tool in various kinds of industrial process (Lundstedt et al. 1998).Conventionally, the classical method (one-at-a-time) provides for changing one independent variable while maintaining all others at a fixed level, which is extremely time-consuming and expensive for a large number of variables. The major disadvantage is the lack of inclusion of the interactive effects among variables. However, it could not lead to real optima in many cases. Consequently, procedures for optimization of factors by multivariate techniques have been encouraged, as they are faster, more economical, and effective and allow more than one variable to be optimized simultaneously (Aslan and Cebeci 2007). Owing to its powerful efficiency, response surface methodology is now being routinely used for optimization of widely various systems. Among the various response surface approaches, it was found that three common multilevel designs such as central composite design, Box–Behnken design, and Doehlert matrix have been frequently utilized for the final optimization of desired processes (Aslan and Cebeci 2007).

Box–Behnken design is a spherical, rotatable, or nearly rotatable second-order design. It is based on three-level incomplete factorial design, which consists of the center point and middle points of the edges from a cube. Their primary advantage is in

addressing the issue of where the experimental boundaries should be, and in particular to avoid treatment combinations that are extreme (Aslan and Cebeci 2007).

From the literature and the experience on the ozone treatment, a range of levels were set for the independent variables i.e. factors to be optimized as shown in the table 5. As the tenacity of the fiber going on decreasing trend through the span of oxidation and weight loss of jute fiber goes on increasing with the ozone treatment. Weight loss of about 7% of the original weight was set as a target not to affect the cellulosic portion of the fiber. As the objective of oxidation in this work was just to remove maximum non-cellulosic content of jute and to save the cellulosic content for further process of hydrolysis to get micro crystals.

Table 5. Values and levels of independent variables

Independent variables	Symbol	Levels		
		Low (-1)	Centre (0)	High (+1)
Oxygen Flow Rate (L/min)	OX	4	5	6
Ozone Generator Power (%)	OP	25	50	75
Ozonation Time (hours)	OT	2	4	6

From these upper, middle and lower values of the independent variables, 15 runs of different settings were designed with the help of software "design expert". After the design of experiment the responses i.e. Loss in tenacity and the weight loss of the fibre after oxidation Ozone treatment were obtained and tabulated in the table 6 alongwith their settings described in the runs.

The mathematical relationship between the three independent variables and response was approximated by the second order polynomial given in Eq. (15) and Eq. (16)

$$\textit{Tenacity (cN/Tex)} = \beta_0 + \beta_1 OX + \beta_2 OP + \beta_3 OT + \beta_{12} OX \times OP + \beta_{13} OX \times OT + \beta_{23} OP \times OT + \beta_{11} OX^2 + \beta_{22} OP^2 + \beta_{33} OT^2 \quad (15)$$

$$\textit{Weight Loss (\%)} = \mu_0 + \mu_1 OX + \mu_2 OP + \mu_3 OT + \mu_{12} OX \times OP + \mu_{13} OX \times OT + \mu_{23} OP \times OT + \mu_{11} OX^2 + \mu_{22} OP^2 + \mu_{33} OT^2 \quad (16)$$

where β_0 and $\mu_0$are model constants; β_1, β_2, β_3 and μ_1,μ_2,μ_3 are linear coefficients; β_{12}, β_{13}, β_{23} and μ_{12}, μ_{13}, $\mu_{23}$are cross product coefficients and β_{11}, β_{22}, β_{33} and μ_{11},μ_{22},$\mu_{33}$are the quadratic coefficients. The coefficients, i.e. the main effect (β_i) (μ_i) and two factor interactions (β_{ij}) (μ_{ij}) have been estimated from the experimental results using the mathematical software package DESIGN EXPERT.

4.3.2 Construction of model equation

The experimental results obtained for tenacity of jute fibre after ozonation and weight loss percentage in Box-Behnken design (Table 6) were fitted to a full quadratic second order model equation by applying multiple regression analysis using the DESIGN EXPERT software. The model equation representing tenacity and weight loss percentage was expressed as a function of OX, OP and OT for actual values of variables as given in Eq. (17) and Eq. (18) respectively.

Tenacity (cN/Tex) =

$$+56.33458 + 2.05542OX - 0.51338OP - 6.98417OT - 6.60000 \times 10^{-3} OX \times OP + 0.47125OX \times OT + 0.010450OP \times OT - 0.53417OX^2 + 2.75333 \times 10^{-3} OP^2 - 0.024167OT^2 \quad (17)$$

Weight Loss (%) =

$$-12.56917 + 0.060417OX + 0.26427OP + 3.08271OT - 0.019600OX \times OP - 0.27125OX \times OT - 9.50000 \times 10^{-3} OP \times OT + 0.27458OX^2 - 4.92667 \times 10^{-4} OP^2 + 8.64583 \times 10^{-3} OT^2 \quad (18)$$

4.3.3 Specifications of Original (Untreated Jute) Sample

Tenacity	=	44.9 cN/Tex
Elongation at Break	=	3.28%
Weight	=	100%

Table 6. Box-Behnken design of experimental runs with results

Run	**Independent variables in Ozonation**			**Observed Response variables**	
	(OF) Oxygen flow rate (L/min)	(OP) Ozonation power (%)	(OT) Ozone treatment time (hrs)	Tenacity (cN/Tex)	Weight loss (%)
1	6	75	4	8.18	9.2
2	5	75	6	5.15	10.5
3	4	25	4	25.89	3.4
4	6	50	6	6.07	9.98
5	5	75	2	20.78	6.1
6	4	50	6	6.98	9.5
7	4	75	4	12.64	8.78
8	6	50	2	21.90	5.85
9	5	50	4	15.98	6.95
10	5	25	6	13.45	7.95
11	4	50	2	26.58	3.2
12	6	25	4	22.09	5.78
13	5	50	4	16.01	6.8
14	5	25	2	31.17	1.65
15	5	50	4	16.05	6.72

4.3.4 Three dimensional surface plots

Corresponding to the runs of design of experiment and described in table 6, three dimensional surface plots along with the contour diagrams for the responses can be drawn. The trend of the interaction of two independent variables keeping the third at constant level can be elaborated by these shapes.

Figures 12 and 13 depict the effect of ozone power and the rate of oxygen flow on tenacity and weight loss of jute fibre respectively. Keeping the third independent variable i.e. time for ozone treatment at mid-level of design, both the variables have direct effect on the change in tenacity and weight loss.

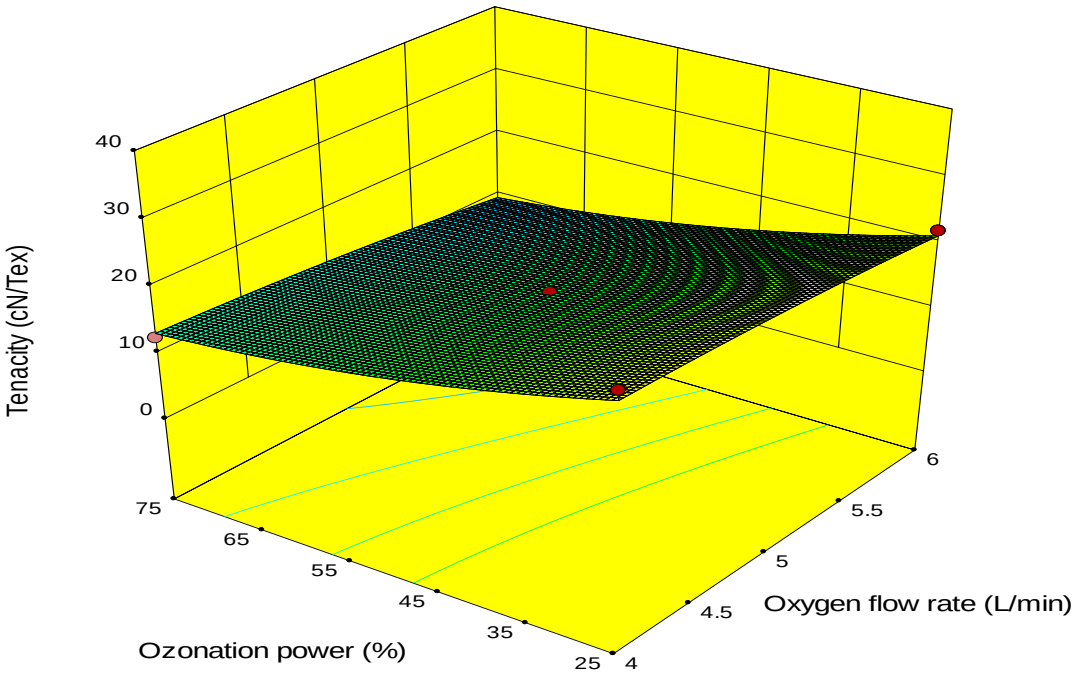

Figure 12. Effect of Ozone power and Oxygen Flow rate on Tenacity of Jute fiber.

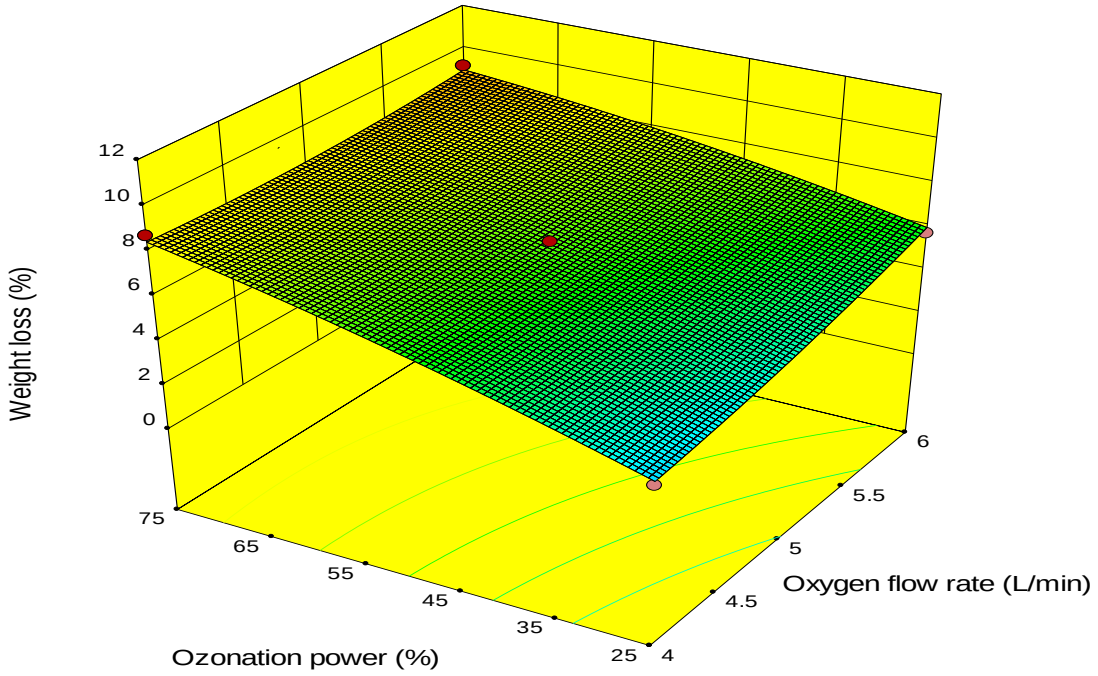

Figure 13. Effect of Ozone power and Oxygen Flow rate on weight loss.

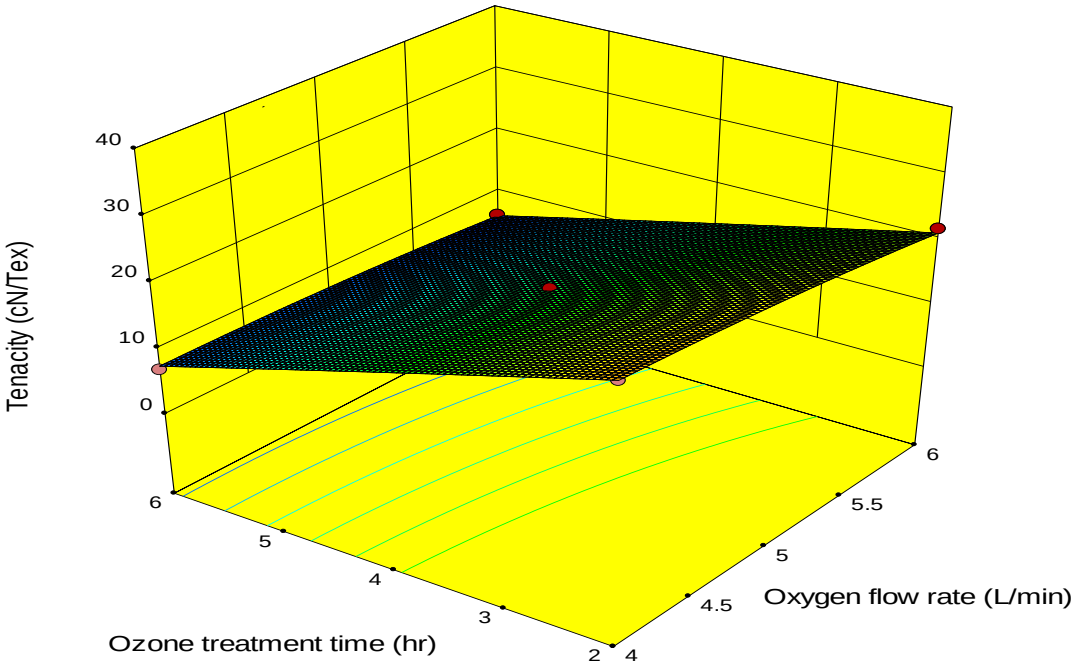

Figure 14. Effect of Ozone Treatment time and Oxygen Flow rate on Tenacity of Jute Fiber.

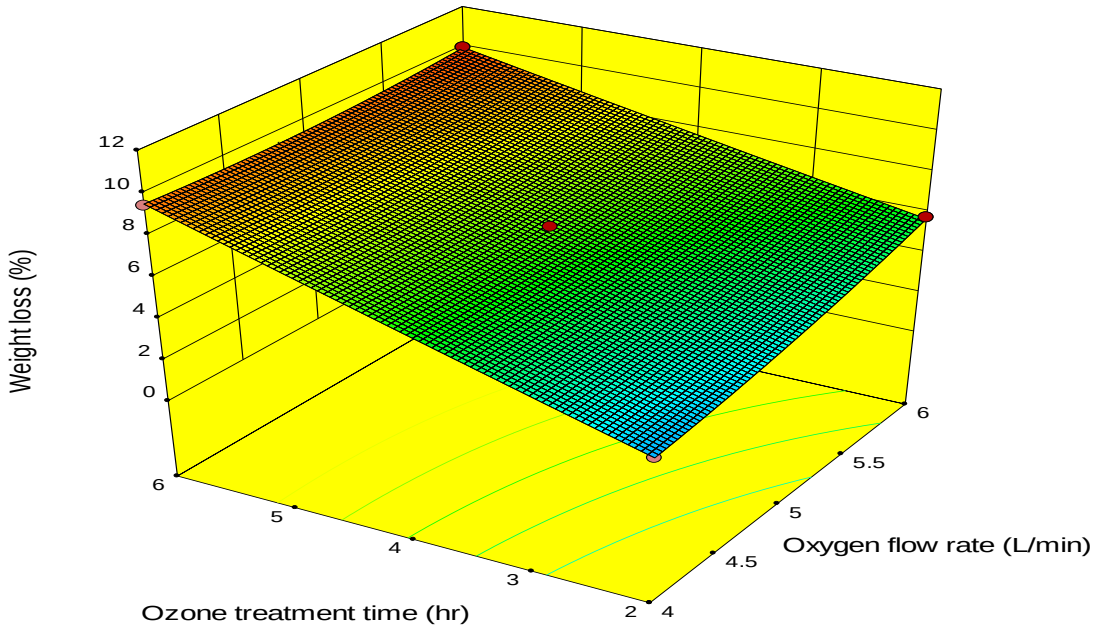

Figure 15. Effect of Ozone Treatment time and Oxygen Flow rate on weight loss.

In figures 14 and 15 relationship of ozonation time and oxygen flow rate is drawn against tenacity and weight loss of jute fibre after oxidation by ozone gas. In this case ozonation power is kept constant at medium level of design i.e. at 50%. The tenacity of the fibre deteriorates with the ozonation time directly and nearly same is the case with the oxygen flow rate from oxygen concentrator. If oxygen is more readily available for the conversion to ozone in the ozone generator, more ozone is being generated giving higher oxidation potential per unit time.

Decrease in tenacity and the weight loss of jute fibre is directly related to the oxidation of the fibre. In figure 16 and 17, ozonation time and the power of ozone generator are plotted against tenacity and weight loss of jute fibre after certain levels of oxidation.

Lignin is a protective layer for the lignocellulosic fibres like jute. First target of oxidation by ozone gas is lignin content in the jute fibre. With the passage of oxidation time, this deterioration effect goes to hemicellulose and then ultimately to cellulose. The responses in this design (tenacity and weight loss) were continually being affected by oxidation process; we have to make some target to get optimum values for response.

As the aim of oxidation was to remove lignin but to a certain limit so that we may not deteriorate the quality of crystal obtained ultimately after enzyme hydrolysis. It is being decided to take the minimum value of tenacity but set target for weight loss was 7%.

4.3.5 Optimised parameters for tenacity and weigth loss after oxidation

Using software of DESIGN EXPERT, independent variable parameters including oxygen flow rate, ozone power and time for ozone treatment was optimized keeping in view minimum tenacity value and target for weight loss of fibers at 7%. Following optimum values were derived from the software after processing the data of design of experiment and the values of responses in the runs designed by the same software.

Oxygen flow rate	=	5.160 Liters per minute
Ozone power of generator	=	50.271% and
Time for ozone treatment	=	4.024 hours

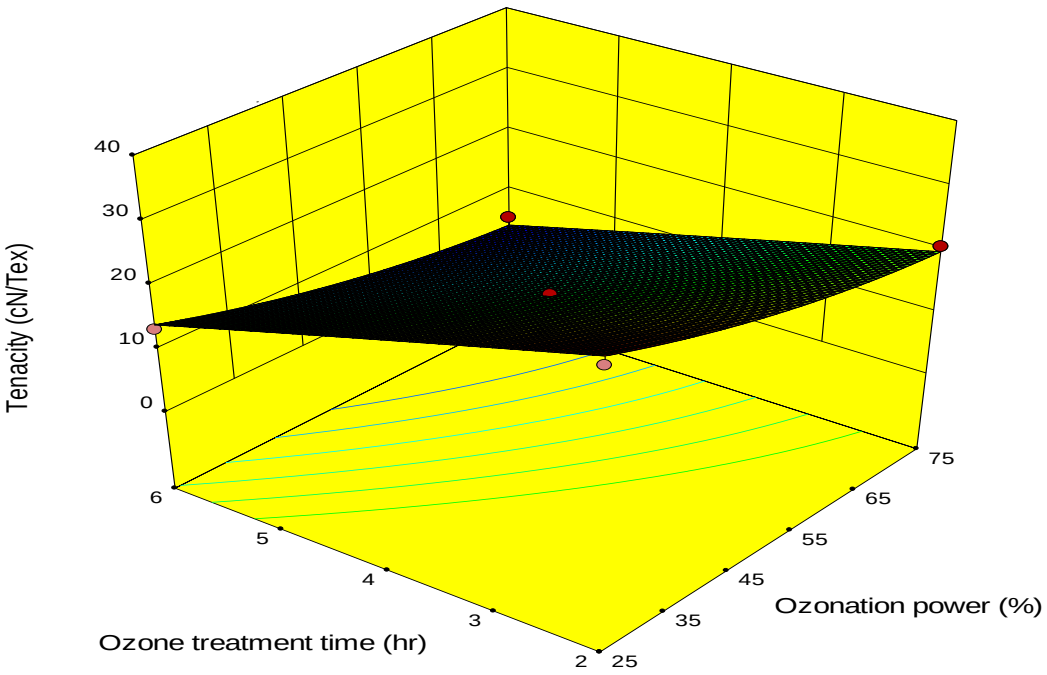

Figure 16. Effect of Ozone Treatment time and Ozone power on Tenacity of Jute fiber.

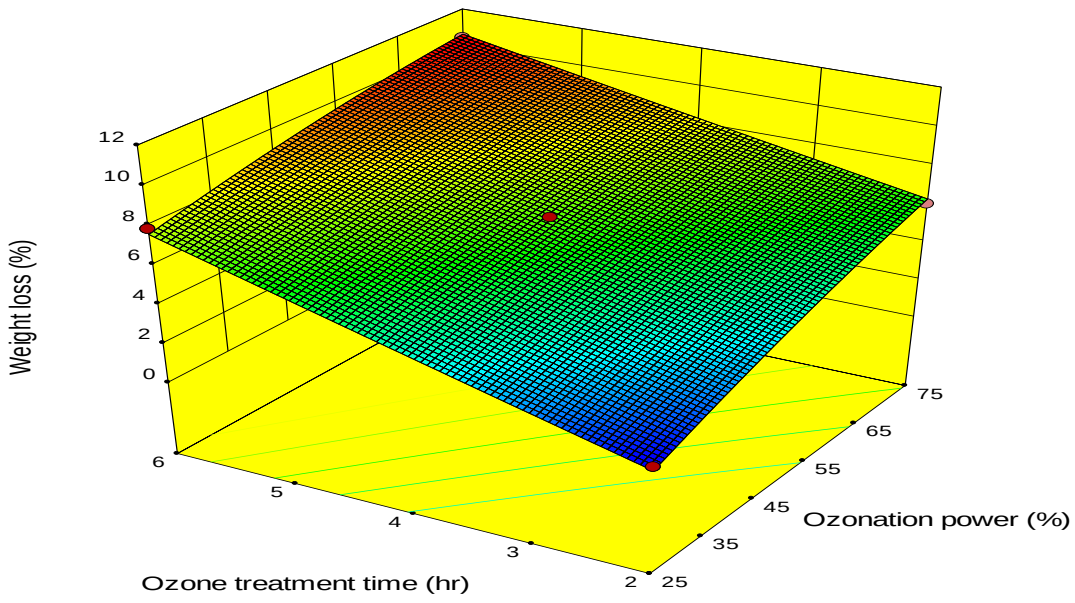

Figure 17. Effect of Ozone Treatment time and Ozone power on weight loss.

4.4 Characterization of Ozonized waste jute fibers

4.4.1 Fiber Topography:

The surface topography of jute fibers (untreated and ozone treated) was observed by scanning electron microscope. An accelerated voltage of 20 kV was selected for SEM images on TS5130-Tescan Scanning Electron Microscope.

4.4.2 FTIR analysis:

Fourier Transform Infrared Spectroscopy (FTIR) analysis was utilized for the quantitative study about the removal of lignin and modification of internal physical microstructure of the jute fibers after ozone treatment. It was done on Nicolet 6700 reflection ATR technique on an adapter with a diamond crystal.

4.4.3 WAXD for evaluation of crystalline structure:

The crystalline structure of the jute substrate before and after the action of Ozone gas, was investigated by the using Wide-angle X-ray Scattering by means of an X'Pert Pro System (PANalytical, Netherlands) with Cu Kα (λ = 0.154 nm) source and operating at 40 kV and 30 mA. Prior to the measurements, the jute fibers were grounded to obtain powder specimens. The diffraction profiles were obtained in the 2θ range 10 – 35° with 0.02° step.

4.4.4 Fiber tensile properties:

VIBRODYNE Lenzing Instruments was used for measuring the tensile properties including fiber Tenacity and Elongation at Break Percentage of untreated and ozone treated jute fibers. A crosshead speed of 10 mm/min, pre-tension of 2000 mg and a gauge length of 10 mm was used for the tensile properties measurement. Average and standard deviation of 50 observed values for each sample were calculated.

4.4.5 Degree of Reflectance and Lightness Value:

Spectraflash600 was being used to measure the degree of reflectance corresponding to the wavelength in the visible light range. L, a & b values were also found out on the same equipment. The change in the shade of the jute samples after Ozone treatment was described by graphical representation of the L (Lightness) values of the samples.

4.4.6 Moisture absorption:

The moisture absorption behavior of untreated and Ozone a treated jute fiber was also assessed by measuring moisture regain percentage values of the samples. For this purpose preconditioned samples in a standard atmospheric conditions (temperature = 20 ± 2°C and relative humidity = 65 ± 4%) for 24 hours were placed in an oven at 105°C for drying up to the point where there was no further loss in mass (Oven Dry mass). Moisture regain percentages of the samples were then calculated using general formula as mass of water present in the material expressed as a percentage of its oven dry mass.

$$\text{Moisture Regain \%} = \frac{Mass\ of\ water\ in\ sample}{Oven\ Dry\ mass\ of\ sample\ to\ constant\ mass}\ x\ 100 \qquad (19)$$

4.4.7 Copper number:

The Copper number is the weight of Copper from Cu^{2+} to Cu^{+} state which is reduced by 100 gm of dry cellulose and is a measure of its inter and intra chain breakdown. It is an expression of the reducing power of degraded celluloses. Oxidation of cellulose can produce ring fission of the glucose residues, resulting in the formation of aldehyde groups at carbon atoms 2 and 3. The copper number was measured using a (CSN 80 0600) standard Czech test method for the determination of the weight of copper in cellulose materials (Maqsood et al. 2016).

CHAPTER 5

SUMMARY OF RESULTS ACHIEVED

5.1 Oxidation of Jute fibers by Ozone

The usage of Ozone gas was increased greatly over the last two decades and have been used for the treatment of ground and industrial wastewaters (Kasprzyk-Hordern et al. 2003). Ozone affects lignin and hemicellulose giving water soluble products without damaging cellulose.

5.1.1 Apparent changes in jute fibers after ozone treatment

All ozonized samples of the jute fibrous waste are displayed in figure 18 and an obvious change in colour relative to the untreated sample is observed.

Figure 18. Apparent change in color of untreated and Ozone treated samples of jute

5.1.2 Lightness Value of jute fibers:

The Lightness values of untreated jute fibers and the fibers after 1-5 hours of ozone treatment were observed. These samples were analyzed at SPECTRAFLASH600

and lightness (L) values of the samples elaborated clearly the bleaching effect of Ozonation (Fig. 19). Corresponding to the results, it is obvious that after one hour of treatment there is significant change in the colour of the fiber. Consequently, it can be seen that with the increase in ozone treatments the colour lightness level of the fiber is also changed, however, after four hours of treatment, there is not marked difference in the L value of the sample. At this stage the shade of the fibers became almost same. For example, the L value of the treated fibers after 4 hours was observed 74.06 in comparison with the L value of 55.52 for untreated jute fibers whereas the value of L for one hour treated fiber was 70.74. The rate of ozone reaction was very rapid during the first hour of treatment as double bonds and other functional groups of chromophores were suddenly slashed by the ozone. After three hours of ozone treatment the brownish shade of jute was faded very slightly.

Results display that with more time of ozone treatment, the degree of lightness was improved as mass transfer efficiency was enhanced by increasing the applied ozone time. In this way more time was available for ozone to react with chromophoric double bonds present in gray jute fibers (Świetlik et al. 2004; Sargunamani and Selvakumar 2006). The lightness of ozonized fiber samples improved with increase in ozone treatment time up to four hours; however, after that there was a very slight improvement in lightness of jute samples but it may have a degrading effect on cellulose. Hence, an ozone treatment of up to four hours was supposed to be optimum time for the acceptable degree of oxidation of cellulose.

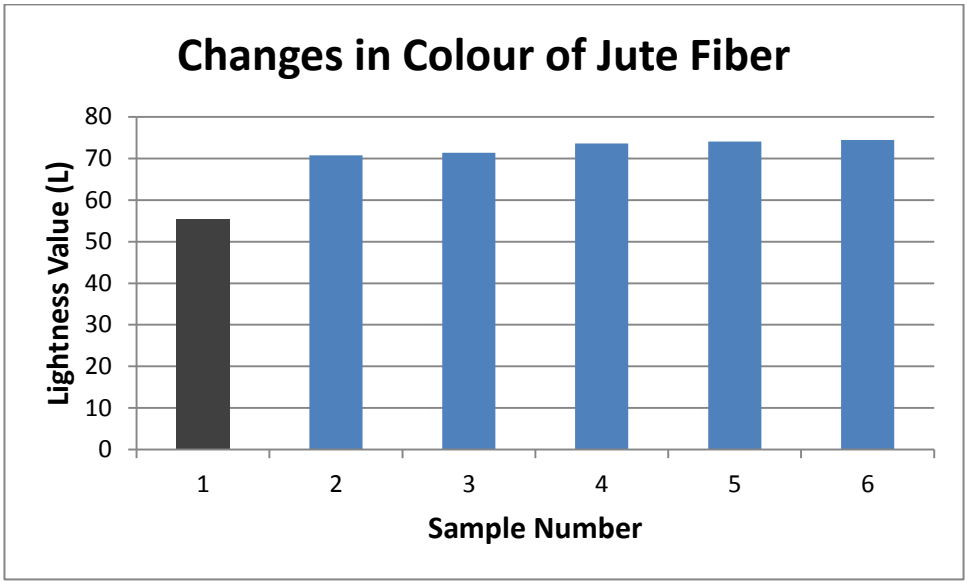

Figure 19. Lightness values of Ozone Treated Jute Fiber (SPECTRAFLASH600)

5.1.3 FOURIER TRANSFORM INFRARED SPECTROSCOPY (FTIR):

Fourier Transform Infrared (FTIR) Spectroscopy results were taken for the untreated and treated Jute samples to check the non-cellulosic contents in the substrate before and after the action of ozone. Functional groups assignments and their respective interactions of Jute fiber can be deduced using FTIR Spectra (Fig. 20). Natural fibrous specific bands and their corresponding bonding interactions have been studied by numerous researchers (Meyabadi and Dadashian 2012; AlMaadeed et al. 2013). There is some variation in the reported bands from one researcher to another; however the difference is not too significant because most natural fibrous materials are made up of celluloses, hemicelluloses and lignin.

Obvious spectral differences in the mid-infrared region (4000-400 cm^{-1}) of jute fiber before and after exposure to ozone gas at different intervals are presented in figure 20. Well-define band at 3341 cm^{-1} in raw jute fiber corresponds to intramolecular bonding of H and OH groups in carbohydrate of cellulose and hemi cellulose. It was decreased to low wave number ~ 3337 cm^{-1} after exposure to ozone gas indicated breaking of breaking of the hydrogen bond between O–H groups of cellulose (Duan and Yu 2015). The peak around 2950 cm^{-1} and 2951 cm^{-1} is specific for C-H stretching vibrations (methyl and methylene group of cellulose and hemi cellulose) in raw biomass were changed to low wave number ~ 2920 cm^{-1} and high wave number ~ 2954 cm^{-1}, respectively. Such changes could be correlated with alteration in organic content of jute fiber (Jabasingh and Nachiyar 2012). The band at 2870 cm^{-1} (CH stretching modes) was disappeared after treatment of jute fiber with ozone for 1, 2, 3 and 4 hours, however, it was observed at 2867 cm^{-1} after 5^{th} hour. Another band at 2852 cm^{-1} in raw biomass was shifted to ~2850 cm^{-1} after treatment.

Bands at 1737 cm^{-1} is attributed to C=O stretching of the carbonyl and acetyl groups in the 4-O-methyl glucano acetyl xylan component of hemicellulose in the raw jute, shifted to low wave number at ~ 1734 cm^{-1}. This decreased in band intensity give evidence of acetylation many ester bonds between jute fiber and ozone (Jabasingh and Nachiyar 2012). It also shows partial removal of hemicelluloses and more cleavage of lignin chains after ozonation treatment (Duan and Yu 2015). So far, two bands at 1594 cm^{-1} and 1504 cm^{-1} represents lignin were disappeared after treatment could be result of improvement in fiber surface by removing lignin (Punyamurthy et al. 2012). Another two peaks at 1537 cm^{-1} (C=C stretching, lignin) and 1424 cm^{-1} (CH_2 bending, cellulose)

were changed to ~ 1539 cm^{-1} and ~ 1428 cm^{-1}, respectively. Peaks at 1647 cm^{-1} (COO^-, pectin) and 1458 cm^{-1} (CH_2 bending, cellulose) was altered to ~ 1644 cm^{-1} and ~ 1455 is attributed to the splitting of lignin aliphatic side chains (Sun et al. 2000).

Peaks at 1370, 1316, 1238, 1157 and 1103 cm^{-1}raw jute fiber samples are due to cellulose related group were changed to variable extent after treatment indicated successful interaction of ozone with jute fiber that may result in removal of impurities from fiber surface. The absorption band at 1316 cm^{-1} can be attributed to the symmetrical deformation of NO_2 in the cellulose azo compound (Islam et al. 2011).

Absorption peaks at 1048 and 897 cm^{-1} are associated with C-O stretching and β-glycosidic linkages of the glucose ring of cellulose were shifted to high wave number (Zhang et al. 2006). These absorptions are consistent with those of a typical cellulose backbone (Sarkar et al. 1948) and showed that the structure of cellulose had not been smashed after the ozonation. It could be summarized that ozone treatments removed most of the lignin and cellulose contents and changed nature of fiber.

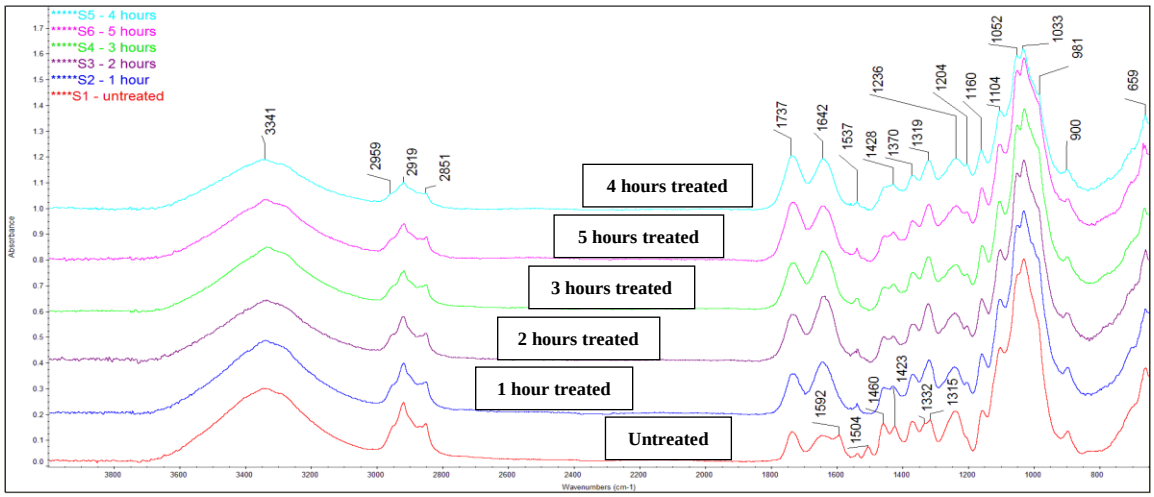

Figure 20. FTIR Spectra of Untreated and Ozone treated Jute samples

5.1.4 Mechanical Properties of Ozone treated Jute Fibers

5.1.4.1 Tenacity:

For the comparative study of the tensile properties of untreated and treated fibers, Standard Test Method for Tensile Strength and Young's Modulus of Fibers (ASTM C1557-14) was followed and the tenacity measured for the untreated jute fiber was

found to be 44.16 cN/Tex. Ozone treated fibers showed declined values of tenacity with the increasing of treatment time (Fig. 22). The treated sample with corresponding time 1, 2, 3, 4 and 5 hours exhibited the value of tenacity as 31.61, 23.12, 19.75, 16.01 and 8.12 cN/Tex respectively. This decrease may be attributed to significant delignification and destruction of cellulosic chains through the ozone treatment (Maqsood et al. 2016).

5.1.4.2 Elongation at Break (%):

The elongation at break examined according to the Standard Test Method for the untreated jute fiber (Saha et al. 2010) and it was observed to be 3.28%. Ozone treated samples showed declined values with the increasing of treatment time as shown in figure 23. The treated samples corresponding to treatment time 1, 2, 3, 4 and 5 hours revealed 2.32, 2.14, 1.89, 1.80 and 1.04 % of Elongation Percentage at Break correspondingly. The elongation at break in these fibers also decreased very much with the increment of treatment time. The fall in elongation at break from 3.28 % to 1.04 % could be correlated to disbanding of amorphous region after ozonation of jute fibers.

Figure 21. Vibrodyne equipment used for tensile properties of Jute fiber.

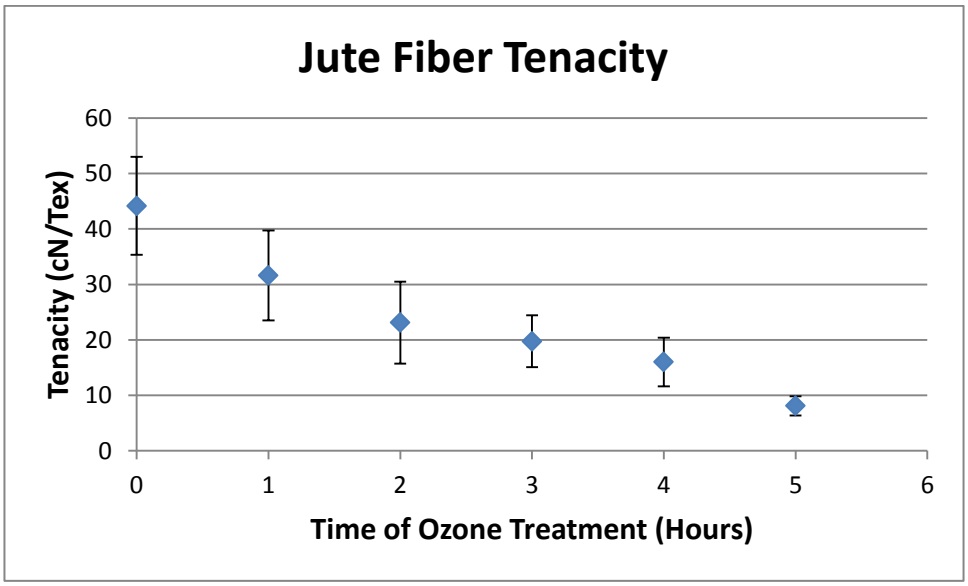

Figure 22. Decreasing trend of Tenacity with ozone treatment time (Error Bars = ± 2δ)

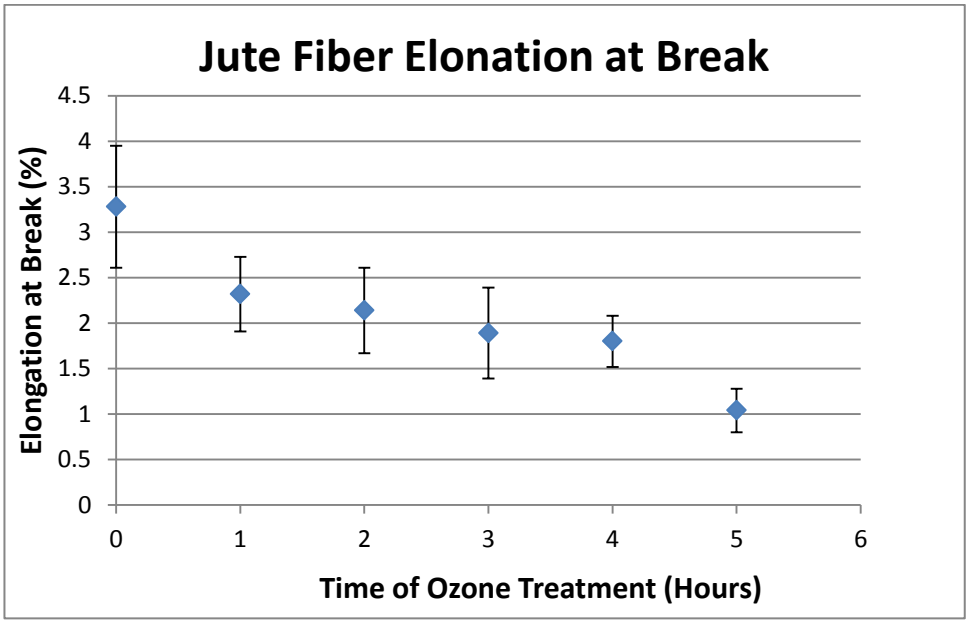

Figure 23. Elongation at Break (%) with Ozone treatment time (Error Bars = ± 2δ)

Many scientists have connected the resulting change in mechanical properties of the treated samples with chemical changes in keratin structure and amino groups. On this basis, the change in the mechanical properties can be correlated with the change in chemical groups and amino acids with the treatment time as detected from FTIR spectra (Fig. 20). The witnessed change in the mechanical properties can be related to the change in both fiber bonding and carboxyl group contents. Generally, the mechanical properties of ozone treated jute samples were changed.

5.1.5 Copper number:

The copper number is the weight of copper from the Cu^{2+} to Cu^{+} state, which is reduced by 100 gm of dry cellulose and is a measure of its inter and intra chain breakdown. It is an expression of the reducing power of degraded cellulose. The oxidation of cellulose can produce the ring fission of glucose residues, resulting in the formation of aldehyde groups at carbon atoms 2 and 3 (Karmakar 1999). It was measured to assess the degradation of cellulose by ozonation and the formation of aldehyde groups in this experiment. Results show that the copper number increased with the increase in treatment time gradually i.e., 2.26 after two hours and 2.35, 2.44, 2.43 after three to five hours respectively (Table 7). The value of the copper number at 4 hour of ozone treatment is high and at this point oxidation is enough for the some useful purposes like production of micro/Nano crystals of cellulose. After five hours of treatment copper number has a slight decrease looking abnormal which may be due to some noise or human error.

Table 7. Copper number of the samples

Jute Fiber	Sample Number	Copper number
Untreated	01	1.2
Treated with O_3	02	2.26
	03	2.26
	04	2.35
	05	2.44
	06	2.43

5.1.6 Moisture absorption:

The moisture absorption tendency of ozonized jute fiber was increased as compared to untreated jute fibers. The moisture regain percentage value of 5 hours ozonized jute fibers was enhanced up to 22.3%, whereas untreated jute fibers had only 10.5% moisture regain. This behavior was observed and it might be the result of increased uneven surfaces of ozone treated jute fibers which increased the pores and specific surface area simultaneously for moisture absorption. The deterioration of

amorphous region after the ozone treatment can be another reason for increased moisture absorbance capacity (Baheti et al. 2016a).

5.1.7 Evaluation of crystalline structure by XRD:

WAXD results were taken for the untreated and ozonized Jute samples to analyze the influence of the ozone treatment on crystalline structure of studied material. In figure 24 the comparison of the X-ray diffraction profiles recorded for all studied Jute samples are presented. In the 2θ range 10 – 32° the characteristic diffraction peaks located at 2θ 14.7°, 16.2° and 22.6° corresponding to (101), $(10\bar{1})$ and (002) lattice planes of α form of native cellulose structure are visible (Kiessig et al. 1939).

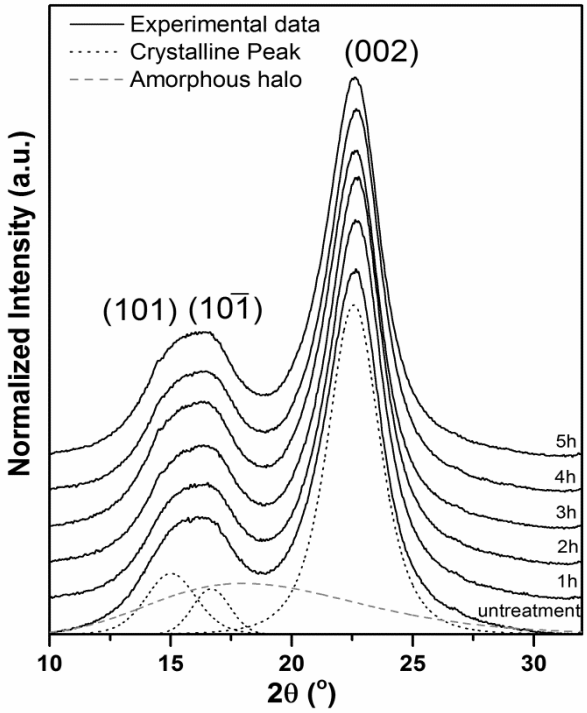

Figure 24. X-ray Diffraction Profiles of Untreated and Ozone Treated Samples of Jute Fiber

The changes between the obtained X-ray diffraction profiles are insignificant therefore, to evaluate the impact of ozone treatment on the crystalline structure were carried out numerical analysis of X-ray profiles and ware estimated structural parameter such as crystallinity degree and size of crystalline area. The analysis of diffraction patterns was carried out using the method of Hindeleh and Johnson, consisting in the best possible fitting the theoretical to experimental curves through the addition of peaks

corresponding to the X-ray diffraction of on crystalline areas and X-ray scattering on amorphous halo (Fig. 24). The theoretical curve determined allowed us to calculate the integration area under the curves of crystalline and amorphous components, which made it possible to determine the content of crystalline phase (*Xc* – crystallinity degree) according to the equation:

$$X_c\ (\%) = \frac{A_C}{A_C + A_A}\ x\ 100 \qquad (20)$$

where A_A and A_C are the integral intensities of the amorphous halo and the peaks from the crystalline phase, respectively. Additionally, the size of crystalline areas perpendicular to lattice planes *(hkl)* was determined by measuring the width of diffraction peak using Scherrer's formula:

$$L_{(hkl)}\ (\%) = \frac{K_\lambda}{B\cos\theta_C}\ x\ 100 \qquad (21)$$

where: $L_{(hkl)}$ – average size of crystalline areas perpendicular to lattice planes *(hkl)* , θ – Bragg angle for planes *(hkl)*, λ – wavelength of X-ray radiation (for CuKα λ = 0,154 nm), B – half width of the diffraction peak for planes *(hkl)*, K – Scherrer's constant that for polymer is equal to 1. The calculation of the all analyzed crystalline structures factors were calculated by the using of WAXSFIT software (Rabiej and Rabiej 2005).

In table 8, change of the crystalline structures factors are presented. As it is clearly presented the surface ozone treatment process increases slightly the crystallinity of the material which also confirms by the growth of crystalline areas.

Table 8. Crystalline parameters of studied samples.

Sample	$L_{(101)}$ **(nm)**	$L_{(10\bar{1})}$ **(nm)**	$L_{(002)}$ **(nm)**	χ_c **(%)**
Untreated	3.63	4.92	3.54	68.5
1h	3.81	4.97	3.60	69.1
2h	3.81	5.18	3.64	69.8
3h	3.82	5.36	3.65	70.1
4h	3.82	5.31	3.68	70.0
5h	3.87	5.32	3.68	70.4

5.1.8 Fiber Topography/SEM Images:

Samples were analyzed under the scanning electron microscope (SEM) to check the changes in fiber surface appearance due to the Ozone treatment (Fig. 25).Clear changes in surface morphologies were observed after ozone treatment. SEM images showed a comparatively smooth surface for untreated fibers; however, after ozonation, all the fibers exhibited uneven surfaces (Castle and Zhdan 1997). Image was taken at grid of 200 micrometer to view the surface of untreated jute fiber in spite of 100 micrometer grid as the fibers were in bundles. The reasoning of SEM images at 100 micrometer grid of treated samples at 4 hours and 5 hours times were as shown in figure 25 (b) and (c) had been taken at a grid of 100 micrometer. The untreated sample viewed with SEM revealed that the fibers were closely packed with each other in bundles. In case of untreated jute fibers, there were many substances like lignin, hemicellulose, pectin and waxy elements etc. on the surface of jute fibers. On the other hand, the ozone gas created many modifications on the surface of the fiber. Comparing figure 25(a) and 25(b, c), the extreme difference in the topography between the treated and untreated fibers can easily be seen. The multi-cellular nature of a jute fiber strand is more clearly shown in figure 25(b, c). Contrary to the untreated fiber, ozonized fibers were free from surface debris and overgrowths. This was certainly the result of the removal of lignin and some part of hemicellulose from both the surface and the intercellular spaces during the ozonation process. With Ozone treatment the bond between individual fibers damaged considerably along with increased rough surface. Results clearly exhibited that with the increase in treatment time of ozone the roughness in fiber surface is also increasing.

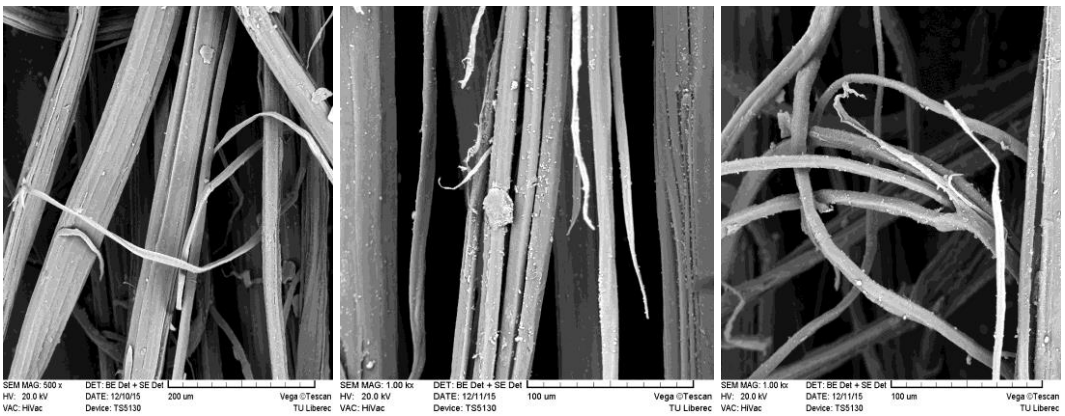

a) Untreated b) 4 hour treatment c) 5 hour treatment

Figure 25. SEM Images of Untreated and Ozone Treated Samples of Jute Fiber

5.2 Preparation for enzymatic hydrolysis of jute fibers

5.2.1 Pre-treatment of short jute fibers

In order to remove the non-cellulosic contents in jute fibers, chemical and ozone pre-treatment was carried out before the enzyme hydrolysis.

5.2.1.1 Chemical pre-treatment.

It was carried out sequentially with 4 % sodium hydroxide (NaOH) at 80 ^{o}C for 1 hour and with 7 g/l sodium hypochlorite (NaOCl) at room temperature for 2 hours under pH 10-11. Subsequently, the fibers were antichlor treated with 0.1 % sodium sulphite at 50 ^{o}C for 20 min.

5.2.1.2 Ozone pre-treatment.

Jute fibers were treated with ozone gas for the duration of four hours. For effective ozone treatment, one humidification system was introduced between Oxygen Concentrator Krober MEDIZINTECHNIK and Ozone Generator TRIOTECH GO 5LAB-K as shown in figure 26. The jute fibers were pre-humidified by spraying 50 % water (w/w) and then vertically hung inside the container for ozone treatment of 4 hours. The ozone concentration 4.5 mg/L with charging time of 1.5 min was used. The oxygen production setting of 5.0 L/minute was used as an input source for the Ozone Generator. After ozone treatment, the jute fibers were washed with 1 g/L nonionic surfactant for 1 hour in order to remove residual ozone. The fibers were then rinsed by distilled water and dried at 105 ^{o}C in an oven for 3 hours.

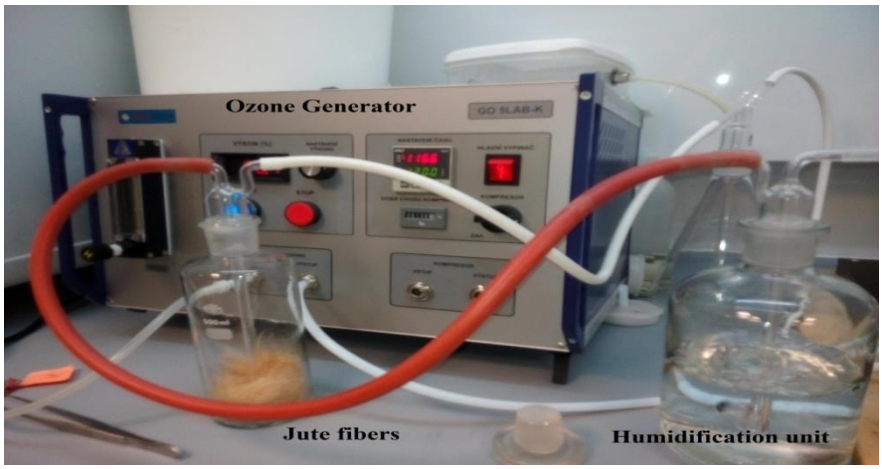

Figure 26. Set up for ozone treatment of jute fibers

5.2.2 Characterization of pre-treated jute fibers

5.2.2.1 Surface topography of pre-treated fibers.

The surface topography of untreated jute fibers (UTJF), chemical treated jute fibers (CTJF) and ozone treated jute fibers (OTJF) was observed using scanning electron microscope. SEM images were taken on TS5130-Tescan SEM at 20 kV accelerated voltage.

5.2.2.2 FTIR analysis.

The removal of lignin and modification of internal physical microstructure of the jute fibers after ozone treatments was evaluated by FTIR analysis. It was performed on Nicolet 6700 reflection ATR technique on an adapter with a crystal of diamond.

5.2.2.3 Single fiber strength.

The single fiber strength of untreated, chemical and ozone treated jute fiber was evaluated from VIBRODYNE Lenzing Instruments in order to know the change in mechanical properties. The single fiber strength was performed with a gauge length of 10 mm at a crosshead speed of 10 mm/min and at pre-tension of 2000 mg. Total 50 readings were taken and then average was calculated. In the end, the additional properties like moisture absorption, whiteness index, etc. were also determined.

5.3 Enzyme hydrolysis of pre-treated short jute fibers

The enzyme hydrolysis was carried out in the test tubes containing 5 g/L untreated, chemical and ozone treated jute fibers under 3 % v/v of cellulase enzyme concentration. The pH of solution was adjusted to 4.8 with the help of 0.05 M acetic acid/sodium acetate buffer. The test tubes were incubated at 55 °C in a heating bath of distilled water for 6 days. Subsequently, the samples were immediately heated to 80 °C for 15 min to deactivate the enzyme and further cooled to room temperature. Then, the mixture was transferred into centrifuge bottles. A Hettich centrifuge EBA 20 (Tuttlingen, Germany) was used to separate the solution from the treated materials. The precipitates were continuously washed with distilled water and centrifuged at 1400 rpm. The obtained suspension was further subjected to ultrasonic treatment in order to separate the individual micro crystals. Later, the suspension was transferred in solvent

isopropanol to avoid hornification of jute micro crystals during drying. In this way, untreated jute micro crystals (UTJMC), chemical treated jute micro crystals (CTJMC) and ozone treated jute micro crystals (OTJMC) were obtained.

5.4 Characterization of jute micro crystals

Particle size distribution of UTJMC, CTJMC and OTJMC obtained after 6 days of enzyme hydrolysis was studied on Malvern zetasizer nano series. Deionized water was used as dispersion medium for the particles. It was ultrasonicated for 5 min with bandelin ultrasonic probe before characterization. Refractive index of 1.52 was used to calculate particle size of jute powder. In addition, morphology of enzyme hydrolyzed UTJMC, CTJMC and OTJMC was observed on scanning electron microscope (SEM) of TS5130-Tescan at accelerating voltage of 20 kV. The amount of 0.01 g of jute powder was dispersed in 100 ml acetone. The drop of the dispersed solution was placed on aluminum foil and gold coated after drying.

5.5 Preparation of PLA composite films

The composite films of 3 wt. % filler content were prepared by mixing the calculated amount of UTJMC, CTJMC and OTJMC into chloroform solution of 5 wt. % PLA using a magnetic stirrer. The stirring was performed at room temperature for 3 hours. The composite mixture was further ultrasonicated for 10 min on Bandelin Ultrasonic probe mixer with 50 horn power. The final mixtures were then casted on a Teflon sheet. The films were kept at room temperature for 2 days until they were completely dried and then removed from the Teflon sheet. One neat PLA film was also prepared without addition of jute micro crystals for comparison purpose.

5.5.1 Differential scanning calorimetry (DSC).

The melting and crystallization behavior of the neat and composite films was investigated on DSC 6 Perkin Elmer instrument using “pyris” software under nitrogen atmosphere with sample weight of 10 mg. The sample was heated from 25 ^{o}C to 200 ^{o}C at a rate of 5 ^{o}C/min. The crystallinity (%) of PLA was estimated from the enthalpy for PLA content in the composites, using the ratio between the heat of fusion of the studied material and the heat of fusion of an infinity crystal of same material from equation (22)

$$\%\,Crystallinity = \left(\Delta H / w \times \Delta H_0\right) \times 100\% \quad (22)$$

where ΔH is heat of melting of sample, ΔH_o is heat of melting of 100 % crystalline PLA i.e. 93 J/g (Baheti and Militky 2013) and w is mass fraction of PLA in composite.

5.5.2 Dynamic mechanical analysis (DMA).

Dynamic mechanical properties of composite films were tested on DMA DX04T RMI instrument, Czech Republic in tensile mode. The measurements were carried out at constant frequency of 1 Hz, strain amplitude of 0.05 %, temperature range of 35-100 ^{o}C, heating rate of 5 ^{o}C/min and jaw distance of 30 mm. The samples were prepared by cutting strips from the films with a width of 10 mm. Four samples were used to characterize each material.

5.5.3 Tensile testing.

Tensile testing was carried out using a miniature material tester Rheometric Scientific MiniMat 2000 with a 1000 N load cell at a crosshead speed of 10 mm/min. The samples were prepared by cutting strips from the films with a width of 10 mm. The length between the grips was kept 100 mm. The total number of ten samples was used to characterize each material. The interaction of jute micro crystals and PLA matrix was investigated from the morphology of composite films using FESEM of Zeiss at 7 kV accelerated voltage.

CHAPTER 6

EVALUATION OF RESULTS AND NEW FINDINGS

6.1 Influence of pre-treatment on jute fibers

6.1.1 Surface morphology of fibers used for enzyme hydrolysis.

The removal of non-cellulosic contents after the action of chemical and ozone pre-treatment was studied from the morphology of jute fibers. According to the SEM photographs shown in figure 27 (a), it can be clearly seen that untreated jute fibers have a smooth surface and the individual fibers are closely packed together in bundle form. However, when jute fibers were subjected to chemical and ozone pre-treatment, the bond between individual fibers weakened significantly. From figure 27 (b), the chemically treated jute fiber revealed significant reduction in fiber diameter and higher fibrillation tendency, which indicated removal of non-cellulosic contents to the greater extent including lignin, hemicelluloses and pectin (Baheti et al. 2014).

Nevertheless, ozone treated jute fibers in figure 27 (c) exhibited uneven rough surfaces, peeling and breaking, which indicated only partial removal of non-cellulosic contents such as lignin but not hemicelluloses or pectin.

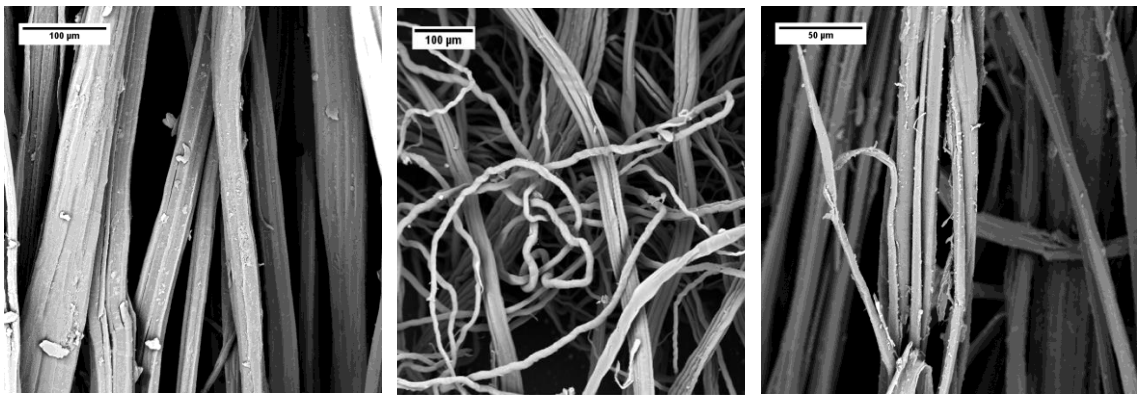

a) UTJF b) CTJF c) OJTF

Figure 27. SEM image of Different Jute fibers used for Enzymatic Hydrolysis

6.1.2 FTIR spectroscopy.

FTIR analysis was carried out to confirm the presence of non-cellulosic contents in jute fibers after the action of ozone pre-treatment. Figure 28 shows the FTIR spectra

of UTJF and OTJF. A broad absorption band in the range of 3300-3500 cm^{-1} represented OH stretching vibrations of cellulose and hemicelluloses. The peak at 1738 cm^{-1} is attributed to acetyl and uronic ester groups of hemicellulose or the ester linkage of carboxylic group of ferulic and p-coumaric acids of lignin and hemicelluloses (Baheti et al. 2014). This peak was found to decrease in the spectrum of OTJF to explain the partial removal of lignin after ozone pre-treatment. The peak at 1642 cm^{-1} represents aromatic vibration of benzene ring in lignin. The absorption band at 1537 cm^{-1} is due to CH_2 bending in lignin, whereas the peak at 1423-1460 cm^{-1} is due to OH in-plane bending (Biagiotti et al. 2004). The band at 1236 cm^{-1} corresponds to C-O stretching of acetyl group of lignin(Neto et al. 2013). The reduced height of these peaks in OTJF confirmed removal of lignin after ozone treatment. The peaks at 1030 cm^{-1} and 995 cm^{-1} are associated with C-O stretching and C-H rock vibrations of cellulose(Neto et al. 2013). The growth of these peaks in spectra of OTJF over UTJF showed increase in the percentage of cellulosic components after ozone treatment.

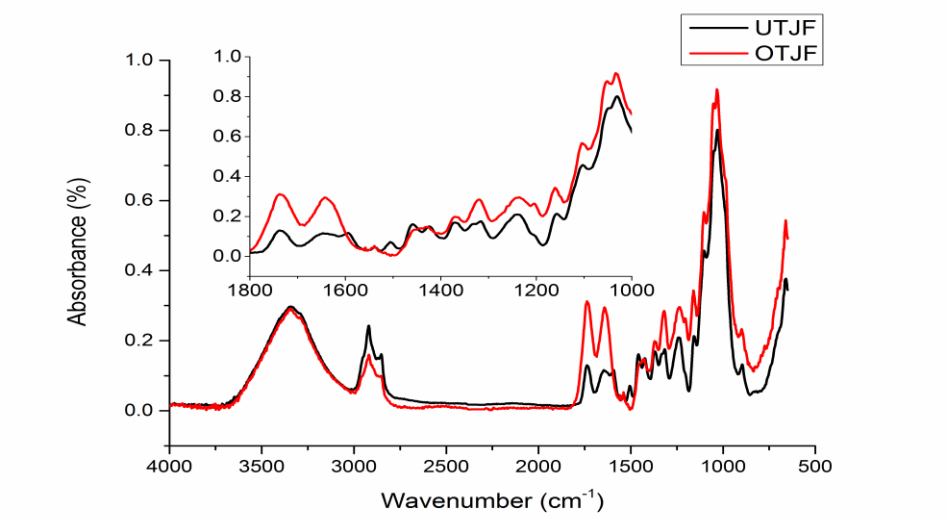

Figure 28. FTIR spectra of untreated and ozone treated jute fibers

6.1.3 Mechanical properties.

From figure 29 and table 9, the tenacity and breaking elongation of jute fibers was found to reduce after chemical and ozone treatment. The maximum reduction in tenacity was observed in case of OTJF, where it dropped from 44.16 cN/tex to 16.01 cN/tex after four hours of ozone treatment. This behavior is attributed to non-uniform removal of lignin and subsequent formation of more uneven rough surfaces, peeling, breaking and fibrillation of jute fibers after the ozone treatment shown in figure 27 (c).

The drop in breaking elongation from 3.28 % to 1.80 % could be related to dissolution of amorphous region after ozone treatment of jute fibers. This clearly showed that crystalline structure of jute fibers could not be disintegrated and rupture of cellulose macromolecules could be avoided by proper control over ozone induced surface modification of fibers. In spite of more fibrillation, CTJF was found to have higher mechanical properties than OTJF. This was due to more uniform removal of non-cellulosic substances from jute fibers after chemical pre-treatment shown in figure 27 (b). Maximum fiber strength of untreated jute fiber is attributed to presence of lignin, which holds the number of fibrils together in bundle form shown in figure 27 (a). The pattern of mechanical properties of UTJF, CTJF and OTJF was also evident from SEM images and FTIR analysis discussed in the previous sections.

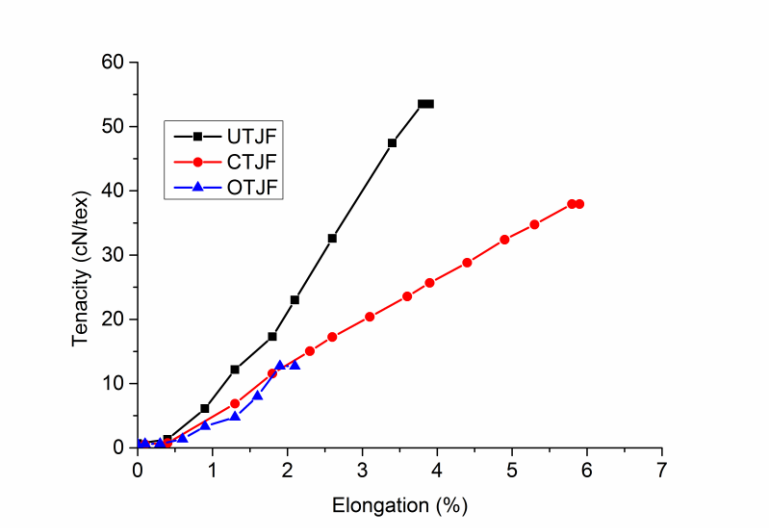

Figure 29. Single fiber strength of untreated and pre-treated jute fibers

Table 9. Mechanical properties of untreated and pre-treated jute fibers

Sample name	Initial modulus YM1 (cN/tex)	Tenacity (cN/tex)	Elongation (%)
UTJF	898.64±140.48	44.16±8.81	3.28±0.67
CTJF	266.28±73.78	28.39±6.34	6.98±1.10
OTJF	201.32±84.74	16.01±4.37	1.80±0.28

6.1.4 Moisture absorption.

The ozone treated jute fiber was found to have maximum moisture absorption tendency than untreated jute fibers. The moisture regain of ozone treated jute fibers was found near 22.3 %, whereas 10.5 % for untreated jute fibers. This behavior is attributed to the increased uneven rougher surfaces of ozone treated jute fibers, which provided additional specific surface area and pores for moisture absorption. Another reason for more moisture absorbency could be weakening of amorphous region after the ozone treatment.

6.1.5 Whiteness index.

The untreated jute fibers showed the apparent change in colour with respect to all treated samples shown in figure 30. The captured images were analyzed in grey scale and whiteness index was measured. The whiteness index of chemically treated jute fiber was found 225, followed by 200 for ozone treated jute fiber and 150 for untreated jute fibers. This is due to uniform and maximum removal of non-cellulosic contents after chemical pre-treatment. Nevertheless, ozone treatment was found promising for oxidation of natural pigments present in jute fibers.

Figure 30. Change in color of jute fibers after pre-treatments

6.2 Influence of enzyme hydrolysis on pre-treated jute fibers

The separated jute micro crystals after 6 days of enzyme hydrolysis are shown in figure 33. The particle size distribution of jute crystals obtained from UTJF, CTJF and OTJF are depicted in figure 32 respectively. The pre-treatment of jute fibers was found to have significant effect on particle size reduction and particle size distribution of obtained jute micro crystals. The average particle size of UTJMC, CTJMC and OTJMC was observed as 5392 nm, 3743 nm and 4238 nm respectively from dynamic light

scattering measurements. This clearly indicated easier separation of individual micro crystals after pre-treatment of jute fibers. On the other hand, the maximum resistance for enzyme hydrolysis was found in case of UTJF due to presence of non-cellulosic contents which hold the fiber bundle together (Abraham et al. 2011).

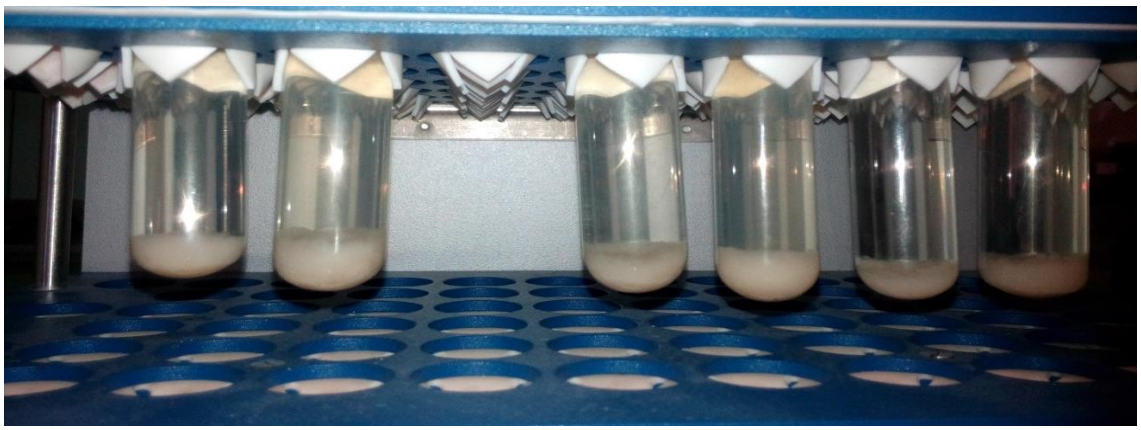

Figure 31. Enzyme hydrolyzed jute micro crystals

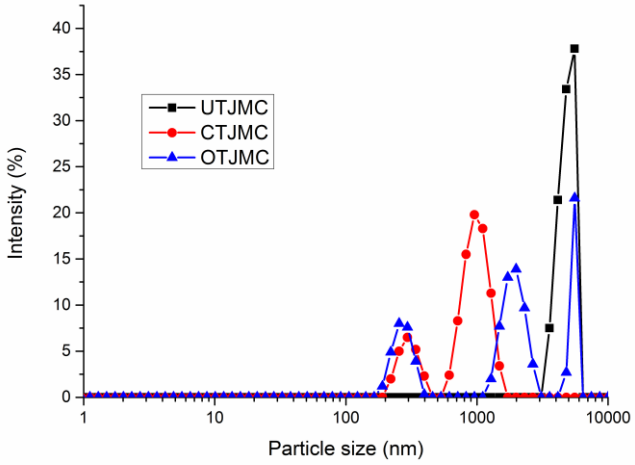

Figure 32. Particle size distribution of jute micro crystals

The enzyme hydrolysis of OTJF was found to result into bigger crystals having wider size distribution than CTJF. This behavior is attributed to non-uniform and partial removal of non-cellulosic contents by ozone treatment, which further offered relatively higher resistance for diffusion of cellulase enzyme into the jute fibrous structure(Satyamurthy et al. 2011). This resulted into uneven dissociation of glucosidic bonds from surface to core of the cellulose in ozone treated jute fibers and consequent non-uniform separation of micro crystals having wider size distribution. The similar results were also evident from SEM images shown in figure 33(a), figure 33(b) and

figure 33(c). The micro crystals obtained after ozone pre-treatment found to exhibit both cylindrical and spherical morphology as shown in figure 33(c), whereas those obtained after chemical pre-treatment revealed only cylindrical morphology with higher aspect ratio shown in figure 33(b).

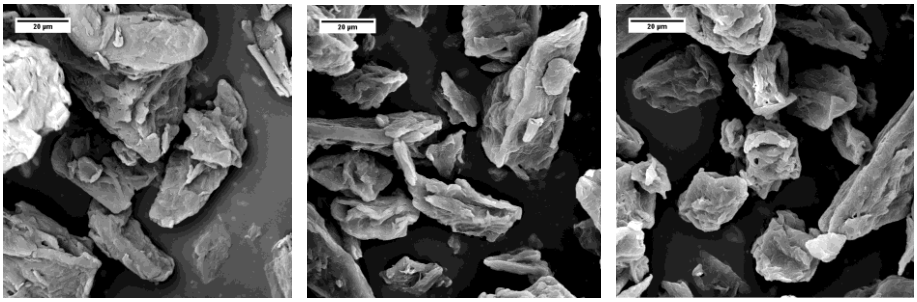

a) UTJMC b) CTJMC c) OJTMC

Figure 33. SEM images of Jute Micro Crystals obtained by Enzyme Hydrolysis

The yield of obtained crystals was calculated from the percentage of ratio of dry mass of micro crystals to the initial dry mass of jute. The obtained lower yield of less than 10 % in all cases indicated significant amount of conversion of cellulose into glucose, cellobiose, cellotriose, and cellotetraose by the action of enzymes (Soni et al. 2015).

6.3 PLA composite films

According to the procedure given in section 5.5, different functional properties of the neat PLA films along with the PLA films incorporated with the jute micro crystals were measured. The descriptions of the measured properties are described below.

6.3.1 Thermal behavior of PLA composite films.

DSC analysis was carried out to study the thermal behavior of PLA after addition of UTJMC, CTJMC and OTJMC. Table 10 shows the results of glass transition (T_g), followed by cold crystallization (T_{cc}), and melting point (T_m). It was observed from figure 34 that T_g value of PLA increased only marginally after incorporation of CTJMC and OTJMC, and reduced after addition of UTJMC. This indicated lesser flexibility of PLA chains due to some improvements in intermolecular interactions, steric effects, and

the cross linking density between pre-treated jute micro crystals and PLA (Krishnamachari et al. 2009). As compared to T_g, the melting temperature T_m of PLA was found to increase significantly after addition of CTJMC and OTJMC. This behavior is attributed to increase of PLA crystallinity after addition of CTJMC and OTJMC as reported in table 10 (Baheti et al. 2013). The lower cold crystallization peak observed in case of composite films of CTJMC and OTJMC further indicated nucleating behavior of pre-treated jute micro crystals for development of crystallinity through trans crystallization phenomena (Dufresne et al. 1999). The absence of cold crystallization peak in UTJMC/PLA sample showed inability of UTJMC to develop PLA crystallinity. This behavior is attributed to the non-cellulosic substances (i.e. wax) present on the surface of UTJMC, which reduced the interaction between PLA and UTJMC.

Table 10. Behavior of neat and composite PLA films on application of heat

Sample	T_g (^oC)	T_{cc} (^oC)	T_m (^oC)	ΔH (J/g)	Crystallinity (%)
Neat PLA	42.35±0.30	98.85±1.10	147.49±0.10	17.33±2.80	18.63
3% UTJMC+PLA	40.01±0.43	-	153.00±0.18	19.26±3.21	21.35
3% CTJMC+PLA	44.84±0.34	96.88±1.39	155.47±0.14	24.53±2.34	27.19
3% OTJMC+PLA	45.01±0.47	96.52±1.22	154.32±0.13	23.09±2.03	25.59

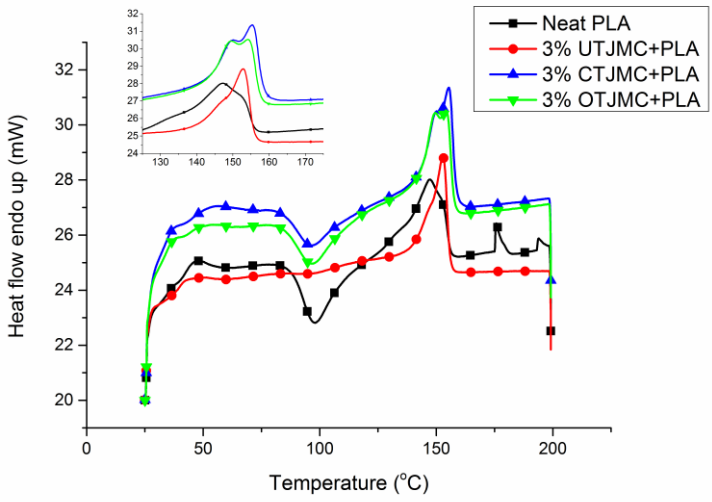

Figure 34. Differential scanning calorimetry of neat and composite PLA films

6.3.2 Thermo-mechanical properties of PLA composite films

The dynamic mechanical analysis was performed to get an idea about reinforcement potentials of jute micro crystals obtained before and after pre-treatments of jute fibers. The load bearing capacity of neat and composite PLA films is shown in figures 35 & 36 along with table 11. From evaluation of figure 35, all samples of PLA composite films were found to exhibit higher storage modulus results at 35 ^{o}C as compared to neat PLA film. This behavior is attributed to the efficient stress transfer from PLA to stiff jute micro crystals at 35 ^{o}C(Petersson and Oksman 2006). The maximum reinforcement was provided by jute micro crystals obtained after pre-treatment (i.e. CTJMC and OTJMC) than those obtained from raw untreated jute fibers (i.e. UTJMC). The storage modulus of PLA composites at 35 ^{o}C increased from 3.09 GPa to the level of 4.11 GPa, 5.16 GPa and 5.13 GPa after the addition of UTJMC, CTJMC and OTJMC, respectively. This trend is attributed to rough surface of OTJMC and less non-cellulosic substances in CTJMC, which dispersed them uniformly within PLA matrix and consequently resulted into maximum surface area of micro crystals interacting with PLA. The least improvement in case of PLA/UTJMC can be attributed to the poor bonding of UTJMC with PLA due to presence of non-cellulosic contents like wax on the surface of UTJMC.

Table 11. Storage modulus of neat and composite PLA films at different temperature

Sample name	E' (35 ^{o}C) (GPa)	E' (60 ^{o}C) (GPa)
Neat PLA	3.09±0.20	0.48±0.02
3 % UTJMC+PLA	4.11±0.72	0.16±0.01
3 % CTJMC+PLA	5.16±0.58	0.24±0.01
3 % OTJMC+PLA	5.13±0.51	0.17±0.01

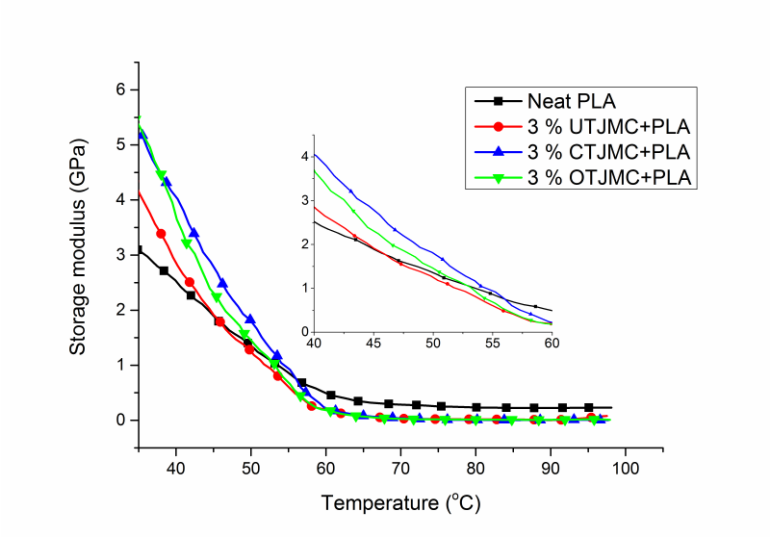

Figure 35. Storage modulus of neat and composite PLA films

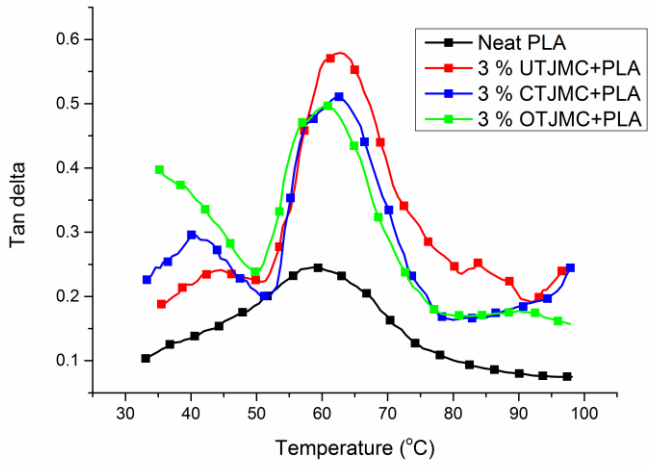

Figure 36. Damping factor of neat and composite PLA films

The concept of addition of jute micro crystals for improvement of load bearing capacity of PLA was found negative at higher temperature of 60 °C. With the increase in temperature from 35 to 60 °C, the storage modulus of PLA composite films was dropped at faster rate than neat PLA film. This showed inability of jute micro crystals to restrict the motion of PLA chains at higher temperature and thus poor transfer of stress from matrix to micro crystals. This behavior was found not in agreement with previous results (Baheti et al. 2013). The reasons could be micro scale dimensions of jute crystals, which were unable to penetrate between the PLA chains.

The ratio of loss modulus to storage modulus is defined as mechanical loss factor or tan delta. The damping properties of the material give the balance between the elastic

phase and viscous phase in a polymeric structure (Baheti et al. 2016b). Figure 36 showed that the tan delta peak of PLA was positively shifted after the addition of all different types of jute micro crystals. The maximum shift of 5 ^{o}C was reported in case of CTJMC/PLA composites due to their clean surfaces for maximum interaction with PLA. This subsequently restricted segmental mobility of the PLA chains around them and improved the damping factor of composites.

6.3.3 Tensile properties of PLA composite films

The stress–strain curve of neat PLA and its composite films is shown in figure 37, whereas average values and standard deviations of mechanical properties are reported in table 12. It is clear from results that PLA composite films of pre-treated jute micro crystals show higher mechanical properties than those jute micro crystals obtained from untreated jute fibers. The maximum increase in tensile strength and initial modulus was found in case of CTJMC/PLA, which is an indication of better stress transfer across the interphase due to good interfacial bonding between CTJMC and PLA matrix(Mathew et al. 2005). This behavior is attributed to less non-cellulosic contents in CTJMC, which consequently improved their compatibility with PLA matrix as compared to other jute micro crystals. The higher mechanical properties of OTJMC/PLA over UTJMC/PLA composite films are attributed to rough uneven surfaces of OTJMC, which provided increased surface area of interaction than UTJMC.

Table 12. Tensile properties of neat and composite PLA films

Sample name	Initial modulus (GPa)	Tensile strength (MPa)	Yield point elongation (%)
Neat PLA	1.04±0.03	25.98±0.13	4.84±0.72
3 % UTJMC+PLA	1.41±0.07	22.72±0.47	1.60±0.50
3 % CTJMC+PLA	1.63±0.04	34.92±0.39	2.14±0.41
3 % OTJMC+PLA	1.55±0.03	30.40±0.41	1.96±0.47

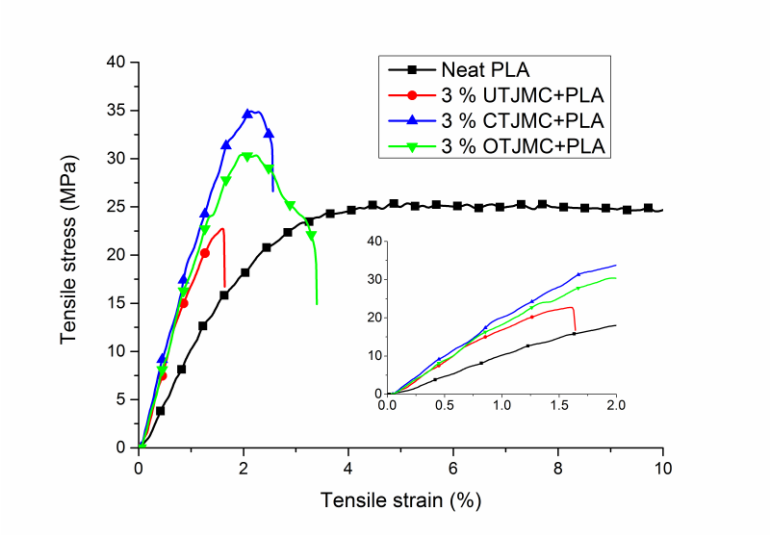

Figure 37. Stress-strain curve of neat and composite PLA films

Moreover, the increase in crystallinity of PLA discussed in section 6.3.1 was also found to have significant effect on mechanical properties. With increase in crystallinity, the brittleness of PLA also increased. This subsequently resulted into reduction in yield point elongation and increase in initial modulus of all PLA composites. In addition, the tendency of stress concentrations due to stiff nature of jute micro crystals could also be considered for reduction in yield point elongation.

6.3.4 Microscopic evaluation of different composite films

In order to get clear idea of interaction between PLA and different jute micro crystals, the morphology of composite films was investigated under FESEM microscopy. The absence of voids, intact position of fillers, interfacial bonding between fillers and matrix, and absence of agglomerations of fillers decide the intensity of filler–polymer adhesion (Garlotta et al. 2003). It is clear from figure 38 (a), 38 (b) and 38 (c) that the presence of non-cellulosic contents and roughness of jute crystals affect the homogeneous dispersion and tendency of agglomerations in composites. From figure 38 (b) and figure 38 (c), the composite films of CTJMC and OTJMC revealed uniform dispersion with minimum agglomerations due to their respective clean and rough surfaces having minimum percentage of non-cellulosic contents. The intact position of CTJMC and OTJMC confirmed stronger interaction between them and PLA due to their uniform wetting. On the other hand, figure 38 (a) for composites films of UTJMC showed significant agglomerations as a result of poor bonding caused by their smooth

surfaces having more non-cellulosic substances. The gap around the surface of UTJMC in PLA confirmed their poor interfacial adhesion.

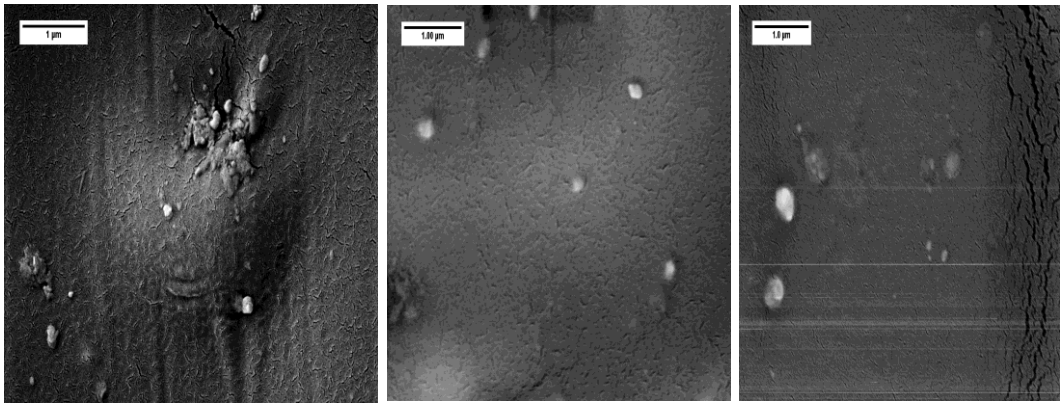

a) UTJMC/PLA b) CTJMC/PLA c) OJTMC/PLA

Figure 38. Morphology of different composite films

6.4 Comparison of experimental results with mechanical models

It was clear from figure 39 that experimental results were situated below the predictions of rule of mixture, Halpin-Tsai, Cox-Krenchel and percolation theories, however relatively close agreement was found up to 3 wt. % loading of JMC. With increase in JMC loading, the difference between experimental results and predicted values of rule of mixture and percolation theories became wider. This indicated lack of filler to filler interaction between individual JMC crystals for formation of percolated network. The effect of higher JMC loading was found negligible for improvement in predicted values of Halpin-Tsai and Cox-Krenchel theories. The constant predicted values of Halpin-Tsai and Cox-Krenchel theories above 3 wt% JMC loading indicated achievement of threshold in improvement of mechanical properties for particular dimensions of JMC. The experimental results were found to fit closely with Cox-Krenchel theory, which indicated random orientation of JMC in PLA composite films. In this way, maximum reinforcement ability of prepared JMC was verified between 1 to 3 wt% loading from mechanical models and experimental results. The following values given in table 13 were used for theoretical calculations:

Table 13. Input parameters of mechanical models

Parameter	Value
Modulus of PLA (E_m)	1.04 GPa
Modulus of JMC (E_r)	70 GPa
Density of JMC (ρ_r)	1.58 g/cm^3
Density of PLA (ρ_m)	1.25 g/cm^3
Diameter of JNF	5000 nm [Fig. 32]
Length of JNF	50 µm

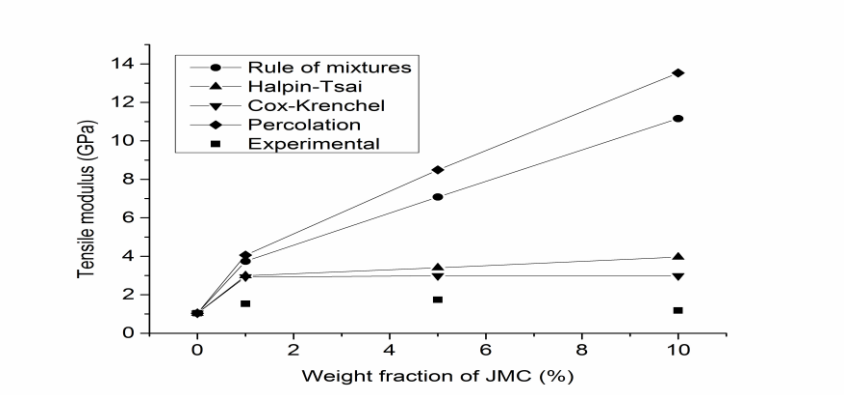

Figure 39. Comparison of Initial modulus with mechanical models

6.5 Prediction Model using Generalized Rule of Mixtures

When we consider simple rule of mixtures, it is often utilized in the prediction of various material properties such as modulus, electrical, thermal conductivity etc. However, in most cases, the prediction models underperform and don't accurately predict the system properties. It is due to the fact that there are various interactions present in the system.

The values of tensile modulus of the composites were plotted against the volume fraction of jute micro crystals and a multiple linear regression is applied.

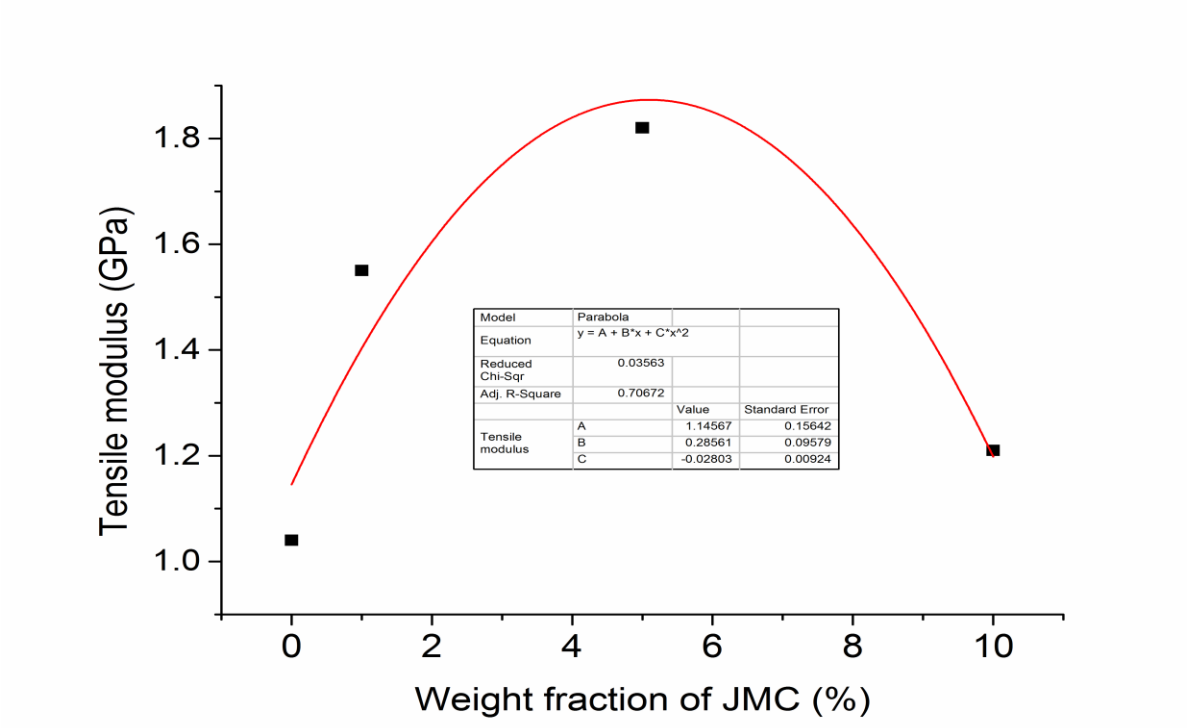

Figure 40. Prediction model using multiple linear regression

Figure 40 shows the multiple linear regression equation of the composite system as described below:

$$Y = 1.146 + 0.286X - 0.028X^2 \quad (23)$$

Corresponding to Eq. (13), Eq. (14) and Eq. (23), we can modify the equation in terms of the composite modulus "*E*" and X_r (the volume fraction of reinforcement i.e. JMC) as follows:

$$E = 1.146 + 0.286X_r - 0.028{X_r}^2 \quad (24)$$

where $1.146 = E_m$; $0.286 = (E_r - E_m + I)$ and $(-0.028) = (-I)$ or

$$E_m = 1.146$$

$$E_r - E_m + I = 0.286$$

$$I = 0.028$$

It is evident that interaction between the volume fractions of reinforcement (JMC) and matrix (PLA) in this particular system of composite films preparation enhances the overall composite system property (Tensile modulus) by at least 2.8%.

It is worth mentioning that the accuracy of generalized rule of mixtures predicts the component system up to 70.67% as shown by R^2 value.

CONCLUSIONS

The present study was focused on the development of environment friendly approach for surface treatment of jute fibers and subsequent separation of individual cellulose micro crystals. The sequential action of ozone pre-treatment followed by enzyme hydrolysis was selected for this purpose. At first, jute fibers were pre-treated with ozone gas for the duration of four hours. For comparison purpose, one sample with chemical treatment of jute fibers was also prepared. The effect of pre-treatments on mechanical properties and surface morphology of jute fibers was investigated. The maximum deterioration in mechanical properties was found in case of ozone treated jute fibers than chemically treated jute fibers. The tenacity was dropped from 44.16 cN/tex to 16.01 cN/tex after four hours of ozone treatment. Under SEM, more uneven rough surfaces, peeling, breaking and fibrillation of jute fibers were observed due to partial removal of non-cellulosic contents after ozone treatment. On the other hand, chemical treatment revealed significant reduction in fiber diameter and higher fibrillation due to maximum removal of non-cellulosic contents. In addition, the moisture absorbency of ozone treated fibers was found higher than untreated and chemical treated jute fibers.

Later, enzyme hydrolysis was carried out to separate longer cellulose micro crystals from jute fibers. The pre-treatment of jute fibers was found to have significant effect on particle size reduction and particle size distribution of obtained jute micro crystals. The rate of refinement of untreated fibers having non-cellulosic contents was found slower than treated jute fibers due to strong holding of fiber bundles by non-cellulosic contents. The average particle size of 5392 nm, 3743 nm and 4238 nm was found for crystals obtained from untreated, chemically treated and ozone treated fibers respectively. This indicated easier separation of individual micro crystals after ozone pre-treatment. The enzyme hydrolysis of ozone treated fibers was found to result into bigger crystals of both cylindrical and spherical morphology having wider size distribution.

When jute micro crystals were incorporated in PLA matrix, the maximum reinforcement was provided by crystals obtained after pre-treatment than those obtained from raw untreated jute fibers. These improvements in mechanical properties are attributed to their rough uneven surface, higher percentage of cellulosic contents and smaller particle size. The SEM morphology of fractured surfaces also confirmed homogeneous dispersion and fewer tendencies of agglomerations due to fewer amounts of non-cellulosic contents and

roughness of jute crystals. Nevertheless, the role of jute micro crystals as reinforcement of PLA was found negative at higher temperature of 60 °C. This showed inability of larger jute micro crystals to restrict the motion of PLA chains at higher temperature and thus poor transfer of stress from matrix to micro crystals. In this way, the present study showed a green process for reusing of waste jute fibers and converting them into useful cellulose powder for reinforcement in composite materials. Moreover, the ozone treatment was found attractive in terms of less energy, time and water with additional advantage of minimum degradation of cellulose.

Finally, experimental results of Initial modulus were compared with predicted modulus of mechanical models. A good level of agreement was observed from 1 to 3wt % loading of jute micro crystals and close fit with Cox-Krenchel theory indicated random orientation of micro crystals in PLA matrix. In this way, this study showed a green process for reusing of waste jute fibers and converting them into useful cellulose powder for reinforcement in composite materials.

By applying quadratic regression to the plotted actual values of obtained tensile modulus of composite corresponding to different volume fraction of jute micro crystals in the system, we got a quadratic equation using generalized rule of mixture explaining interaction of the volume fraction of jute micro crystals and PLA as well. Using this generalized rule of mixture the predicted model can be utilized for the prediction of tensile modulus corresponding to volume fraction of reinforcement and the interaction between volume fractions of reinforcement and matrix.

REFERENCES

Abraham E, Deepa B, Pothan LA, et al (2011) Extraction of nanocellulose fibrils from lignocellulosic fibres: A novel approach. Carbohydr Polym 86:1468–1475. doi: 10.1016/j.carbpol.2011.06.034

Agarwal BD, Broutman LJ, Chandrashekhara K (2006) Analysis and performance of fiber composites. John Wiley & Sons

Alemdar A, Sain M (2008) Isolation and characterization of nanofibers from agricultural residues–Wheat straw and soy hulls. Bioresour Technol 99:1664–1671.

AlMaadeed MA, Kahraman R, Khanam PN, Al-Maadeed S (2013) Characterization of untreated and treated male and female date palm leaves. Mater Des 43:526–531.

Angles MN, Dufresne A (2000) Plasticized starch/tunicin whiskers nanocomposites. 1. Structural analysis. Macromolecules 33:8344–8353.

Arooj F, Ahmad N, Shaikh IA, Chaudhry MN (2014) Application of ozone in cotton bleaching with multiple reuse of a water bath. Text Res J 84:527–538.

Aslan N, Cebeci Y (2007) Application of Box–Behnken design and response surface methodology for modeling of some Turkish coals. Fuel 86:90–97.

Azeredo H, Mattoso LHC, Avena- Bustillos RJ, et al (2010) Nanocellulose reinforced chitosan composite films as affected by nanofiller loading and plasticizer content. J Food Sci 75:N1–N7.

Baheti V, Maqsood HS, Wiener J, Militky J (2016a) Reinforcement of ozone pre-treated and enzyme hydrolyzed longer jute micro crystals in poly lactic acid composite films. Compos Part B Eng 95:9–17.

Baheti V, Militky J (2013) Reinforcement of wet milled jute nano/micro particles in polyvinyl alcohol films. Fibers Polym 14:133–137.

Baheti V, Militky J, Marsalkova M (2013) Mechanical properties of poly lactic acid composite films reinforced with wet milled jute nanofibers. Polym Compos 34:2133–2141. doi: 10.1002/pc.22622

Baheti V, Militky J, Mishra R, Behera BK (2016b) Thermomechanical properties of

glass fabric/epoxy composites filled with fly ash. Compos Part B Eng 85:268–276. doi: 10.1016/j.compositesb.2015.09.049

Baheti V, Mishra R, Militky J, Behera BK (2014) Influence of noncellulosic contents on nano scale refinement of waste jute fibers for reinforcement in polylactic acid films. Fibers Polym 15:1500–1506. doi: 10.1007/s12221-014-1500-5

Bax B, Müssig J (2008) Impact and tensile properties of PLA/Cordenka and PLA/flax composites. Compos Sci Technol 68:1601–1607.

Benli H, Bahtiyari Mİ (2015) Combination of ozone and ultrasound in pretreatment of cotton fabrics prior to natural dyeing. J Clean Prod 89:116–124. doi: 10.1016/j.jclepro.2014.11.007

Biagiotti J, Puglia D, Torre L, et al (2004) A systematic investigation on the influence of the chemical treatment of natural fibers on the properties of their polymer matrix composites. Polym Compos 25:470–479.

Brito BSL, Pereira F V, Putaux J-L, Jean B (2012) Preparation, morphology and structure of cellulose nanocrystals from bamboo fibers. Cellulose 19:1527–1536.

Cao X, Habibi Y, Lucia LA (2009) One-pot polymerization, surface grafting, and processing of waterborne polyurethane-cellulose nanocrystal nanocomposites. J Mater Chem 19:7137–7145.

Castle JE, Zhdan PA (1997) Characterization of surface topography by SEM and SFM: problems and solutions. J Phys D Appl Phys 30:722.

Celzard A, Fierro V, Kerekes R (2009) Flocculation of cellulose fibres: new comparison of crowding factor with percolation and effective-medium theories. Cellulose 16:983–987.

Chakraborty A, Sain M, Kortschot M (2005) Cellulose microfibrils: a novel method of preparation using high shear refining and cryocrushing. Holzforschung 59:102–107.

Chauve G, Heux L, Arouini R, Mazeau K (2005) Cellulose poly (ethylene-co-vinyl acetate) nanocomposites studied by molecular modeling and mechanical spectroscopy. Biomacromolecules 6:2025–2031.

Chazeau L, Cavaille JY, Canova G, et al (1999) Viscoelastic properties of plasticized PVC reinforced with cellulose whiskers. J Appl Polym Sci 71:1797–1808.

Chen P, Yu H, Liu Y, et al (2013) Concentration effects on the isolation and dynamic rheological behavior of cellulose nanofibers via ultrasonic processing. Cellulose 20:149–157.

Choi Y, Simonsen J (2006) Cellulose nanocrystal-filled carboxymethyl cellulose nanocomposites. J Nanosci Nanotechnol 6:633–639.

Das K, Ray D, Bandyopadhyay NR, et al (2011) Physico-mechanical properties of the jute micro/nanofibril reinforced starch/polyvinyl alcohol biocomposite films. Compos Part B Eng 42:376–381.

de Menezes AJ, Siqueira G, Curvelo AAS, Dufresne A (2009) Extrusion and characterization of functionalized cellulose whiskers reinforced polyethylene nanocomposites. Polymer (Guildf) 50:4552–4563.

Deepa B, Abraham E, Cherian BM, et al (2011) Structure, morphology and thermal characteristics of banana nano fibers obtained by steam explosion. Bioresour Technol 102:1988–1997.

Dhakal HN, Zhang ZY, Richardson MOW (2007) Effect of water absorption on the mechanical properties of hemp fibre reinforced unsaturated polyester composites. Compos Sci Technol 67:1674–1683.

Diniz JMBF, Gil MH, Castro J (2004) Hornification—its origin and interpretation in wood pulps. Wood Sci Technol 37:489–494.

Duan L, Yu W (2015) Novel and Efficient Method to Reduce the Jute Fibre Prickle Problem.

Dufresne A (2013) Nanocellulose: from nature to high performance tailored materials. Walter de Gruyter

Dufresne A, Kellerhals MB, Witholt B (1999) Transcrystallization in Mcl-PHAs/cellulose whiskers composites. Macromolecules 32:7396–7401.

Eren HA, Anis P (2009) Surface trimer removal of polyester fibers by ozone treatment. Text Res J 79:652–656.

Eren HA, Avinc O, Uysal P, Wilding M (2011) The effects of ozone treatment on polylactic acid (PLA) fibres. Text Res J 81:1091–1099.

Eren HA, Ozturk D, Eren S (2012) Afterclearing of disperse dyed polyester with gaseous ozone. Color Technol 128:75–81.

Fathi-Azarbayjani A, Qun L, Chan YW, Chan SY (2010) Novel vitamin and gold-loaded nanofiber facial mask for topical delivery. Aaps Pharmscitech 11:1164–1170.

Favier V, Chanzy H, Cavaille JY (1995) Polymer nanocomposites reinforced by cellulose whiskers. Macromolecules 28:6365–6367.

Filson PB, Dawson-Andoh BE, Schwegler-Berry D (2009) Enzymatic-mediated production of cellulose nanocrystals from recycled pulp. Green Chem 11:1808–1814.

Garlotta D, Doane W, Shogren R, et al (2003) Mechanical and thermal properties of starch-filled poly(D,L-lactic acid)/poly(hydroxy ester ether) biodegradable blends. J Appl Polym Sci 88:1775–1786. doi: 10.1002/app.11736

Gashti MP, Pournaserani A, Ehsani H, Gashti MP (2013) Surface oxidation of cellulose by ozone-gas in a vacuum cylinder to improve the functionality of fluoromonomer. Vacuum 91:7–13. doi: 10.1016/j.vacuum.2012.10.015

Gashti MP, Willoughby J, Agrawal P (2011) Surface and Bulk Modification of Synthetic Textiles to Improve Dyeability. Text Dye. doi: 10.5772/800

Gómez-del Río T, Poza P, Rodríguez J, et al (2010) Influence of single-walled carbon nanotubes on the effective elastic constants of poly (ethylene terephthalate). Compos Sci Technol 70:284–290.

Grunert M, Winter WT (2000) Progress in the development of cellulose reinforced nanocomposites. Polym Mater Sci Eng 82:232.

Grunert M, Winter WT (2002) Nanocomposites of cellulose acetate butyrate reinforced with cellulose nanocrystals. J Polym Environ 10:27–30.

Guo J, Guo X, Wang S, Yin Y (2016) Effects of ultrasonic treatment during acid hydrolysis on the yield, particle size and structure of cellulose nanocrystals.

Carbohydr Polym 135:248–255. doi: 10.1016/j.carbpol.2015.08.068

Habibi Y, Chanzy H, Vignon MR (2006) TEMPO-mediated surface oxidation of cellulose whiskers. Cellulose 13:679–687.

Habibi Y, Lucia LA, Rojas OJ (2010) Cellulose nanocrystals: chemistry, self-assembly, and applications. Chem Rev 110:3479–3500.

Helbert W, Cavaille JY, Dufresne A (1996) Thermoplastic nanocomposites filled with wheat straw cellulose whiskers. Part I: processing and mechanical behavior. Polym Compos 17:604–611.

Horrocks AR (1996) Recycling textile and plastic waste. Elsevier

Islam MS, Hamdan S, Rahman MR, et al (2011) Dynamic Young's modulus, morphological, and thermal stability of 5 tropical light hardwoods modified by benzene diazonium salt treatment. BioResources 6:737–750.

Jabasingh SA, Nachiyar CV (2012) Process Optimization for the Biopolishing of Jute Fiberswith Cellulases from Aspergillus Nidulans AJ SU04. Int J Biosci Biochem Bioinforma 2:12.

Jabbar A, Militký J, Madhukar Kale B, et al (2016) Modeling and analysis of the creep behavior of jute/green epoxy composites incorporated with chemically treated pulverized nano/micro jute fibers. Ind Crops Prod 84:230–240. doi: 10.1016/j.indcrop.2015.12.052

Johnson S, Kang L, Akil HM (2016) Mechanical behavior of jute hybrid bio-composites. Compos Part B Eng 91:83–93. doi: 10.1016/j.compositesb.2015.12.052

Jonoobi M, Harun J, Mathew AP, Oksman K (2010) Mechanical properties of cellulose nanofiber (CNF) reinforced polylactic acid (PLA) prepared by twin screw extrusion. Compos Sci Technol 70:1742–1747.

Jonoobi M, Khazaeian A, Tahir PM, et al (2011) Characteristics of cellulose nanofibers isolated from rubberwood and empty fruit bunches of oil palm using chemo-mechanical process. Cellulose 18:1085–1095.

Kalia S, Kaith BS, Kaur I (2011) Cellulose fibers: bio-and nano-polymer composites:

green chemistry and technology. Springer Science & Business Media

Karmakar SR (1999) Chemical technology in the pre-treatment processes of textiles. Elsevier

Kasprzyk-Hordern B, Ziółek M, Nawrocki J (2003) Catalytic ozonation and methods of enhancing molecular ozone reactions in water treatment. Appl Catal B Environ 46:639–669.

Khait K, Carr SH, Mack MH (2001) Solid-state shear pulverization. CRC Press

Khalil HPSA, Bhat AH, Yusra AFI (2012) Green composites from sustainable cellulose nanofibrils: a review. Carbohydr Polym 87:963–979.

Kiessig H, Hess K, Sobue K (1939) Das System Cellulose–Natrium hydroxyd–Wasser in Abhangigkeit von der Temperature. Z phys chem 43:309–329.

Klemm D, Schumann D, Kramer F, et al (2006) Nanocelluloses as innovative polymers in research and application. In: Polysaccharides Ii. Springer, pp 49–96

Köhnke T, Lund K, Brelid H, Westman G (2010) Kraft pulp hornification: A closer look at the preventive effect gained by glucuronoxylan adsorption. Carbohydr Polym 81:226–233.

Krenchel H (1963) Fibre reinforcement; Akademisk Forlag: Copenhagen, 1964.

Krishnamachari P, Zhang J, Lou J, et al (2009) Biodegradable Poly(Lactic Acid)/Clay Nanocomposites by Melt Intercalation: A Study of Morphological, Thermal, and Mechanical Properties. Int J Polym Anal Charact 14:336–350. doi: 10.1080/10236660902871843

Lee M, Lee MS, Wakida T, et al (2006) Chemical modification of nylon 6 and polyester fabrics by ozone-gas treatment. J Appl Polym Sci 100:1344–1348.

Lee S-Y, Chun S-J, Kang I-A, Park J-Y (2009) Preparation of cellulose nanofibrils by high-pressure homogenizer and cellulose-based composite films. J Ind Eng Chem 15:50–55.

Leitner J, Hinterstoisser B, Wastyn M, et al (2007) Sugar beet cellulose nanofibril-reinforced composites. Cellulose 14:419–425.

Li R, Fei J, Cai Y, et al (2009) Cellulose whiskers extracted from mulberry: A novel biomass production. Carbohydr Polym 76:94–99.

Li W, Yue J, Liu S (2012) Preparation of nanocrystalline cellulose via ultrasound and its reinforcement capability for poly (vinyl alcohol) composites. Ultrason Sonochem 19:479–485.

Liimatainen H, Sirviö J, Haapala A, et al (2011) Characterization of highly accessible cellulose microfibers generated by wet stirred media milling. Carbohydr Polym 83:2005–2010.

Liu DY, Yuan XW, Bhattacharyya D, Easteal AJ (2010) Characterisation of solution cast cellulose nanofibre–reinforced poly (lactic acid). Express Polym Lett 4:26–31.

Lopez A, Ricco G, Ciannarella R, et al (1999) Textile wastewater reuse: ozonation of membrane concentrated secondary effluent. Water Sci Technol 40:99–105.

Lu P, Hsieh Y-L (2010) Preparation and properties of cellulose nanocrystals: rods, spheres, and network. Carbohydr Polym 82:329–336.

Lundstedt T, Seifert E, Abramo L, et al (1998) Experimental design and optimization. Chemom Intell Lab Syst 42:3–40.

Lunt J (1998) Large-scale production, properties and commercial applications of polylactic acid polymers. Polym Degrad Stab 59:145–152.

Man Z, Muhammad N, Sarwono A, et al (2011) Preparation of cellulose nanocrystals using an ionic liquid. J Polym Environ 19:726–731.

Manning TJ, Little B, Purcell J, et al (2002) Ozone decomposition data for kinetics exercises. Chem Educ 7:278–283.

Maqsood HS, Wiener J, Baheti V, et al (2016) Ozonation: a Green Source for Oxidized Cotton. FIBRES Text East Eur 24:19–21. doi: 10.5604/12303666.1168523

Marcovich NE, Auad ML, Bellesi NE, et al (2006) Cellulose micro/nanocrystals reinforced polyurethane. J Mater Res 21:870–881.

Mathew AP, Oksman K, Sain M (2005) Mechanical properties of biodegradable composites from poly lactic acid (PLA) and microcrystalline cellulose (MCC). J Appl Polym Sci 97:2014–2025. doi: 10.1002/app.21779

Meyabadi TF, Dadashian F (2012) Optimization of enzymatic hydrolysis of waste cotton fibers for nanoparticles production using response surface methodology. Fibers Polym 13:313–321.

Militký J, Jabbar A (2015) Comparative evaluation of fiber treatments on the creep behavior of jute/green epoxy composites. Compos Part B Eng 80:361–368. doi: 10.1016/j.compositesb.2015.06.014

Mohanty AK, Misra M, Drzal LT (2005) Natural fibers, biopolymers, and biocomposites. CRC Press

Morin A, Dufresne A (2002) Nanocomposites of chitin whiskers from Riftia tubes and poly (caprolactone). Macromolecules 35:2190–2199.

Nakayama R, Imai M (2013) Promising ultrasonic irradiation pretreatment for enzymatic hydrolysis of Kenaf. J Environ Chem Eng 1:1131–1136. doi: 10.1016/j.jece.2013.08.030

Neto ARS, Araujo MAM, Souza FVD, et al (2013) Characterization and comparative evaluation of thermal, structural, chemical, mechanical and morphological properties of six pineapple leaf fiber varieties for use in composites. Ind Crops Prod 43:529–537.

Nielsen LE (1978) Predicting the properties of mixtures. M. Dekker, NY

Noishiki Y, Nishiyama Y, Wada M, et al (2002) Mechanical properties of silk fibroin–microcrystalline cellulose composite films. J Appl Polym Sci 86:3425–3429.

Ohkawa K, Hayashi S, Nishida A, et al (2009) Preparation of pure cellulose nanofiber via electrospinning. Text Res J 79:1396–1401.

Oksman K, Mathew AP, Bondeson D, Kvien I (2006a) Manufacturing process of cellulose whiskers/polylactic acid nanocomposites. Compos Sci Technol 66:2776–2784.

Oksman K, Niska KO, Sain M (2006b) Cellulose nanocomposites: processing, characterization, and properties. Amer Chemical Society

Oksman K, Skrifvars M, Selin J-F (2003) Natural fibres as reinforcement in polylactic acid (PLA) composites. Compos Sci Technol 63:1317–1324.

ORTS WJ, IMAM SH, SHEY J, et al (2004) Effect of fiber source on cellulose reinforced polymer nanocomposites. In: ANTEC... conference proceedings. Society of Plastics Engineers, pp 2427–2431

Paillet M, Dufresne A (2001) Chitin whisker reinforced thermoplastic nanocomposites. Macromolecules 34:6527–6530.

Pan N, Chen K, Monego CJ, Backer S (2000) Studying the mechanical properties of blended fibrous structures using a simple model. Text Res J 70:502–507.

Parvinzadeh Gashti M, Ebrahimi I, Pousti M (2015) New insights into corona discharge surface ionization of polyethylene terephthalate via a combined computational and experimental assessment. Curr Appl Phys 15:1075–1083. doi: 10.1016/j.cap.2015.06.009

Parvinzadeh Gashti M, Hegemann D, Stir M, Hulliger J (2014) Thin film plasma functionalization of polyethylene terephthalate to induce bone-like hydroxyapatite nanocrystals. Plasma Process Polym 11:37–43. doi: 10.1002/ppap.201300100

Parvinzadeh M, Ebrahimi I (2011) Atmospheric air-plasma treatment of polyester fiber to improve the performance of nanoemulsion silicone. Appl Surf Sci 257:4062–4068. doi: 10.1016/j.apsusc.2010.11.175

Pasquini D, de Morais Teixeira E, da Silva Curvelo AA, et al (2010) Extraction of cellulose whiskers from cassava bagasse and their applications as reinforcing agent in natural rubber. Ind Crops Prod 32:486–490.

Perincek S, Bahtiyari MI, Körlü AE, Duran K (2008) Ozone treatment of Angora rabbit fiber. J Clean Prod 16:1900–1906.

Perincek SD, Duran K, Korlu AE, Bahtiyari İM (2007) An investigation in the use of ozone gas in the bleaching of cotton fabrics. Ozone Sci Eng 29:325–333.

Petersen K, Nielsen P V, Olsen MB (2001) Physical and mechanical properties of biobased materials starch, polylactate and polyhydroxybutyrate. Starch-Stärke 53:356–361.

Petersson L, Mathew AP, Oksman K (2009) Dispersion and properties of cellulose nanowhiskers and layered silicates in cellulose acetate butyrate nanocomposites. J

Appl Polym Sci 112:2001–2009.

Petersson L, Oksman K (2006) Biopolymer based nanocomposites: Comparing layered silicates and microcrystalline cellulose as nanoreinforcement. Compos Sci Technol 66:2187–2196. doi: 10.1016/j.compscitech.2005.12.010

Plackett D, Andersen TL, Pedersen WB, Nielsen L (2003) Biodegradable composites based on L-polylactide and jute fibres. Compos Sci Technol 63:1287–1296.

Platt DK (2006) Biodegradable polymers: market report. iSmithers Rapra Publishing

Prabaharan M, Rao JV (2001) Study on ozone bleaching of cotton fabric–process optimisation, dyeing and finishing properties. Color Technol 117:98–103.

Prasad BM, Sain MM, Roy DN (2005) Properties of ball milled thermally treated hemp fibers in an inert atmosphere for potential composite reinforcement. J Mater Sci 40:4271–4278.

Punyamurthy R, Sampathkumar D, Srinivasa CV, Bennehalli B (2012) Effect of alkali treatment on water absorption of single cellulosic abaca fiber. BioResources 7:3515–3524.

Qua EH, Hornsby PR, Sharma HS, et al (2009) Preparation and characterization of poly (vinyl alcohol) nanocomposites made from cellulose nanofibers. J Appl Polym Sci 113:2238–2247.

Rabiej M, Rabiej S (2005) Analysis of synchrotron WAXD curves of semicrystalline polymers by means of the OptiFit computer program. Fibres Text East Eur 13:75–78.

Ranganathan N, Oksman K, Nayak SK, Sain M (2016) Impact toughness, viscoelastic behavior, and morphology of polypropylene-jute-viscose hybrid composites. J Appl Polym Sci 133:n/a–n/a. doi: 10.1002/app.42981

Reddy N, Yang Y (2005) Structure and properties of high quality natural cellulose fibers from cornstalks. Polymer (Guildf) 46:5494–5500.

Rojas J, Bedoya M, Ciro Y (2015) Current Trends in the Production of Cellulose Nanoparticles and Nanocomposites for Biomedical Applications.

Rosa MF, Medeiros ES, Malmonge JA, et al (2010) Cellulose nanowhiskers from

coconut husk fibers: Effect of preparation conditions on their thermal and morphological behavior. Carbohydr Polym 81:83–92.

Rowell RM (2012) Handbook of wood chemistry and wood composites. CRC press

Rwawiire S, Tomkova B, Militky J, et al (2015) Development of a biocomposite based on green epoxy polymer and natural cellulose fabric (bark cloth) for automotive instrument panel applications. Compos Part B Eng 81:149–157. doi: 10.1016/j.compositesb.2015.06.021

Saha P, Manna S, Chowdhury SR, et al (2010) Enhancement of tensile strength of lignocellulosic jute fibers by alkali-steam treatment. Bioresour Technol 101:3182–3187. doi: http://dx.doi.org/10.1016/j.biortech.2009.12.010

Saïd Azizi Samir MA, Alloin F, Paillet M, Dufresne A (2004) Tangling effect in fibrillated cellulose reinforced nanocomposites. Macromolecules 37:4313–4316.

Samir MASA, Alloin F, Sanchez J-Y, Dufresne A (2004) Cellulose nanocrystals reinforced poly (oxyethylene). Polymer (Guildf) 45:4149–4157.

Sanchez-Garcia MD, Gimenez E, Lagaron JM (2008) Morphology and barrier properties of solvent cast composites of thermoplastic biopolymers and purified cellulose fibers. Carbohydr Polym 71:235–244.

Sargunamani D, Selvakumar N (2006) A study on the effects of ozone treatment on the properties of raw and degummed mulberry silk fabrics. Polym Degrad Stab 91:2644–2653.

Sarkar PB, Mazumdar AK, Pal KB (1948) 4—THE HEMICELLULOSES OF JUTE FIBRE. J Text Inst Trans 39:T44–T58.

Satyamurthy P, Jain P, Balasubramanya RH, Vigneshwaran N (2011) Preparation and characterization of cellulose nanowhiskers from cotton fibres by controlled microbial hydrolysis. Carbohydr Polym 83:122–129. doi: 10.1016/j.carbpol.2010.07.029

Siqueira G, Bras J, Dufresne A (2010) Cellulosic bionanocomposites: a review of preparation, properties and applications. Polymers (Basel) 2:728–765.

Soni B, Hassan EB, Mahmoud B (2015) Chemical isolation and characterization of

different cellulose nanofibers from cotton stalks. Carbohydr Polym 134:581–589. doi: 10.1016/j.carbpol.2015.08.031

Sorrentino L, Aurilia M, Forte G, Iannace S (2011) Anisotropic mechanical behavior of magnetically oriented iron particle reinforced foams. J Appl Polym Sci 119:1239–1247.

Stevens C, Müssig J (2010) Industrial applications of natural fibres: structure, properties and technical applications. John Wiley & Sons

Sun RC, Tomkinson J, Wang YX, Xiao B (2000) Physico-chemical and structural characterization of hemicelluloses from wheat straw by alkaline peroxide extraction. Polymer (Guildf) 41:2647–2656.

Suryanarayana C (2004) Mechanical alloying and milling. CRC Press

Świetlik J, Dąbrowska A, Raczyk-Stanisławiak U, Nawrocki J (2004) Reactivity of natural organic matter fractions with chlorine dioxide and ozone. Water Res 38:547–558.

Tang L, Weder C (2010) Cellulose whisker/epoxy resin nanocomposites. ACS Appl Mater Interfaces 2:1073–1080.

Thomas S, Pothan LA (2009) Natural fibre reinforced polymer composites: from macro to nanoscale. Archives contemporaines

Tzitzi M, Vayenas D V, Lyberatos G (1994) Pretreatment of textile industry wastewaters with ozone. Water Sci Technol 29:151–160.

Wallenberger FT, Weston N (2004) Natural fibers, plastics and composites natural.

Wang B, Sain M (2007) Isolation of nanofibers from soybean source and their reinforcing capability on synthetic polymers. Compos Sci Technol 67:2521–2527.

Wang Y (2006) Recycling in textiles. Woodhead publishing

Wang Y, Cao X, Zhang L (2006) Effects of cellulose whiskers on properties of soy protein thermoplastics. Macromol Biosci 6:524–531.

Wu Y-P, Jia Q-X, Yu D-S, Zhang L-Q (2004) Modeling Young's modulus of rubber–clay nanocomposites using composite theories. Polym Test 23:903–909.

Yuen CWM, Cheng YF, Li Y, Hu JY (2009) Preparation and characterisation of nano-scale cotton powder. J Text Inst 100:165–172.

Zhang C, Price LM, Daly WH (2006) Synthesis and characterization of a trifunctional aminoamide cellulose derivative. Biomacromolecules 7:139–145.

Zuluaga R, Putaux JL, Cruz J, et al (2009) Cellulose microfibrils from banana rachis: Effect of alkaline treatments on structural and morphological features. Carbohydr Polym 76:51–59.

LIST OF RESEARCH ARTICLES PUBLISHED

8.1 Publications in journals

1. Ozonation: a Green Source for Oxidized Cotton.

Fibers and Textiles in Eastern Europe ***(Published)***

2. Reinforcement of Enzyme Hydrolyzed Longer Jute Micro Crystals in Poly(lactic acid).

Polymer Composites ***(Published)***

3. Reinforcement of ozone pre-treated and enzyme hydrolyzed longer jute micro crystals in poly lactic acid composite films.

Composites Part B ***(Published)***

4. Ozone Treatment of Jute Fibers.

Cellulose ***(Reviewed)***

5. Development and characterization of solution cast cellulose reinforced poly(lactic acid) thin film.

Bulletin of Material Science ***(Under Review)***

6. Cationization of Cellulose fibers for composites.

The Journal of Textile Institute ***(Accepted)***

7. Effect of Cellulose Coating on Properties of Cotton Fabric.

Materials Science Forum ***(Published)***

8. Impact of Filling Yarns on the woven fabrics performance.

Fibers and Textiles in Eastern Europe ***(Accepted)***

9. Optimization of parameters for Oxidation of Jute by Ozone Treatment.

(In Process)

8.2 Contribution in conference proceeding

1. Surface treatment /cationization of cellulose fibers for composites.

   ICCMME 2016

2. Stress Strain Curves for PES Fiber and Yarns.

   STRUTex 2014

3. Effect of cellulose coating on properties of cotton fabric.

   ICCMME 2016

4. Ozonation: a Green Source for Oxidized Cotton.

   Svetlanka Workshop 2014

5. Thermal Properties of Yarn.

   Svetlanka Workshop 2015

6. Reinforcement of cationized cellulose in anionic matrix.

   Bila Voda Workshop 2016

7. Enzyme hydrolysis of ozone pre-treated jute fibrous wastes.

   44th TRS IIT Delhi 2016

APPENDIXES